

The Observation of Stars and Background Radiation in the
1600-3000A range with Low Resolution Photoelectric
Spectrophotometers carried on Unstabilised
Skylark Rockets.

George C. Sudbury M.A.

submitted for the requirements of the Degree of
Doctor of Philosophy

University of Edinburgh

1970.



SUMMARY

Four ultraviolet spectrophotometric instruments, designed and built at the Royal Observatory Edinburgh, were launched on E.S.R.O. unstabilised Skylark rockets. For two of these instruments, use of controlled roll-rate and aspect sensors led to a hundred received stellar signals being identifiable with stars. Forty-three of the best spectra, at 200\AA resolution, are presented. One of the instruments also gave information on the spatial distribution and intensity of the background radiation near 2500\AA .

Problems encountered in the experimental work were in the fields of physical and electronic optics, electronics, systems and environmental engineering, organisation, and cost-analysis. Effort devoted to laboratory ultraviolet intensity calibration did not, for practical reasons and in the author's opinion, solve the problem adequately. In this instance, reliance on a "comparison star" was supplemented by preflight tungsten ribbon lamp measurements.

To handle the substantial quantities of spectral data in a reproducible and consistent fashion, computer programmes were developed to identify the wavelength and extract the continua at suitable resolution via fitted polynomials. An extensive study is made of the resulting random and systematic errors, for both photon counting and direct current measurements.

The reduced spectra are tabulated at 50\AA intervals within the 1700-3000 \AA range (where the intensity was adequate) and are summarised in graphical form. The graphs show self-consistent photometry in agreement with published summary data.

Anomalies discussed include emission line and "peculiar A" stars; the latter have ultraviolet fluxes in accord with the spectral classifications of Osawa. Information on the interstellar flux, additional to that already published by Sudbury and Ingham, is obtained by summing the individual spectra, the contribution of which appears to be substantially less than that of fainter stars.

C O N T E N T S .

	Page.
Chapter I. Introduction	1
Chapter II. General Design	20
Chapter III. Calibration, Integration, Checkout and Flight Performance	53
Chapter IV. Data Reduction and Analysis.	75
Chapter V. Results and Discussion.	103

REFERENCES

ACKNOWLEDGEMENTS

APPENDICES

TABLES

INDEX

	<u>Page</u>
Chapter I. Introduction.	1
1.1 Historical Background	1
1.1.1. General Organisational Background	1
1.1.2. Scientific Background	2
1.1.3 Technical Background	7
1.1.4. Environment and Organisation	9
1.1.4.1 The Environment	9
1.1.4.2 The Organisation	11
1.1.5 Financial Background	13
1.2 Timetable of the Project	16
Chapter II. General Design.	20
2.1 Design Criteria and Limitations	20
2.2 General Design Description	25
2.3 Optical Design - Features and Problems	27
2.4 Mechanical Design - Features and Problems	31
2.4.1. Contamination, Paints and Scattered Light	36
2.5 Electronic Design Problems	40
2.5.1. D.C. Measurement Techniques	40
2.5.1.1 Frequency Response	40
2.5.1.2 Cathode High Potential Problems	42
2.5.1.3 Wide Measuring Range	43

	<u>Page</u>
2.5.2 Counting Systems	46
2.5.2.1 Noise	47
2.5.2.2 Count Rate Limitations	48
2.5.2.3 Discriminator Setting	49
2.5.3 Photomultiplier Selection	50
Chapter III. Calibration, Integration, Checkout and Flight Performance	53
3.1. Calibration	53
3.1.1 The Need for Calibration	53
3.1.2 Absolute and Relative References	56
3.2 The Calibration of the Spectrophotometer	60
3.2.1. Calibration Data	66
3.3 Payload Integration and Test	68
3.4 Flight Performance	70
Chapter IV. Data Reduction and Analysis	75
4.1 Nature of the Data	75
4.2 Attitude Solution	78
4.3 Reduction of Data	82
4.3.1. Measurement	83
4.3.2. Background Evaluation	84
4.3.3. The Zero Order	85
4.3.4. Smoothing and Curve Fitting	86
4.3.5. Reddening Correction	89

	<u>Page</u>
4.4. Sources and Amounts of Errors	91
4.4.1. The Counting Channel	91
4.4.1.1 Gross Errors	91
4.4.1.2 Random and Systematic Errors	93
4.4.1.3 Calibration Error	95
4.4.1.4 Tabulated Star Errors	98
4.4.2. D.C. System Errors	99
Chapter V. Results and Discussion	103
5.1. Presentation of the Data	103
5.2. The Stellar Data	104
5.3. Interstellar Reddening	108
5.4. The Galactic and Extragalactic Background	109
5.5. Conclusions and Prospects	113

Appendices

- Appendix I. Design Aims of Experiment R63.
- Appendix II. Approximate Cost Breakdown of one Spectrophotometer.
- Appendix III. The Sky Background Experiment (ROE-D).
- Appendix IV. ALGOL Programmes:-
 SNORE
 COMT
 AMPL
 FOLGEN
 SPLOT
- Appendix V. Reprints of Published Papers:-
 Applied Optics 8, 2013 (1969)
 Nature 226, 526 (1970),
 (in cover pocket).

LIST OF FIGURES

- Figure 1. Height-Time Curve for Payload S27-1, 3rd Dec 1968
(following page 15).
- Figure 2. Optical Diagram of Stellar Spectrophotometer.
(following page 25).
- Figure 3. (a) The R65(2) Spectrophotometer
(b) Cutaway Diagram of Spectrophotometer
(following page 25)
- Figure 4. The S27-1 Payload (undergoing vibration tests)
(following page 26)
- Figure 5. Circuits of DC Amplifier System R65(2)
(following page 41)
- Figure 6. Main Amplifier output, R65(2) DC Spectrophotometer
(following page 45)
- Figure 7. Calibration and Response Curves of Pulse Counting
Spectrophotometer
(following page 64)
- Figure 8. Output of Pulse Counting Spectrophotometer when
Calibrated with Ribbon Lamp
(following page 66)
- Figure 9. Section of S27-1 telemetry record showing signals
due to star β Cephei
(following page 72)
- Figure 10. Effective Bandpass under various conditions for
R65(2) counting channel.
(following page 75)

Figure 11. Across Slit residual plot, S27/1 attitude solution
(following page 81)

Figure 12. Relation between Spectral Type and Normalised
Brightness for

(a) 1850A

(b) 2000A

(c) 2200A

(d) 2500A

(following page 104)

Figure 13. Main sequence data compared to values by Blondelot
(following page 106)

Figure 14. Comparison of present observations and published data
(following page 106)

Figure 15. (a) to (f) Plots of Spectral distribution for 36
stars.

(following page 106)

I. INTRODUCTION.

1. 1. Historical Background.

1. 1. 1. General Organisational Background.

This thesis describes work, carried out between late 1962 and early 1970, directed to obtaining data on the low spectral resolution intensity distribution of light received from early type stars in the ultra-violet shortwards of 3000A - the ozone cutoff. All of it was done while the author was working with what is now the Space Research Division of the Royal Observatory Edinburgh (R.O.E.) in the post of Senior Research Fellow or (since November 1965) Senior Scientific Officer. It was funded through the Observatory budget (which has appeared on the Science Research Council budget since 1965) as part of the British National Space Research programme. The European Space Research Organisation (E.S.R.O.) was responsible for the integration of the instruments into payloads, the launches, and the post flight attitude reconstitution.

The author's own role was to define the instrumental requirements, to initiate the particular instrumental approach, and, as Project Manager of the experiments, to be entirely responsible for all the day to day planning and organisation of the project. This meant that he

personally carried out much of the design, development, testing, calibration, round integration and final launch preparation of the instrument and reduction of the resultant data. As the acknowledgements make clear, however, as well as the several external organisations involved, other members of the R.O.E. Space Research Division played a considerable and, in some cases, vital part in much of the work.

1. 1. 2. Scientific Background.

Since, for reasons largely beyond the author's control (see section 1.2.) the work extended over a far longer period than had at first been envisaged, it is necessary to view the project first within the limitations of the state of stellar rocket ultraviolet observations in 1962.

The early solar observations of the NRL and, latterly, AFCRL groups had confirmed that the ozone absorption, which prevents celestial observation from the ground shortwards of 3000A, became unimportant above 80 - 100km and hence that clear observation to less than 1850A was possible above this altitude. The Schumann-Runge and Lyman-Birge-Hopfield absorptions become important at shorter wavelengths, requiring altitudes near 200km to make good observations at 1400A.

The British Cuckoo-boosted Skylark rocket gave access to these altitudes with payloads of greater than 100kgs during the early 1960's, as the Viking and Aerobee rockets had done for the U.S.A. in the preceeding decade or so. Apart from the arguments of pure natural philosophy that one-and-a-half octaves of radiation, equivalent in span to the entire spectrum used by conventional astronomers at that time, should not go unexplored, there were certain particular matters which could already be expected to be worthy of observation. The early type (O-B) stars emit the greater part of their energy in the ultraviolet so that measurements made longwards of 3000A required substantial extrapolation to predict the effective temperatures, and hence the total fluxes and the evolutionary rates, of these stars. Van de Hulst had already predicted that great differences might occur in the ultraviolet interstellar extinction due to different possible compositions of the interstellar material. When high resolution spectra became possible, it was to be expected that the resonance lines of many stellar elements would be observable and, ultimately, lines due to interstellar absorption; low resolution measurements would pave the way for such work.

There had, in the late 1950's and early 1960's been a number of flights, with differing success, of

various stellar photometric instruments (e.g. Chubb & Byram 1963, Boggess & Dunkelmann 1958, Kupperian, Boggess & Milligan 1958, Alexander, Bowen & Heddle 1963). The main significance of these was to show that fluxes from early type stars at the shortest wavelengths (the 'ion-chamber' region shortwards of 1500A) were less, by amounts probably exceeding a stellar magnitude, than those indicated by the theoretical models of the time (Underhill 1956, 1960, 1961, 1962 & 1963, Cavannaglia & Pecker 1953, Saito 1954, 1956, Cayser 1958, de Jager & Neven 1957) which did not allow for the cumulative effects of line absorption (blanketing). The measures in the 2200 - 2800A region, on the other hand, were more or less in accord with the models. The first flight of an objective dispersion (spectrophotometric) instrument (Stecher & Milligan 1962) also seemed to show quite astonishing deficiencies in stellar fluxes, beginning at 2500A and amounting to one or two stellar magnitudes compared to the current models by 1900A; the Stecher & Milligan data also showed at least one startling difference in spectrum between stars of similar spectral type and class. The data of Alexander, Bowen & Heddle at 1900A was not of high quality but seemed to show deficiencies about half of those obtained by Stecher & Milligan. Such deficiencies would indeed have substantial effect on the evolution of early type

stars or on our ideas of circumstellar absorption. It seemed clear to me that only further spectral scans could verify or otherwise such data and cast more light on its nature. This therefore was one reason for embarking on the programme.

Over the intervening years however these anomalies have been largely resolved by:-

- (a) Improvements in the models to allow for line blanketing (Mihalas 1966, Elst 1967, Housiaux 1969, Adams & Morton 1968, review by Davis & Webb 1970) which has the effect of reducing the ultraviolet fluxes and raising the "visible" flux for a given effective temperature T_{eff} (thus causing T_{eff} to be overestimated from ground-based measurements).
- (b) Improved UV observations and calibration. (Stecker 1969, Bless et al 1968).
- (c) Reconsideration of the T_{eff} criteria from ground-based measures (Heintze 1969, Peters & Aller 1970, Kodaira 1970). In fact, the remaining discrepancies, about 0.5 mag around 1200-1400Å, are now comparable to the likely residual absolute calibration errors at these wavelengths.

Much of the above theoretical work has in fact been stimulated by rocket measurements.

The separate problem of the interstellar material is still undergoing a development which has been greatly stimulated by the far ultraviolet measurements. The nature of the reddening curve in the 1500-2500A region is far more sensitive to the variations of grain size and composition, to the extent that relatively crude measures at a number of points in this region are sufficient to reject models which would only give a very small departure from the nearly linear relation between extinction and reciprocal wavelength which is a characteristic of the 3000 - 8000A region (Wickramasinghe 1967). This fact has been a particular stimulus for the continuation of the project. Other uses of broad band data have been expounded elsewhere by Wilson (1968).

Finally, the general gathering of data of a relatively new type on a very substantial number of individual observables (stars in this case) has in the past often justified itself by producing unexpected information of which the data on background brightness from this project is a good example. The practical experience gathered by the Royal Observatory Edinburgh by this work has also been of inestimable value in providing a background for a number of aspects of the more uniquely valuable and complex S2/68 scanning satellite project.

1. 1. 3. Technical Background.

The general constraint of scientific advance by the current state of engineering and technology applies with especial force in the field of space observations. Some of the detailed technical problems and bounds affecting this project are discussed in section 2. and they, like the science, changed in many ways in the course of six years. One particular constraint, however, determined above all the scope of the observations and the nature of the instrument; the measurements had to be made from an unstabilised Skylark rocket. Although the lunar-stabilised Skylark existed conceptually, and star-pointing rockets were a long-range possibility, in 1962 (as in 1968) the only immediately available suitable vehicle was the standard Skylark. To have a reasonable prospect of obtaining the spectra of a substantial number of stars from this vehicle, dictated that photo-electric measurements, with an instrument viewing perpendicular to the (longitudinal) spin axis of the rocket, were the only possibility. The quick optimisation study which was carried out in 1963 and which is reproduced verbatim in appendix I. showed that, although a handful of stars, down to a visual magnitude of 3 - 3.5, could probably be observed with $\sim 100\text{\AA}$ resolution under a wide variety of rocket rotational dynamics,

nevertheless because of the then rapidly growing body of statistics indicating the wide dispersion of roll and precession rates of Skylark, the addition of the (then existing) roll rate control unit would greatly increase the chances of substantial success. As detailed in Section 1. 2. the failure in August 1965 finally convinced ESRO of this fact. The use of this unit is also vital to the present design concept since it allows optimisation of the frequency response characteristics of the detector output measuring systems (amplifier or pulse counter) for the spectral resolution.

The acceptance of the low resolution implied by the need to observe a reasonable number of stars in a random scan of the sky has always implied that spectral line measurement was not the aim - nor, therefore, the measurement of continua in the exact stellar spectroscopic sense of the word. The data are, in fact, measures of the total received flux from a star in a sequence of overlapping bands, the bands being relatively narrow in wavelength terms compared to the traditional UBV bands, though comparable (~ 10) in resolving power. Only by implication, from available resolved spectra or reliable models, could such data give information on the strength of spectral lines.

Because, also, the main labour of this research has been the overcoming of many practical limitations

and problems imposed by the very nature and novelty of ultraviolet stellar research from rockets, much of this thesis is concerned with detailing these problems and their solution whenever this was satisfactorily found. The tabulation and commentary on the spectral brightness of some 40 of the stars observed, and the astrophysical deductions from the sky background measures, represents the extent of the solution of these problems.

1. 1. 4. Environment and Organisation.

In addition to all the normal everyday problems of any scientific research, space research experimenters face two particular problem areas the full magnitude of which have only gradually come to be generally realised over the past decade.

1. 1. 4. 1. The Environment.

The rocket-borne instrument has to survive, and sometimes operate in, a hostile environment involving:-

- (a) Vibration levels which (for Skylark) are some 5 - 10g at the motor end of a payload but which payload resonances can multiply by a factor of five or ten; since the sounding rocket structure unlike that of a satellite or its launcher, is

relatively rigid, a poorly designed experiment can receive enough energy to factor this significantly again.

- (b) Kinetic heating of boundary layer air flowing over the rocket skin, which may reach 1000°C ; however if this air is kept out and heat shielding used near sensitive parts, the thermal time constant of typical structures and components means that no substantial thermal effects need be encountered.
- (c) Decompression to the state of high vacuum which is, of course, necessary for our observations and which must be aided by venting of otherwise closed volumes and choice of low outgassing materials and finishes; however, it represents a particular hazard to the corona breakdown of high voltage equipment- which it must be recalled is not always trouble free even under normal laboratory conditions.
- (d) Variable "steady" acceleration, reaching 12g near the end of the boost phase, to be followed by the "free fall" condition until re-entry.
- (e) Complete lack of control over the rocket and its contents from the moment of motor ignition, when the entire round becomes an independent entity the success of which hangs on the care

and forethought in its design, and which, for an astronomical instrument of substantial collecting area, must involve the mechanical ejection of the kinetically heated air protection i.e. a hatch or nose cone.

- (f) The far from favourable ground environment which generally exists during range preparation and checkout.

1. 1. 4. 2. The Organisation.

Even at the sounding rocket level, space research activities suffer from the problems attendant on a "big science" activity, involving extensive finance, good will, effort and co-ordination from a number of bodies and individuals, outside the experimenter's own line of control and appeal. This impacts particularly in respect of the timetable. Firstly almost all details of the interfaces with the payload system have to be defined before the flight models have been constructed and generally before the prototype has been evaluated. At that stage also, especially in the case of payloads integrated by an industrial contractor, a timescale to launch must be agreed: the desire for speedy results tends to make this one without much "float" but there is then strong moral and (potentially) financial

pressure from all sources to keep to this schedule. The payload team, normally with extensive backing resources and usually assembling production items to a standard routine, is more favourably placed for this exercise than the experimenter with his limited resources and "one-off" developments.

Equally, when the need for a substantial change of timescale or technical requirement arises, this tends to require considerable time-consuming negotiation through appropriate "political" channels. As the launch date draws nearer, the time-pressure becomes substantially greater when firing in the ESRO system from Sardinia, due to the operation of limited period firing "campaigns"; the extension or duplication of these campaigns has, again, cost implications which may be of the same magnitude as the actual experiment cost. Finally, once at the range, aiming for a firing "slot" of limited (seven days in a month) duration, with further limitations of hours of firing, very temperamental weather conditions, and (for local reasons) substantial extra range costs being incurred for every night when a count-down is scheduled, the conditions are far removed from those of most traditional laboratory or observational science. Perhaps eclipse observations are the nearest analogue in the field of conventional astronomy.

Subsequent to firing, the experimenter becomes dependent upon the facilities, co-operation and skill of the data-processing organisation to present his data in usable form and, in the case of this programme, to co-operate in deriving a sufficiently accurate aspect solution. Only then can the astrophysical reduction begin.

1. 1. 5. Financial Background.

Particularly in view of the general reputation of space research as being an outstandingly expensive form of research, on a par with nuclear physics, but also as this thesis is a part time one with funding and support staff not drawn from the University, it may be of especial interest to summarise the cost of the data obtained. A detailed breakdown of the component cost as bought in is given in appendix 2. It will be seen that this is dominated by the current price of a selected Ascop photomultiplier when this is used. A generous rounding up to include procurement costs, spares etc. would reach a total of £2,000. In addition each instrument requires a total of some four months of laboratory technician time to manufacture, say £400. excluding overheads. Two unflown "spare" models, used as prototypes, especially for vibration testing, have

also been made in addition to the four models flown, so we may cost each model at effectively £3,660. This figure increases to some £5,500 if we include about six months each of a Senior Scientific Officer/Senior Research Fellow (i.e. myself) and an Experimental Officer at current mean scales. Travel, freight etc probably increases this to £6,000.

Such figures are of course dwarfed by the cost of the rest of the payload, its integration and launch. The roll control unit, when supplied by Space General Corporation, costs about another £5,500 while total current costs of payload (excluding experiments) integration, and launch for an unstabilised Skylark is some £50,000. As the round is shared with another experimenter only a part of this is attributable to an individual instrument, so the total cost attributable to launching four instruments to date on three rockets must be some £60,000, giving an inclusive total of £84,000. This is just over £2,000 for each star usefully observed; as the successful round carried two spectrophotometers, we might assess this, with a weighting factor for quality of spectrum according to the brightness observed, as about £100 per useful item of data. However, additional data, of comparable importance has been obtained from the background brightness (Section 5.4) which shows the problems of a

cost assessment of this type. This costing is considered further in a space research context at the end of this paper.

The initial design and development of the unit was in fact done in a substantially cost-limited environment, the total Division vote for bought in items, including laboratory build-up from nothing, being £2,000 for 1962/3 and £5,000 for 1963/4; this was shared with one other experimenter. The corresponding budget for rocket work alone, shared between three experimenters, has been around £10,000 for 1968 and 1969.

Assistance available since 1964 has been, on average, one Experimental Officer and one Laboratory (workshop) Technician (mechanical or electrical) during the time that the programme was active (see Section 1.2.)

TABLE (1)

ESRO Payload Designation	Integration by	Spectrophotometer Designation	Date of Firing	Success or reason for failure	Apogee
D 4 = S05/1	E S T E C	R63-F1	August 1965	Faulty telemetry, Moon sensors, Pitch-yaw lock-in leading to low roll rate	208kms
D 4 = S05/2	E S T E C	R63-F2	May 1967	? Loss of adjustment or optical contamination/overheating	200kms
S27/1	British Aircraft corporation	R65-2 FLA (DC) FLB (Countg)	December 1968	Success	199kms (Fig. 1)

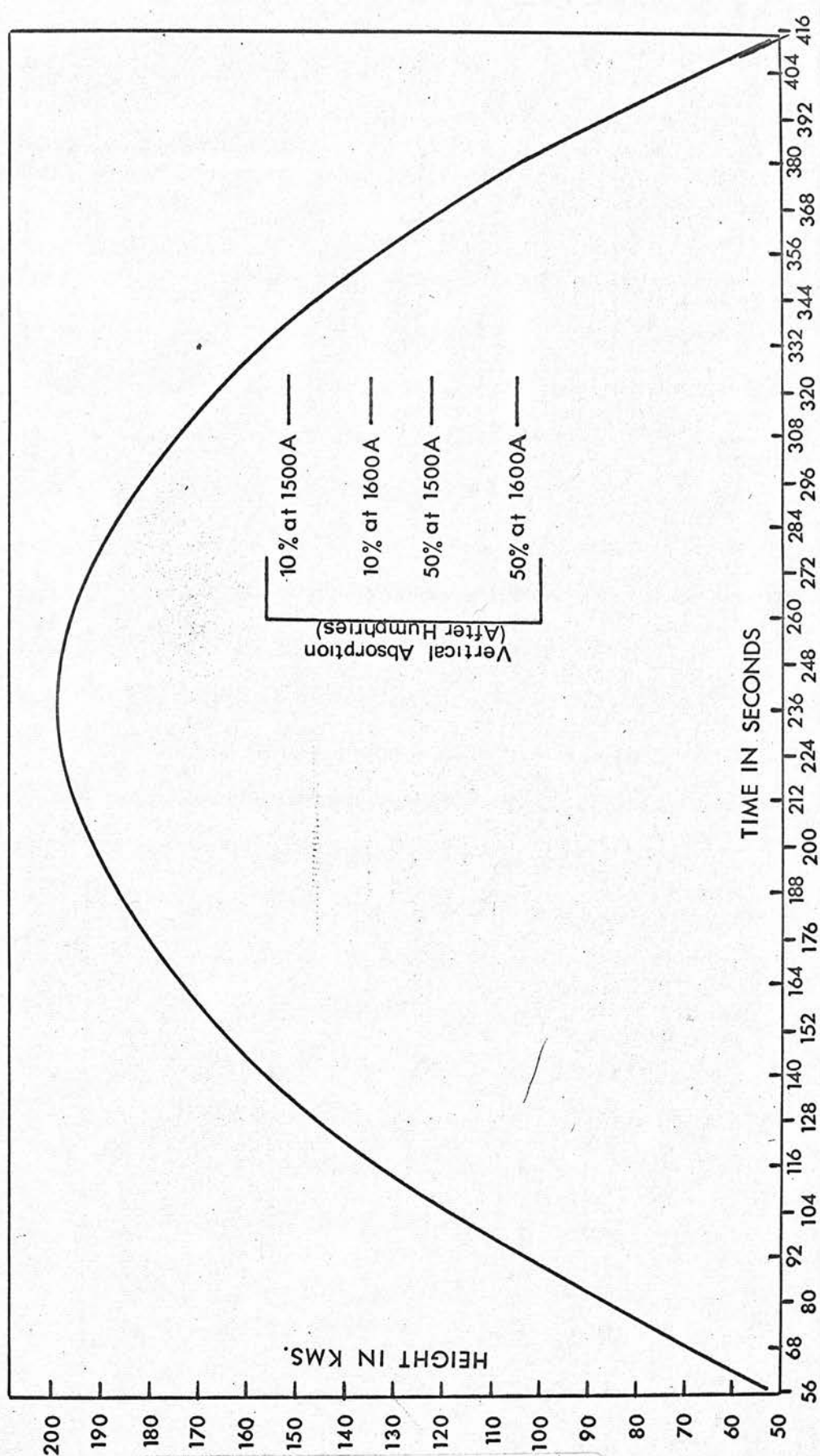


FIG 1 HEIGHT - TIME CURVE FOR
PAYLOAD S27-1 3/12/1968.

1. 2. Timetable of the Project.

Although the programme has been in existence since 1962, when this Ph.D. course was entered, it has in fact been in abeyance for a substantial part of the time. A timetable is presented below to make this clear. Table I provides a key to the labels and timing of the three rounds involved.

1962 Summer	Application of Optical scheme conceived.
Autumn	Optical breadboard devised and tested.
Winter	Application made to E.S.R.O. Preparatory Commission (COPERS) for round space.
1963 Spring	Experiment accepted as R-63 for firing in ESRO D-4 payload scheduled March 1964.
Summer	Prototype mechanical/optical system designed and tested.
September	Payload D-4 postponed by up to one year. Work halted on R-63 spectrophotometer to allow group's Sky background photometer experiment (ROE-D) to proceed.
1964 March	Roll control unit formally requested of ESRO.
July	Roll control unit refused by ESRO.
September	ROE-D completed and despatched. Work restarted on R-63.

1965 Feb/March Vibration tests on D-4 experiments.

Some redesign carried out.

April Integration and vibration tests both
D-4 (S05) flight payloads.

June Calibration completed R-63, F1 and F2.

August Payload S05/1 fired. Partial telemetry
failure, Pitch-yaw lock-in, Moon sensor
failure. Experiment R-63 operated and
observed spectra but no attitude
solution possible.

Autumn Roll control units approved for ROE
rounds.

Winter Redesign of photomultiplier block in R-63
second model (F.2.) to accomodate longer
slit.

1966 Summer R-63, F.2. recalibrated, reintegrated.

July Firing cancelled on second possible launch
night owing to faulty moon sensors.

1967 Spring. F.2. recalibrated, integrated & launched
(payload S05/2 May). High steady back-
ground, only three stars recognisable.
Ph. D. studies suspended.

Autumn/
Winter Experiment R-65(2) on payload S-27
modified to become two spectrophotometers.
Pulse counting system developed.
Prototype vibration tests.

1968 Spring/ Summer	Decision to "split" pair of S27 payloads. S27/1 flight model built, tested, integrated.
Autumn	Flight model calibrated. Firing postponed one month due to photomultiplier failure in another experiment and payload electrical noise problems and a further month due to range facilities not being ready.
1968 December 3rd.	Payload S27/1 successfully launched. Apogee 199km, all systems necessary to R-65(2) functioned successfully.
1969 Jan/Feb	First attitude solution received from ESRO, checked on two stars.
March	Second attitude solution received. 75 stars identified.
Apr/Oct.	Reorganisation of S1/2/68 satellite project virtually halts data reduction.
October	Fresh attitude solution requested especially to establish roll rate.
December	Third attitude solution and accurate roll rate tabulation received. Full data reduction started.
1970 February	Main analysis of "background" light completed.
April	Fully reduced spectra of over 30 stars computed.

The foregoing shows that, discounting the nugatory effort in repeating the S05/2 preparation, work was actually in progress on this programme for a total of just over three years prior to the 1968 firing and for some nine months since then. From late 1966 until October 1969 the writer's time was largely engaged on the S1/2/68 satellite project and this has continued to be a partial (about 50%) commitment. Some official assistant effort, totalling about two man-months has been made available for the routine reduction procedures.

II GENERAL DESIGN.

2. 1. Design Criteria and Limitations.

As already indicated, the scientific aim was to obtain stellar spectra, and the basic technological limitation of the unstabilised Skylark rocket meant that such spectra must be photoelectric, the spectral resolution not being better than about 100Å in order to observe a useful number of stars (appendix 1.). The latter restriction assumes that the instrument has its line of sight orthogonal to the rocket longitudinal axis , to make use of the roll scanning motion of the rocket, rather than along the axis where, although the scan rate is generally much lower, the direction of scan (in rocket axes) is continually changing due to the roll motion and the rate of scan is quite unpredictable. For a completely unstabilised Skylark, however, the roll motion has also a very large range of values; on the statistics available in 1962/3 the indications were of a mean value around the desirable $20-30^{\circ}/\text{sec.}$ but also with values which might be higher than $100^{\circ}/\text{sec.}$ or only a few degrees per second. The relatively high precession rate which was associated with the latter values meant that the instrument would have to be able to obtain its individual spectra in a short scan, clearly conflicting with the high rate situation;

nevertheless it seemed necessary to design the instrument to function to some effect in either situation. Of course, by the eventual provision by E.S.R.O. of the roll-rate control, following the pitch-yaw lock-in experience on S05-1 (this process transfers virtually all angular momentum from roll to precessional motion) the dilemma was partially resolved; by this time sufficient statistics had accumulated to show that the desirable roll rate hardly ever occurs. As, potentially lock-in could still occur before roll rate stabilisation, substantial precession rates remained a danger, however, leading to the choice of a higher-than-optimum scan rate for round S05-2.

Other criteria (some of which have been discussed in more detail by me elsewhere) (Sudbury 1969) for a stellar ultraviolet instrument can also be set down.

- (a) It should have as large a collecting area as possible--this is the general rule for all stellar work.
- (b) Notwithstanding (a) above it should be as compact as possible - to avoid excessive constructional and environmental problems, allow for flying of more than one instrument in a payload, and (of rather less importance in a sounding rocket) to economise in weight.
- (c) Notwithstanding (a) and (b), the instrument

should have as high an efficiency as possible. Even with the overcoating techniques developed by Tousey, Hunter and Haas during the 1950's, reflectivities of more than 75% are not easy to obtain in the rocket ultraviolet, while the combination of shortness of observing time, limitations of collecting area, and small percentage of stars having substantial fluxes in this region make efficiency much more vital than for ground-based observations; hence folding of the optical path purely for volume limitation should be avoided if possible.

- (d) The instrument should have a high rejection for visible radiation, again on account of the excess of stars having peak output in the visible region. Such rejection may be by optical baffling or vignetting, multiple dispersion, and the use of visual blind (alkali telluride) photo cathodes, separately or in combination. All these methods tend to conflict with the efficiency requirement (c) above; in particular the tellurides have peak quantum efficiencies two or three times smaller than the best antimony caesium cathodes; this is in practice compensated at very low light levels by their negligible dark current at ordinary

temperatures. The rejection requirement is exacerbated by the next condition (e).

- (e) It should have a fairly wide field. Although the highly concentrated distribution of early type stars does cause a substantial blending problem, a random scan in a rocket flight can only scan a relatively small part (about 20 - 25% for a 3° field) of the accessible hemisphere. Hence a field greater than a degree is desirable. Such a width also increases the possibility of repeat observations during a flight or between one flight and another, leading to increased confidence in the observations, and diminishes the percentage of dubious "grazing" measurements. With a proper solution of the rejection problem, the signals strong enough to be useful are not in fact generally background limited.

- (f) For reasons of reliability, there should ideally not be any moving parts, other than those required for the jettisonable skin section which protects the instrument during ascent through the atmosphere.

All of these criteria were in mind when the original choice of instrument was being made, the only exception being that the ultraviolet background was not

known. Such in-flight information as was available (Stecher & Milligan loc.cit., Boggess, verbal communication 1964) suggested that in fact background might well be a limitation, perhaps being comparable to the signal from a third or fourth magnitude star. Since this parameter was such an important one in respect of field size for all stellar experiments, but especially for this instrument in determining the wave-length resolution as well, it acted as an additional impetus for the Division in its decision to fill the programme hiatus which occurred in 1963-4 by building an instrument (known as R.O.E.-D) to measure this background. As the draft description which was prepared of ROE-D. did not reach publication and as it has technical as well as scientific relevance a brief description is given in Appendix 3. However on account of the motor failure on the round to measure night background the necessary scientific data was not obtained, while in the outcome the pulse-counting version of the spectrophotometer itself has been able to make such measurements (Sudbury & Ingham 1970).

2. 2. General Design Description.

An outline description of the design of the instrument used in these investigations is given now for the sake of putting the succeeding design discussion into context, a fuller description having been given in a reference (Sudbury 1969) which forms an addendum to this thesis.

Optically the spectrophotometer comprises (Fig.2) a 216mm diameter (210mm clear aperture) paraboloid of around 390mm focal length collecting light to feed a 58cm square (52cm square clear ruled aperture) plane reflecting diffraction grating (600 lines/mm, 2000A blaze) placed 4.25 degrees off axis in the convergent beam. The dispersed light is focussed in the plane of a slit having a field length of 3 degrees and spectral width some 150 - 200A. The exact dispersion scale depends on the precise mirror focal length and mirror-grating spacing and is around 1000-1250A per degree of rotation of the instrument.

Behind the slit lies a Fabry (field) lens of fused silica or calcium fluoride imaging onto a photomultiplier cathode of caesium telluride deposited on the rear of a fused silica or sapphire window. The slit, lens, and detector are mounted in a single unit (Fig 3) while separate cell systems hold the mirror and grating.

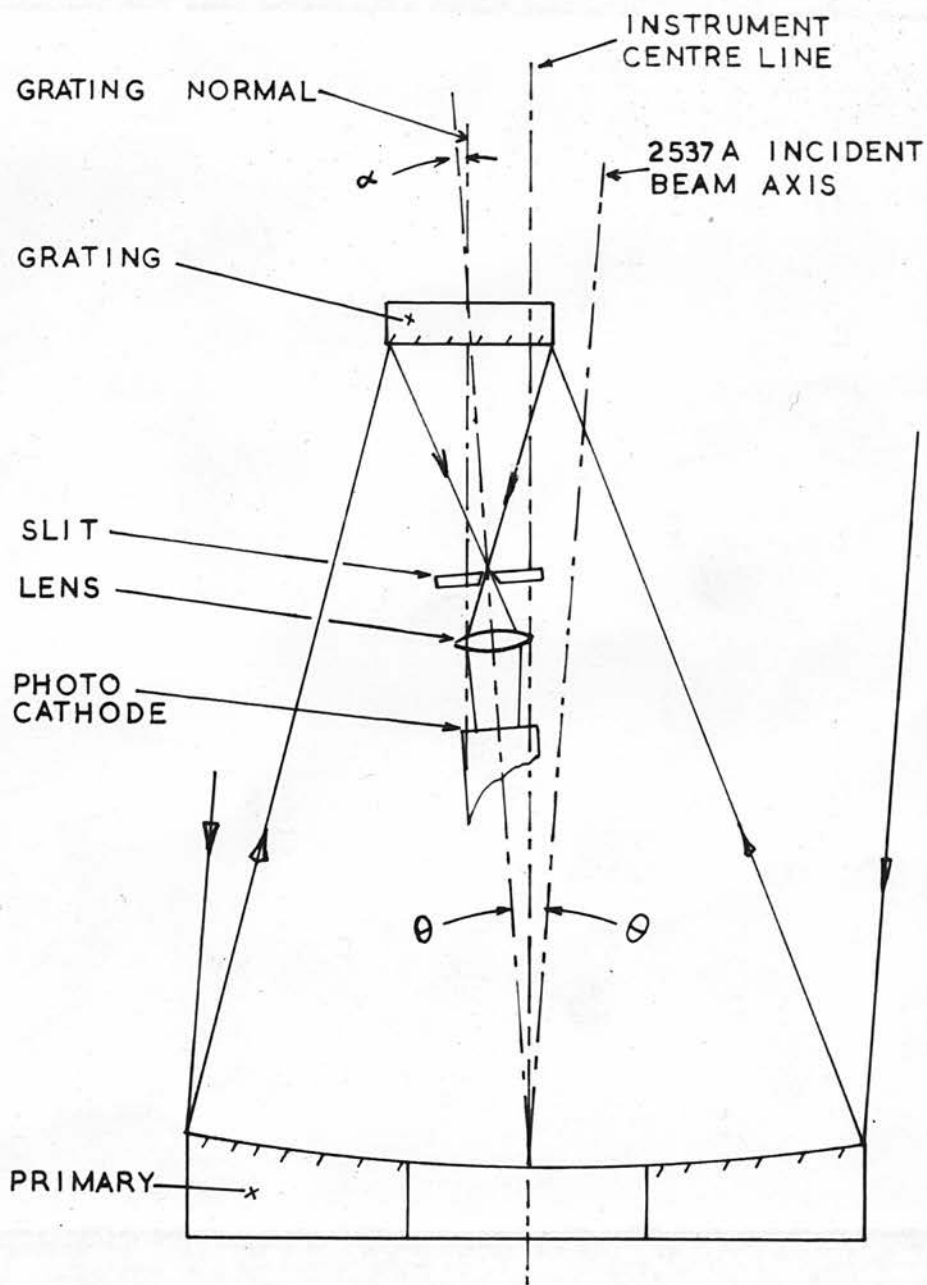


FIG.2 OPTICAL DIAGRAM OF STELLAR SPECTROPHOTOMETER.

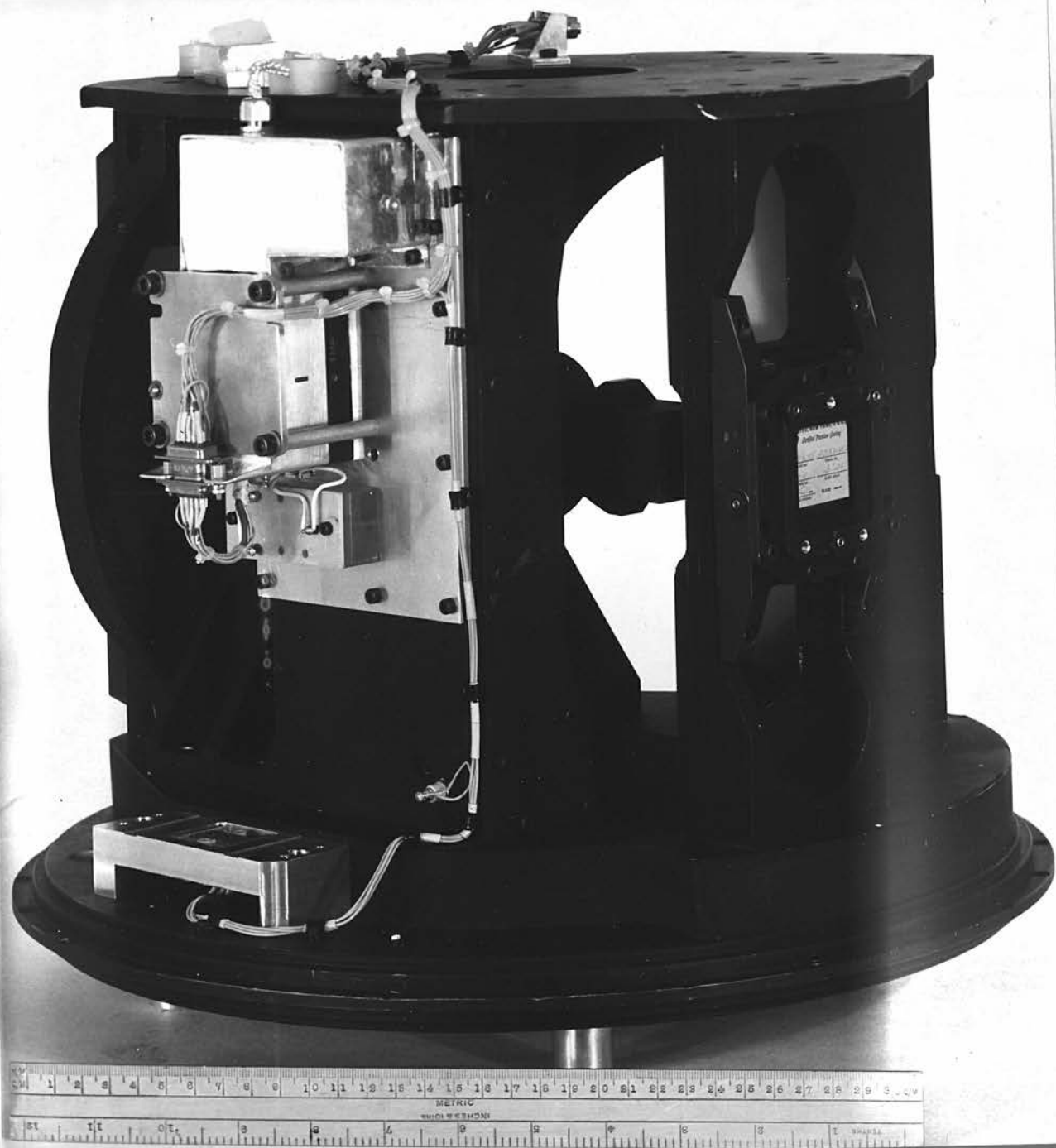


FIG.3a THE R65(2) SPECTROPHOTOMETER.

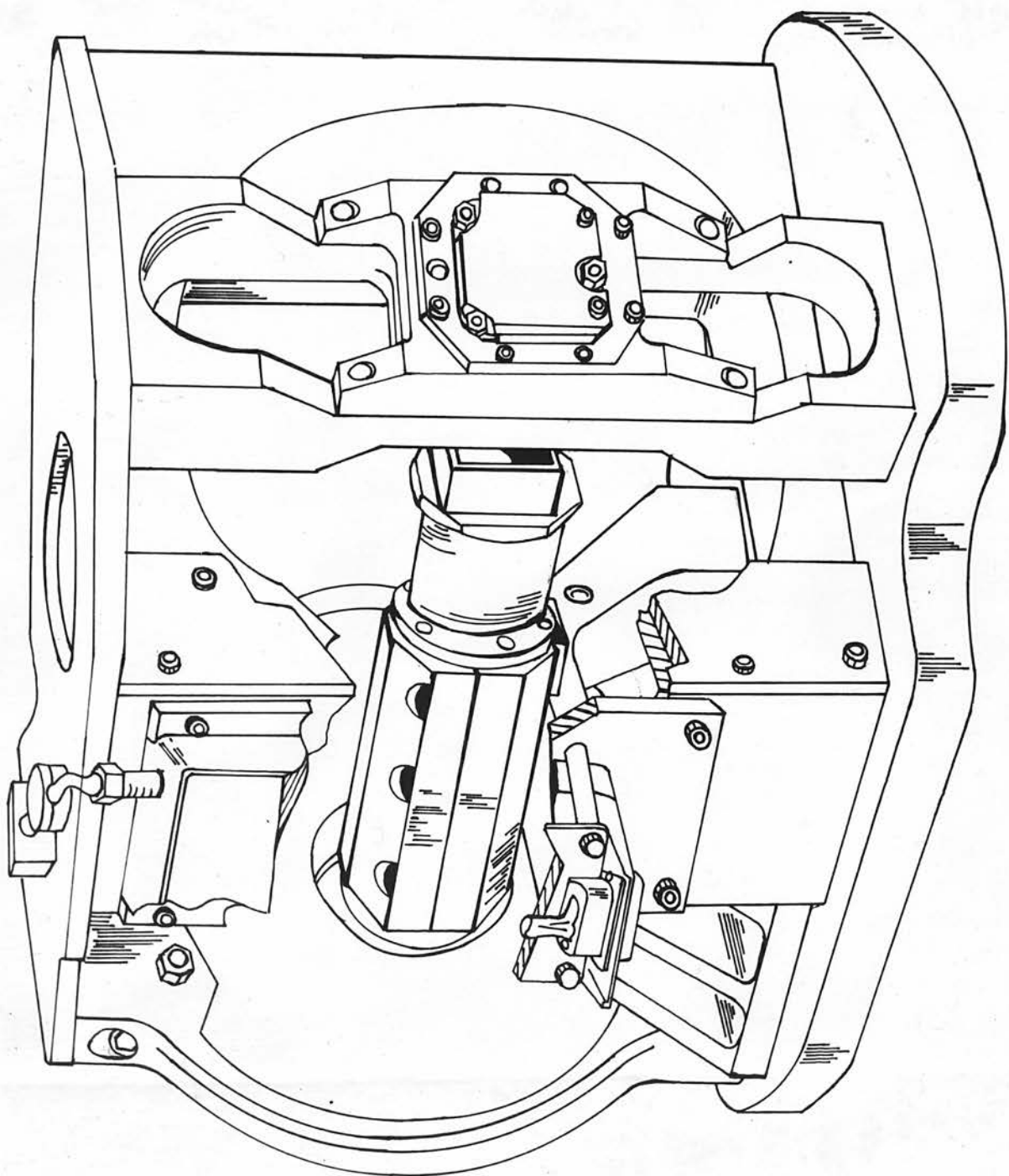


FIG. 3b CUTAWAY DIAGRAM OF SPECTROPHOTOMETER.

The detector block is then mounted from the ribbed casting comprising the "floor" of the unit (which has now been flown also in the inverted orientation) while the grating and mirror mounts are held between this and a top plate. The top plate is made rigid by means of a central box-shaped casting in which is the near circular entrance baffle of the system. The entire unit mounts in a single 337mm high Skylark parallel body section (Type 8) and views the sky through an aperture which is covered with an ejectable plate during ascent through the atmosphere.*

High voltage (E.H.T.) for the photomultiplier is provided from the payload main 28v DC supplies by an inverter (transformer) stabilised system. Signal detection is by non-linear D.C. amplifier or, latterly, photon pulse counting (Beattie & Paterson 1970).

* See Fig. 4.



R65-2
ELECTRONICS

R65-2 D.C.
SPECTRO-
PHOTOMETER

R65-2 PULSE
COUNTING
SPECTRO-
PHOTOMETER

TELEMETRY

BATTERIES/
SWITCHING

MOON SENSORS
& MAGNETERS

TWIN U-V.
PHOTOMETERS

STELLAR
SENSOR

SINGLE U.-V.
PHOTOMETER

ROLL CONTROL
UNIT &
TRACKING
LAMPS

NOSE
CONE

TYPE 8
13" BODY
SECTION

TYPE 8
BODY

TYPE 7
12" BODY

BATTERY
BAY

ATTITUDE
BAY

TYPE 8
BODY

ATTITUDE
BAY

SPACER

TYPE 8
BODY

SPECIAL
BAY

VIBRATOR

FIG 4 S27-I PAYLOAD
(UNDERGOING VIBRATION TESTS)

2. 3. Optical Design - Features and Problems.

In the context of the criteria of 2. 1., the scheme of Murty (1962) which reached the author at the time most of these criteria had been evolved, seemed well suited to our purposes and capable of realisation in series production without the heavy expenditure on imported optics which would be required for a system of the Stecher & Milligan (loc. cit.) type. Through the initiative of H.E. Butler a "breadboard" model, already possessing some of the principal constructional appearance of the final design, was made, optimised for 3000A. It was immediately apparent from the study of the mercury spectrum that the system had quite sufficient spectral resolution over the necessary wavelength range, within the slit width resolution limitations imposed by the scan rate. The author also carried out a test on bright stars to assess the problems of background as well as the relative brightness and location problems for the zero order light. This test confirmed that the system was practical and had approximately the right parameters.

The detailed aspects of this, and general, convergent beam systems are fully covered by Sudbury (loc.cit.) and Murty (loc.cit.) and their references and will not be repeated here. Two particular, and related, problems

of the design as used must be mentioned here. Generally, optical systems have a clearly defined entrance aperture stop from which the collecting area of the instrument can be specified. It also has a particular role in photo-electric work as being the object plane which the Fabry or field lens of the system will image onto the photocathode, thereby (in principle) eliminating problems due to the non-uniformity of the cathode sensitivity, when light enters the system from different parts of the field of view. Now it is a feature of our optical system that at wavelengths away from the optimum (first negative order 2500A) the beam pencil defined by the near circular entrance baffle, through which incoming light first passes, is subsequently vignetted chordwise at the diffraction grating and (to a lesser extent) in a lune shape by the primary mirror. Thereby a non-linear spectral attenuation is provided restricting the zero order and suppressing other unwanted orders. Clearly the disadvantage is that the stop boundary away from the optimum wavelength is a composite of the baffle, the mirror, and the grating boundaries. The Fabry imaging in such circumstances can only be approximate, although the problem is mitigated by the very short focus essential for the Fabry lens to produce suitably sized images. There is no evading the fact that the image itself is of a variable (though reproducible) shape and

size as vignetting proceeds. The matter is further complicated by the fact that, if transfer optics or a large grating are not to be used, the slit, Fabry lens, photomultiplier and their mounts intrude well into the optical system, causing obstruction (again varying with angle) of the incoming and (more significantly) the convergent beam (Fig.2). The grating mount itself also causes a slowly moving obstruction of the entering beam.

Otherwise, the system satisfies our criteria in the following ways:-

- (a) It is compact while having the minimum number of reflections possible, for a dispersive system having as large a collecting area as is reasonable in a sideways viewing Skylark experiment. (A single concave grating, which would be simpler, would not be available with such an aperture, aperture ratio, and blaze, apart from the exorbitant cost of such a ruled area).
- (b) Because the dispersion scale is dependent on the grating-focus distance, the dispersion is of about 1000-1200A/degree of rotation or low enough to accomodate substantial precession rates. At 20° /sec. roll rate, a precession of 2° /sec. would only affect some 15% of stars.
- (c) The instrument can accomodate a field of up to 3° without major design or optical problems.

- (d) The vignetting, especially at the grating, of zero and unwanted orders eliminates the need for the inefficiencies and complexities of venetian-blind field restricting baffles, when a visual blind photocathode is also used.
- (e) The only in-flight operations needed are hatch ejection and E.H.T. switch on.

2. 4. Mechanical Design - Features and Problems.

The central mechanical problems are:-

- (1) To mount glass optical parts in such a way as to allow them to be adjusted in all necessary ways and yet be held firmly, without damage or distortion under vibration.
- and (2) To mount photomultipliers so as to avoid submitting them to excessive shock (to fracture them) or vibration (to change the internal electrical characteristics).

The first problem has been complicated by the desire to use the maximum size of primary mirror and the minimum of obstruction by the grating mount; hence from the initial designs these two components have been mounted without the use of a subsidiary optical cell having a separate adjustment. They have been held directly by three sets of three nylon tipped screws, acting on front, edge and back of the component, thereby retaining it directly within the surrounding cell structure and yet enabling adjustment as needed. In the case of the grating, which is square, adjustment about the normal is necessary to bring the rulings parallel to the roll axis. The principal edge screws are at the 'top' centre and 'bottom' ends for this purpose and additional lateral screws are tightened for restraint after final adjustment.

Equally, it was found essential to stop the circular primary from rotating by having flats ground on the edge at the points where the screws bear. For both components the single centrally placed screw was at the "top" from the boost acceleration point of view - the recent pair of successful spectrophotometers in fact flew with the 'base plate' uppermost i.e. inverted from fig. 3 .

Early faults with the mounting method arose from three causes:-

- (a) The nylon area was not large enough to stand the dynamic vibration loading and underwent cold flow, solved by using larger screws, eventually 3/8 in. diameter, for the rim of the primary.
- (b) Vibration-proof locking after final adjustment was a major problem. The commercial locking fluid Loctite, which only sets in a metal-metal interface, has a very unfortunate tendency to creep over surfaces and hence contaminate the optics; where it sets it causes particulate contamination and thread damage if subsequent adjustment is necessary. Screws with nylon inserts in the thread (Nylok) were found to take up a skew angle to the tapped thread, thereby not bearing properly on the optical component, and not allowing enough 'feel' for adjustment, i.e. the useful holding force was not responsible for

a sufficient proportion of the adjustment torque. Eventually, double locking nuts and washers were used throughout except for the lateral retaining screws of the mirror where, for geometric reasons, an orthogonal grub screw system or a more complex hexagonal keying lock were required and feasible.

- (c) The grating mount, in particular, which had been a simple 'H' type structure fabricated out of two simple $\frac{1}{4}$ inch thickness bars screwed to the square grating cell, suffered from a very large 'Q' amplification factor under lateral vibration. When redesigned more as a θ -type structure made out of a single piece of alloy, this problem was overcome; as already described (Sudbury 1969)(loc.cit.) the grating cell and mask assembly was eventually devised as a separate unit to enable mounting and storage to be apart from the main structure. Increases in section of material and in strength of mounting arrangements were also carried out on the mirror mount in course of development, though this had only two elements, the cast ring and a backplate.
- The photomultiplier mount had started with a similar 'H' philosophy, a block mounted

between two upright bars which were screwed to the sheet aluminium alloy top and bottom plates; the problem of this was compounded by the phenomenon, unknown to the Group at that time, of 'plate resonance' whereby very large 'Q's' occur at the centre of a vibrated plate fixed in its periphery. For the R-63 instruments (S05) the photomultiplier block was mounted on an inverted Y casting cantilevered forward from the base of the mirror casting (the centre of the baseplate being removed), but this was replaced in the current design by a bridge type of mounting (V) fixed near the periphery of the much stiffened (cast magnesium) baseplate. The photomultiplier block was adjustable on the mount by running in a shallow channel and held in place by screws passing through slotted holes.

The experience of the ROE-D experiment, where a photomultiplier was recovered with the envelope intact after free fall from a 170km apogee, showed that silicone rubber pre-cast rings were a fully satisfactory method of mounting detectors. The R.63 mounts had the photomultiplier mounted into a central cylindrical cavity, in a square block, with rectangular section rings, and restrained longitudinally with

L-section rings in end pieces; the high voltage lead termination at the rear was subsequently encapsulated. This technique ran the risk of placing an insufficiently definable longitudinal compression on the tube via the window; furthermore the proximity of the rubber to the window appeared to aggravate the problems of running the cathode at high potential for D.C. work. It was also awkward to remove the tube, which it was expected might be necessary with the less reliable E.M.I. tubes. In the R.65 design, therefore, a substantially longer block was divided diametrically (held together by eight screws) and the tube could then be placed in this after it had been adjusted in its notched rectangular section rubber rings. The adhesion of the encapsulation of the rear end of the tube was relied on to provide primary longitudinal restraint; a step in the mounting diameter at the point of attachment of the lens/slit holder assisted in limiting the forward excursion at resonance.

The whole initial mechanical construction was shown by full scale testing in 1965 to be insufficiently rigid laterally under vibration resonance; the addition of the box-shaped baffle casting improved the situation greatly but for R.63 the need to mount the quite massive power unit boxes then in use at the free end (top) of the instrument limited the possible

improvement. For R.65(2) the situation was further aided by the use of miniaturised E.H.T. units which could be mounted on the baffle plate, the mounting of the main electronics separately in the round, and the use of high damping magnesium alloy for the cast structures.

2. 4. 1. Contamination, Paints, and Scattered Light.

These are interrelated problems for an ultraviolet space instrument. The problem of contamination on optical surfaces is a major one in the ultraviolet, where organic materials are opaque and may even fluoresce, and where, simply because of the shorter wavelength, a much thinner layer of material is effective in stopping transmission or causing spurious interference effects. Such contamination may arise from vacuum oils backstreamed into the test chamber, from organic materials comprising part of the payload (plastics, silicone rubbers, paints) or from external contaminants (industrial 'haze', fuels and exhausts and human volatiles). The most severe problem arises from the so-called VCM (volatile condensate material) which are substances of relatively low vapour pressure but which can transfer, in a closed or vacuum environment, onto the optical surface, where they will

tend to remain indefinitely. Because of their relatively low vacuum pressure, it is difficult to remove these compounds from a substance by vacuum and heating over a reasonable period (Muraca 1965).

Very early in the programme, before the systematic work of Muraca had become available, I realised that black paint, in particular, might be a very dangerous source of such contaminants, on account of its essentially complex organic nature and the large area it presents to the optical surfaces when used to reduce stray light. at the time, black anodisation seemed to offer the most attractive alternative by producing a protective and adherent surface of intrinsically low reflectivity and one in which the pigment would be at least surfactantly bound. The difficulty of producing a really matt finish was partly overcome by sandblasting before anodisation and by 'ploughing' those surfaces which were within, and more or less parallel to, light paths with triangular grooves, to trap the highly reflected near-grazing incident light. (This is an extension of the traditional practice of threading the inside of optical tubes).

Several factors led to the abandonment of this process for the final pair of instruments. Principal among these were:-

- (1) The lack of control over a relatively complex process; this led to such problems as loss of dimensions, and, in one case detected by chance, the application of lanolin by a contractor in order to produce a more matt surface.
- (2) Information that the black azo-dyes used in the process were a major outgassing source (though not necessarily a contaminant).
- (3) The tendency of anodised surfaces to absorb contaminants.
- (4) The availability of epoxy matt black paints of high adhesion and good stability, which would withstand prolonged baking to reduce the residual contaminant level.

At the present time, the existence of 3M401 'Nextel' black paint and an established post cure cycle for it, confirmed by the success of the OAO, means that this problem has a satisfactory solution.

Much has been studied and written about backstreaming from oil vacuum pumps during the period of this project (Fischer 1965). In particular, it is now apparent that 'optically tight' baffling, preferably with liquid nitrogen cooling, is necessary if backstreaming in diffusion pumps is to be trapped, while the problem of backstreaming from rotary pumps at

pressures less than 0.1 torr has been highlighted and prevented (Baker & Laurenson 1966). It is quite possible that such contamination may have contributed to or caused the failure of the instrument in the S05/2 payload, and for the subsequent instruments a baffle array was fitted to the pump system as well as taking rotary pump pressure precautions. This problem also is thoroughly covered by the use of ion pumps and foreline traps.

Controls have also been introduced on the use of loctite thread locking fluid, with its elimination wherever possible, on the silicone rubber usage, and on handling (with nylon gloves only).

2. 5. Electronic Design Problems.

2. 5. 1. D.C. Measurement Techniques.

Traditionally, light detection with a photomultiplier has been made quantitative by measuring the anode (direct) current. A number of the disadvantages of that method, realised or reinforced in the course of our work, have been well summarised by Beattie and Paterson (1970). Three which are more specific to the present project and deserve expansion are:-

- (a) the relatively high signal frequency response demanded by the instrument,
- (b) for current measurement, practical systems require the anode output near earth potential and so the photocathode at high voltage.
- (c) the need, common to space astrophysics, for a wide, automatic, measuring system range.

2. 5. 1. 1. Frequency Response .

The design criteria of Section 2.1 have led to a low dispersion, $\sim 1000^{\circ}/\text{deg}$, and a substantial roll rate, $15\text{--}30^{\circ}/\text{sec}$. Such conditions imply that, to utilise the practicable spectral resolution ($100\text{--}200\text{\AA}$), a system response up to 500Hz is needed. Generating amplifier outputs exceeding one volt, without input noise

predominating, from 10^{-8} amp~~s~~anode photocurrent, requires electrometer resistors of the order of 100megohms. Clearly to achieve full frequency response at this current requires stray input capacitances do not exceed a few pfd which is very difficult within the limitations of a sounding rocket experiment. Although, given suitable connectors as are now available, the floating inner screen technique could reduce lead capacitance, there would still be the tube and amplifier stray capacitances. Therefore a rolloff characteristic which in practice starts at about 100HZ at the rate of 3db/octave for a 120M Ω input resistor, is intrinsic to the main electrometer amplifier; on the 1967 flight some compensation was obtained by shunting the feedback loop with a small capacitor and hence increasing the gain above 100HZ. This technique could only give improvement to about 200HZ before 'ringing' set in. For the R-65(2) flight, since two telemetry channels were available, and in view of the ready availability of encapsulated transistorised operational amplifiers by this time, the output of the main electrometer was processed to give high-frequency gain compensation to 500HZ and a DC gain of two. This was passed to the high frequency response telemetry channel, the remaining one having only a response to 160HZ and therefore only usable for the direct output as

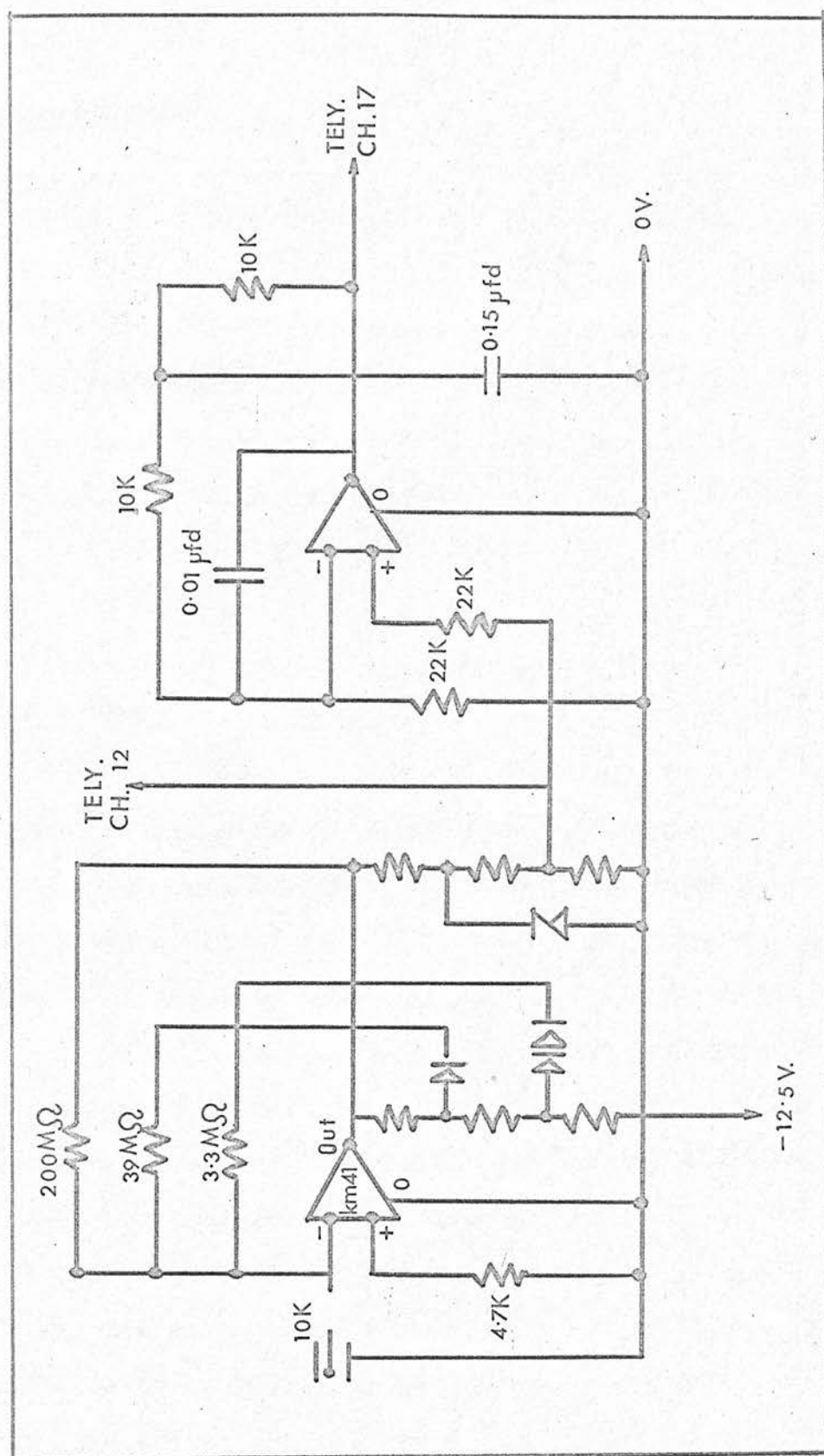


FIG.5. CIRCUITS OF DC AMPLIFIER SYSTEM R65(2)

redundant information in case of in-flight problems. The wide frequency band, in addition to passing more intrinsic noise, was also more susceptible to interference and, for R.63, inverter interference at 1kHz had been the main limitation. Higher frequency inverters and improved line filtering techniques (demanded by the pulse counting channels) made this source of noise negligible on the R65(2) DC channel.

2. 5. 1. 2. Cathode High Potential Problems.

When the cathode is run at high (negative) potential with respect to earth, spurious discharges arise at the window giving rise to pulse outputs which at the anode may exceed 10^{-8} coulombs. The source of these discharges is not, apparently, fully known but the effect is almost certainly some form of non-destructive breakdown in the window due to the proximity of earth potentials. The magnitude of this interference, observed with sapphire-windowed caesium telluride cathode Ascop tubes, rises rapidly with voltage overall between 2 and 3kv (voltages of this amount being necessary to obtain gains of $10^6 - 10^7$ with such tubes) and may reach several per second of 10^{-8} amps peak. One such tube where the effect had increased to a severe point during a year's storage in

the instrument, was greatly improved by cleaning the tube window with acetone and outgassing and cleaning the silicone rubber ring which, at that time, bore on the window. Presumably this improved the insulation path externally. As the record (Fig. 9) shows, the use of a tube selected for sufficient gain at a lower voltage, and the elimination of the ring near the window made the effect relatively unimportant for the Ascop flown in R 65(2). Clearly, had more gain been usable, the frequency response problem of 2.5.1.1. would have been much alleviated by the reduction in input resistor value.

2. 5. 1. 3. Wide Measuring Range

The astronomer's choice of a logarithmic magnitude scale is indicative of the large dynamic range required to study stars. For our instrument, to achieve the justifiable 10% measurement accuracy on early type stars of magnitude 3.5 while avoiding saturation on zero magnitude stars, a useful dynamic range of 250:1 is required. Since the combined limitations of telemetry and calibration accuracy are in the region of 25-50 mV a range of between 4:1 and 8:1 is all that can be achieved with a single linear amplifier having 2V full scale output. Given telemetry capacity, the successive

outputs of cascaded amplifiers (or an attenuated string from a single amplifier) would raise this to the n th power where n is the number of channels available. This solution was first reported by Stecher & Milligan (ibid 1962) and J.W. Campbell has adopted it using commutation of wide-band IRIG channels; his two output channels could give 64:1 if optimised. Another solution is the logarithmic amplifier; this has some peculiar disadvantages:-

- (a) Since a really accurate and stable logarithmic characteristic is hard to achieve, accurate calibration is difficult;
- (b) Analogy with the familiar "square law" detector shows that the dynamic response differs from the DC response (Chater 1969) making (a) more difficult; this is particularly significant in low-light-level detection where fluctuation noise is large (Pao et al 1966);
- (c) A small DC offset (due to drift in the amplifier or telemetry) has a relatively large effect on the calibration of the high level signals.

With such an amplifier at the limit of 25 mV total resolution (including drifts) on a 2V scale we could achieve 40:1 dynamic range, which is still really insufficient for our purposes. The compromise which was adopted for the spectrophotometer DC channels was that described by Fastie (1963), of using a multiple

feedback loop configuration with the diode isolation of the lower value, shunting resistors, breaking down as the output voltage rises and the diodes conduct. This gives a "multilinear" sensitivity characteristic of straight lines joined by logarithmic "knees" which can be made relatively sharp with an amplifier having a substantial output voltage swing and two or more diodes in series. Such characteristics are shown in Fig. 6 a & b, which gives the characteristics of the electrometer amplifiers on the S27-1 flight of 1968.

A more subtle disadvantage of such non-linear amplifiers is akin to the offset problem and arose when considering the lack of data on the 1967 S05-2 flight (although it was not responsible for the problem). In the presence of a substantial, though well established, background level, the sensitivity to faint signals is drastically reduced - e.g. measurement at the 10^{-9} amp level becomes impossible for a 10% optimised scale in the 10^{-8} - 10^{-7} amp range, even though the photon fluctuation noise may allow measurement at such a level. Clearly what one needs is a kind of self-setting and self-recording offset to "back-off" the major part of the output. Such a system is conceptually possible in DC systems but is obviously much more straight-forward in pulse counting systems where the information is already in digital form; in essence the problem becomes similar

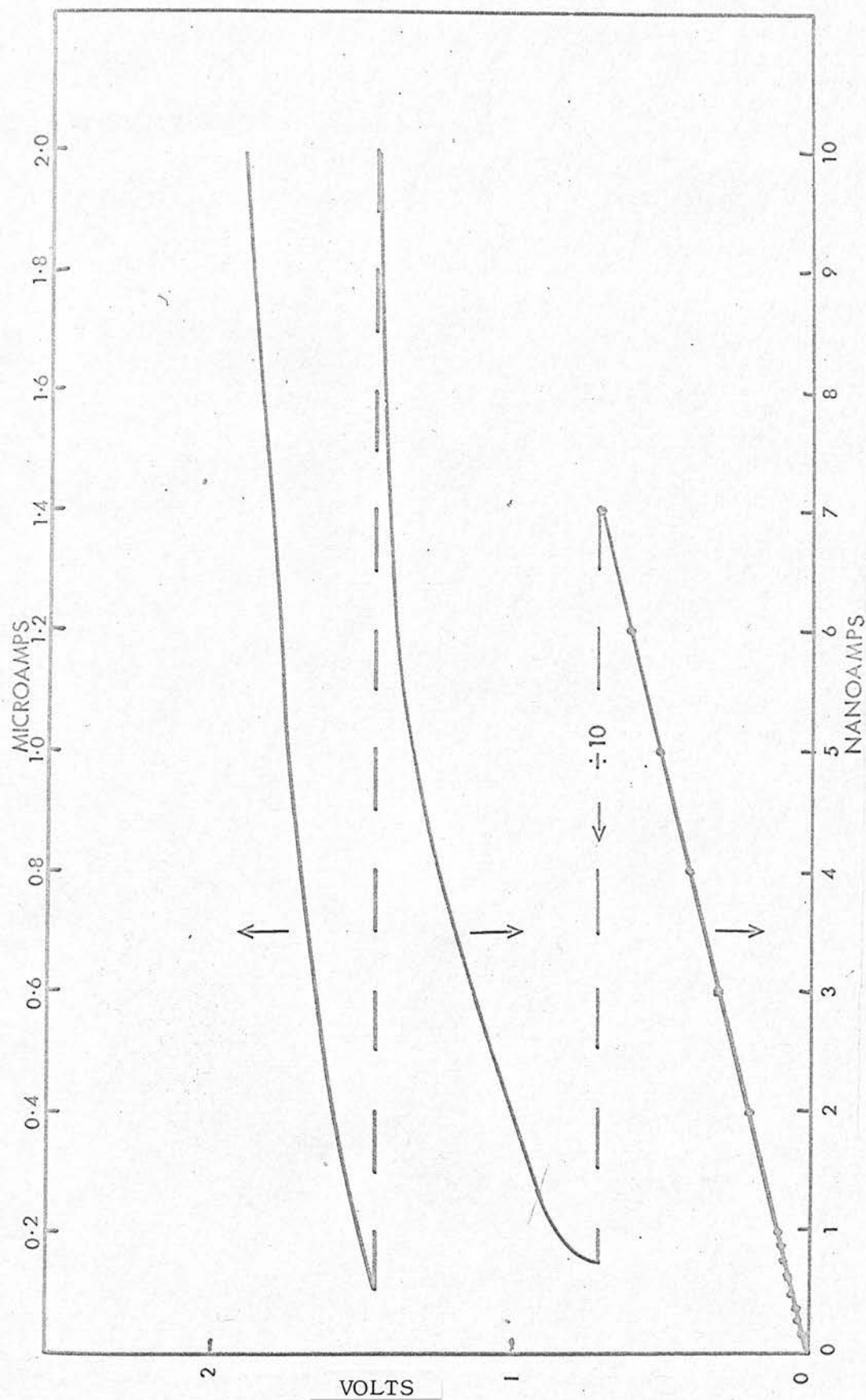


FIG 6a DC CHARACTERISTICS OF ELECTROMETER AMPLIFIER OUTPUT

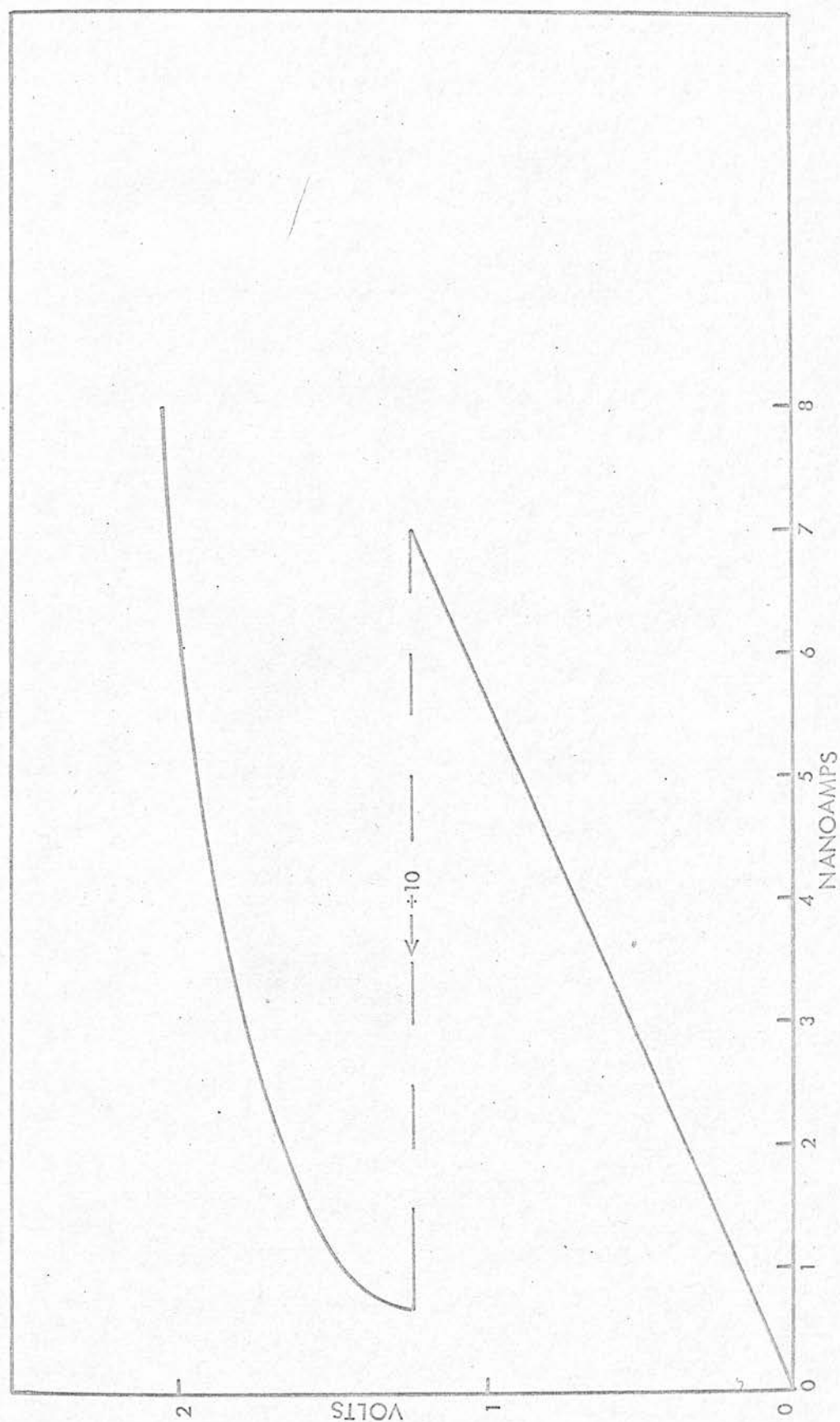


FIG 6b DC CHARACTERISTICS OF FREQUENCY COMPENSATED OUTPUT (CH. 17)

to the standard satellite one of operating in floating point format and accepting the most significant bit (in binary code) as automatically being present.

2. 5. 2. Counting Systems

Fulfilling the counting system requirement just mentioned was completely within the experience and competence of C.H. Paterson, who had joined the Division in 1967. The problem was defined by me as being one of devising a system which would

- (a) Operate on two IRIG analogue telemetry channels, one for the "range" or "exponent" part and one for the fine reading or mantissa.
- (b) Provide sampling rates of about 500/sec without substantial "dead-time" loss.
- (c) Count at rates up to 10^6 /sec and display down to 2×10^{-3} /sec.
- (d) Provide a display accuracy that would not substantially degrade the intrinsic accuracy limit due to photon fluctuations, over most of the range, i.e. the display "steps" should be substantially less than \sqrt{N} where N is the actual count reading.
- (e) Cost less than £150 (1967) for components.

The pulse counting and encoding system which was devised to meet these requirements (Beattie & Patterson 1970) is so successful that it can be regarded as having solved that part of the problem; perhaps the only remaining developments needed are a method of synchronisation in order that the data may be digitised directly on to computer tape, and the possible future adaptation to P C M telemetry. The merits of the system for the solution of the problems peculiar to this application are supplementary to the demonstrated superiority of pulse counting as a low-light-level measuring technique (Alfano & Ockman 1968; Young 1968).

However, there were some systems problems associated with the use of pulse counting and it is appropriate to mention these in general terms now.

2. 5. 2. 1. Noise

With P.M. tube gains of order 10^7 , the pulses at the anode are only around ten millivolts and impulsive noise at this level is readily generated within a rocket payload. The most severe source is the E.H.T. inverter; in particular, although pulse counting enables the photocathode to be placed at the desirable earth potential, this has the effect of making the full E.H.T. ripple voltage appear at

the tube output. The principle component of this ripple from a well stabilised E.H.T. inverter is a sequence of spikes of microsecond width at the inverter frequency which is therefore duly counted as such by the pulse counting system. Shunting capacitors of 0.1 microfarads with a series resistor of less than one megohm were found to be enough to reduce the output ripple itself; however, the dominant source of noise then became the "reflected" noise from the impulsive input current to this, and other, inverters, picked up on power lines. L.C. filters adjacent to their inputs were necessary. In the integrated payload, interference was also received from the electrically driven calibration timer and the rate gyro of the roll-control unit, although the latter was self-contained for power. A series stabiliser and filtering on all lines entering that payload section was found to be necessary for the roll control unit.

2. 5. 2. 2. Count Rate Limitations

Although, with this instrument, count rates greater than 3×10^5 are only exceeded for two or three stars in a flight, count rates of 10^6 are easily reached when calibrating with a mercury low-pressure lamp if the problem of attenuating the lamp is going to be avoided. Such count rates raise a

number of practical problems, two of which are particularly pertinent to pulse-counting. Firstly, the anode pulses which are some 100ns wide start to overlap in a significant number of cases, a condition known as a "pile-up of pulses". Such piled up pulses either overlap and fail to trigger the pulse-shaping device a sufficient number of times or, in an extreme case, raise the zero-base-line and are discriminated out as "noise". Secondly, unless a rather low impedance dynode resistor chain is used (or capacitors shunted between the later dynodes) pulse gain can vary due to substantial instantaneous currents being drawn at the late dynodes.

There are, in addition, the normal hazards of cathode fatigue or late dynode heating. Cathode fatigue is more severe with the semi-conducting telluride cathodes than the simple bi-alkali ones.

2. 5. 2. 3. Discriminator Setting

This is rather an arbitrary process especially when, as in this instance, the commercial pulse-height analyser (Baird-Atomic) was found to be unreliable due to its unpredictable saturation characteristics at relatively low count levels, far below its specified rating. In practice the E.M.I. D 104 tube selected was found to exhibit quite a distinct "plateau" in the counting rate as the

discriminator level was adjusted, provided a sufficiently high overall potential ($\sim 1800\text{V}$) was applied. Because external rather than tube noise was a major source of concern, it was necessary to set the discriminator towards the higher voltage side of this plateau but under these conditions over 90% of pulses were counted and 50 volt variations in E.H.T. (far greater than the expected drift) produced only a few per cent change in the count. This relative insensitivity to E.H.T. variation is, of course, one of the well known merits pulse-counting has versus D.C. measurement.

2. 5. 3. Photomultiplier Selection

Certain photomultiplier tube characteristics are particularly suited to this application; however, obtaining such characteristics is not straightforward. Investigation of the market, and experience, showed that there were only two suitable sources of one-inch diameter CsTe photocathode P.M.'s, the Electro-mechanical Research (Ascop) 541F-05 series and the E.M.I. Electronics D 104 development tube. The former tube has become increasingly expensive (in sterling terms) over the years (see Appendix 2). However, it is fully ruggedised, has an encapsulated dynode chain system, and generally good properties. The requested selection criteria for this included gain $>10^6$ at 2000V (to avoid voltages at which the

the "photocathode high" pulses become too disturbing while attaining reasonable outputs, with D.C. operation), quantum efficiency $>5\%$ (since quantum noise is limiting in this work) and long-wavelength rejection, to keep down stray light from later type stars. The specification for the rejection was a ratio of 100:1 between the 2537A and 3650A sensitivities. It is particularly necessary to specify all these criteria at the same time, since excess photocathode caesi-ation, which improves the gain and quantum efficiency, reduces the long-wavelength rejection.

The E.M.I. D 104 tubes are semi-rugged and have an internal dynode resistor system (within the envelope) to avoid external corona problems and because of the difficulty of supplying sufficient pins on a one-inch base for a 13-stage tube. They were supplied at very favourable rates on a customer selection accept-or-return basis and, at the time of selection (1968), E.M.I. were experiencing substantial problems with outgassing of the internal resistors. As a result a number of the tubes were sooner or later rejected owing to internal breakdown. On this, and other, criteria, out of some ten tubes screened three finally gave satisfaction. The selected tube for flight had a gain exceeding 10^6 at 1800V overall, quantum efficiency 6-7%, and a relative long-wave length



rejection comparable with the Ascop criteria;
the pulse discrimination qualities have already
been mentioned.

For all tubes the photocathode and first dynode
were not internally linked but the "link point"
brought out on leads so that the photodiode DC quantum
efficiency (which may in fact differ from the pulse-
counting efficiency) could be measured.

III CALIBRATION, INTEGRATION, CHECKOUT AND FLIGHT
PERFORMANCE.

3. 1. Calibration.

3. 1. 1. The Need for Calibration.

The calibration of flight instruments for ultra-violet stellar observations, especially in absolute terms, has increasingly come to be realised as a major problem in the field. In Europe, for example, at the time of writing an extensive effort is being made in connection with the S2/68 instrument for the TD1 satellite; in spite of an expenditure on this problem much greater than the total cost of the instruments so far flown in the R.O.E. spectrophotometry programme, the final knowledge of the sensitivity of the S2/68 telescope is not expected to be substantially better, in absolute terms, than about 30%. Equally, it now seems probable that the early data of Stecher and Milligan relating to flux deficiencies below 2400Å arose primarily from a change of spectral sensitivity of the instrument between calibration and flight. The situation differs fundamentally from the existing in ground-based optical astronomy where virtually all measurements are made on a relative scale and until the late

nineteen fifties the absolute fluxes corresponding to the zero-point of the traditional astronomical photometric measures were poorly known (Code 1960, Willstrop 1958,1960, Kharitonov 1963). The necessity for such calibration, both in ground based and space astronomy, has the following principal origins:-

- (1) The ability, developed during the nineteen fifties, of theoreticians to compute more or less meaningful models of stellar atmospheres and the spectral distribution of their resultant flux.
- (2) The need to have a systematic basis on which to place the "colour indices" arising from space ultraviolet and visible fluxes, compounded by:-
- (3) The necessarily random sky coverage of observations prior to the availability of pointing rockets and satellites, and
- (4) The fact that equipment is normally lost after each set of observations.

The third of these factors has, fortunately for the present data, become increasingly unimportant for spectral work as the number of published photometric observations has increased, making it possible to find data on a significant number of the brighter stars in any reasonably random sample of thirty or

forty bright Northern Hemisphere accessible stars.

A further minor impetus to absolute calibration has come from the need to intercompare results in other parts of the electromagnetic spectrum and also to derive integrated fluxes; however, the state of the art is such that 30-50% accuracy should readily suffice for these purposes.

Naturally, if spectral observations can be made from space over a wide enough range to overlap with ground calibrations, a good relative calibration suffices. However, in the absence of sophisticated calibration apparatus, the problem does not differ greatly in the sources of errors which are most important. In the case of the R63/R65(2) instrument, the throughput is quite low around 3000\AA (mainly due to the high rejection of the telluride photocathode for longer wavelength light) and the "overlap" method is of limited scope. Some investigation of ground based measurements shortwards of the Balmer jump has been carried out and is discussed in Section 5.2.

3. 1. 2. Absolute and Relative References

The traditional primary reference for optical purposes is the black body at the melting point of platinum. This is clearly somewhat restricted in its practical application and is mainly of value in the visible and near infra-red region. By its means, however, secondary detector (thermopile) and source (ribbon lamp) standards can be calibrated and used as transfer systems (Bless et al 1968). Thermopiles present problems with sensitivity, limited area, spectral blackness, uniformity, and dependence on thermal conditions. Ribbon lamps require prior knowledge of the emissivity of the tungsten (which may be a function of the metallic grain structure) (Schurer 1968), need a window, and have poor and steeply falling output shortwards of 3000Å.

Four other kinds of local or transfer standard are available in the ultraviolet:-

- (1) The narrow bore low pressure mercury lamp (Childs 1962) which gives out most (90%) of its energy monochromatically in the narrow 2537Å resonance line and with a flux which is relatively independent of current over the range 10-15mA. Another particular advantage of this lamp is that

its power output is quite small, about $\frac{1}{4}$ watt, and the source narrow ($\sim 1\text{mm}$) which makes it possible to calibrate sensitive instruments by the "distant light" method.

- (2) The high pressure mercury lamp (Kreff et al 1937) is a bright (250W) wide bore one giving all the listed mercury lines at considerable strength although the 2537A line is very broad and self-absorbed. Both the ratio of the line fluxes and their absolute values (under the stable running conditions) have been given by various workers (Dejadin et al 1965). However, because of the brilliance of the lamp it is not possible to use it directly as an absolute standard for photoelectric measurements. With a suitable non-spectrally-selective detector it is possible to measure spectrograph transmissions from the line ratios but a standard source is still needed to turn such knowledge into absolute values.
- (3) Fluorescent detectors, especially sodium salicylate. This latter has in fact been the best studied of these detectors, perhaps because it is the easiest to obtain and

apply (Samson 1967). It has a more or less constant conversion efficiency between some 500A and 3000A, giving an output around 4500A. Problems with its use include the possibility of spectrally non-uniform quantum efficiency under certain conditions, especially when "aged", and the need to use a broad band visible sensitive detector with it, the sensitivity of the system to visible light therefore usually being substantially more than to ultraviolet. Nevertheless, it is widely used and is probably in itself accurate to 10-20% when carefully applied to a substantial thickness ($> 1 \text{ mg cm}^{-2}$). We have used the "spray gun" application method as being the most reproducible.

- (4) The parallel plate ion chamber using nitric oxide has been shown (Samson 1964) to be a very reliable laboratory standard in the 1100-1200A region, where the theoretically derived quantum efficiency of 78% can be realised. This device has not been available to Edinburgh where we have in any case only recently developed sources

with reliable output at these wavelengths. The use of such a detector is mainly in checking the absolute efficiency of other transfer standard detectors (thermopiles, salicylate).

Other methods (branching ratio, synchrotron radiation, cascade arc) do exist for absolute and relative intensity sources, but are more esoteric in the facilities and techniques they require. The first two are particularly applicable to the extreme ultraviolet (below 1000Å).

3. 2. The Calibration of the Spectrophotometer

Our problem, then, became one of applying the foregoing source/detector methods to the objective dispersion spectrophotometer. It cannot be said to have been satisfactorily solved, for a variety of unconnected reasons and the ensuing description is included to give a background to this lack of high confidence. At the time of writing a vastly more extensive and costly effort than the author could have undertaken has been mounted to ensure that the S2/68 telescope is calibrated to the standard which would have been desirable for his instrument; the current undertaking has used much of the experience, albeit often negative, acquired in the programme described below.

The calibration procedure comprised two parts, that carried out in a vacuum chamber and that done in air over a long path.

For the vacuum system, the Wadsworth-principle monochromator, the collimator and the turntable, were of the author's own devising and design. (The principle used in the monochromator has since been described independently by Schroeder (1966)). However, the combination of the monochromator and the light source has been identified as one major cause of inaccuracy in the calibration owing to the non-

uniformity of the resultant collimated beam. The ingeniously simple idea used by Stecher of having a rough ground lithium fluoride disc as a diffuser at the light source window to improve its angular distribution would not have been sufficient in this application because the tripartite blazed grating, used at $f:5$ gave a very considerable "target pattern" (i.e. variation in efficiency over the diffracting surface), and one that appeared to vary from wavelength to wavelength. Although this problem had been identified by the time of the 1968 calibration, and has led to the design and construction of an elaborate "X-Y" beam mapping device for the new R.O.E. satellite calibration facility, the use of such a system was not, after careful consideration, felt to be justified for the 1968 calibration on the following grounds:-

- (a) The extensive mechanical and electrical work needed to make such a device function reliably and accurately in vacuum. About one man-year has been consumed in the construction of the device for the new facility.
- (b) The time needed to carry out the mapping at some 200 points and perhaps 30 wavelengths, which time would not, without the use of fully automatic recording devices, have been available in the preparation timetable.

- (c) The experience with the DC discharge sources had indicated that the working lifetime before electrode contamination and window deterioration (Warneck 1965) necessitated renovation was only a few hours; apart from the extra time consumed by such renovation, it may well have altered the optical uniformity. The microwave sources, which have a much better life and stability, had not been sufficiently developed at that time within the Division.
- (d) There are problems peculiar to the use of a highly non-uniform beam with this particular optical design of instrument which have been, in part, discussed earlier (Section 2.3). Since the grating blaze efficiency, optical resolution, and obstruction are a function both of wavelength and position in the entrance aperture, this function would require to be known on a relative basis before any values for absolute calibration could be deduced from the collimated beam, i.e. it really needs an "X-Y" scan of the instrument at all useful wavelengths with a collimated "pencil" beam. This is clearly an undertaking of magnitude comparable with, perhaps greater than, the collimator beam scanning although there are, in principle, ways which one could devise of

combining the two operations.

It is the author's view, therefore, that the laboratory calibrations which were carried out on the instruments flown were of value only in giving a general assurance of the operation of the instruments over the full range of wavelengths, in the sense that a major loss or lack of sensitivity could have been detected.

The distant light calibrations are limited in value for somewhat different reasons. The problem of the steep fall in output and variable emissivity of tungsten have been mentioned (Section 3.1.2). There are other practical problems, such as the ageing of the lamp and the dependence exacerbated by working on the extreme short-wave part of the spectral distribution curve, on the ribbon temperature and hence on the local temperature and (more easily) the current. Ideally the current should be monitored by digital voltmeter across a standard resistor but it has not so far been possible to arrange this; a sub-standard pointer meter has been used which has reading and calibration errors each of about $\pm 0.2\%$. The total output of the ribbon approximately follows the (current) ^{$8/3$} and the emitted flux per unit wavelength at this part of the Planck distribution increases by some $1\% / ^\circ\text{K}$ for temperatures around 2500°K . Hence $\pm 0.3\%$ error in the current alone leads to about 5% error in flux output.

Additional error in the distant standard source techniques can arise from contamination of the fused silica window and, in the case of the low pressure mercury lamp, absorption from locally generated ozone. Oke and Schild (1970), calibrating at wavelengths $>3000\text{\AA}$, have found that absorption over the total path can be substantial and vary considerably, although Oke has indicated (private verbal communication) that local industrial pollution was the cause (see also Hayes (1970)). This is most unlikely to have been present at the Sardinia range. Uncorrected contamination and absorption both lead to an underestimation of the sensitivity of the instrument and comparison of the results of the author's own ground calibration with the calibration against Stecher's β Tauri published data suggests that this has in fact happened (Fig. 7). An extensive discussion of the many other sources of error fundamental, systematic, and random which can affect ribbon lamp calibration has been given by Bless et al (1968). Undoubtedly the careful use of improved incandescent sources (e.g. Quinn & Barber (1967)) will improve the situation.

In the vacuum calibration the pulse counting channel, which provided the best in-flight data, suffered from an additional unexpected trouble; both the E.H.T. of the D.C. discharge (the supply was that used for the cleaning

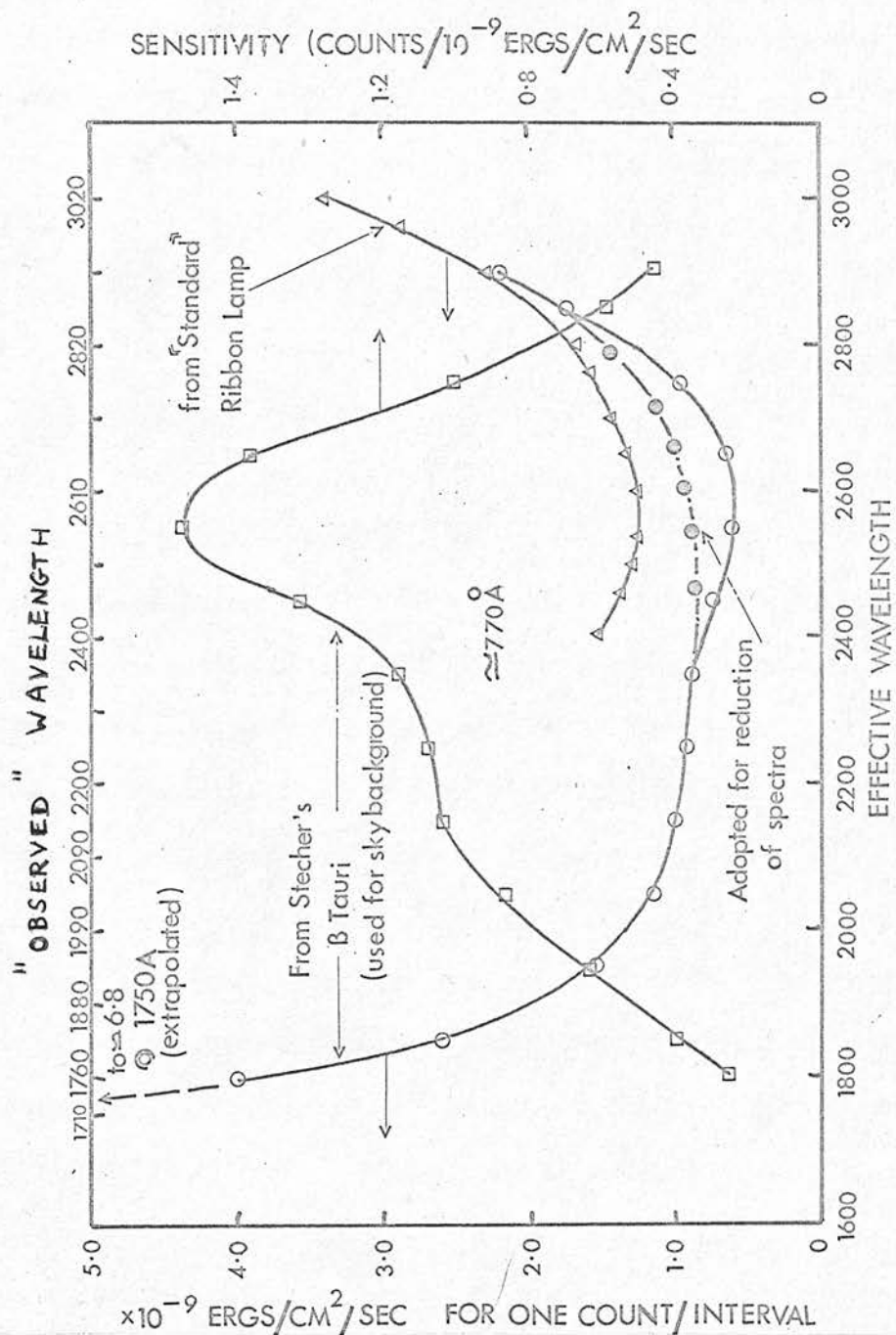


FIG.7 CALIBRATION AND RESPONSE CURVES OF PULSE COUNTING R65(2) SPECTROPHOTOMETER.

discharge of the 36-inch coating plant) and the output of the microwave unit (a medical one) suffered from severe mains ripple which had not affected earlier calibration due to the very limited frequency response of the D.C. laboratory electrometers used. The range changing facility of the pulse counting instrument made the ripple particularly troublesome as it was impossible to read meaningful "average" values of the analogue output on low frequency response meters. Some measurements were made, on an ultraviolet recorder, but in the circumstances of the calibration problems earlier outlined and since some "comparison stars" have been observed, it has not been thought worthwhile to undertake the very substantial labour of reducing them by hand.

It was possible, and indeed is desirable, to run the low pressure mercury lamp, used for range calibrations, from a stable D.C. supply, a relatively small (10-15 mA) current being required. Under these conditions the lamp discharge was struck by an R.F. Tesla coil probe (Edwards leak tester).

3.2.1. Calibration Data.

Fig. 8 shows the actual count rates measured when calibrating the R65(2) pulse counting instrument with a distant ribbon lamp, both before despatch from Edinburgh and at the launching range a week before flight. Due to practical limitations, the source-instrument distances were quite different; the change in size of the defocussed image alters the spectral resolution profile, the two calculated profiles also being shown in Fig. 8. The rapid change in lamp spectral output over such a bandpass required the flux input to be computed by convoluting the output curve with the calculated profile (programme WMESCAN). Some of the disparity of up to 20% between the two count rate curves, after allowing for the inverse square law, is due to the profile change, together with the error sources just discussed and the small real changes which no doubt occurred. Because of the higher count rate, the shorter distance Edinburgh measurements appear more reliable in the interesting 2500-2800⁰Å region, and have been used in the curve of Fig. 7.

As the earlier discussion has indicated, the nature and extent of the sources of systematic error

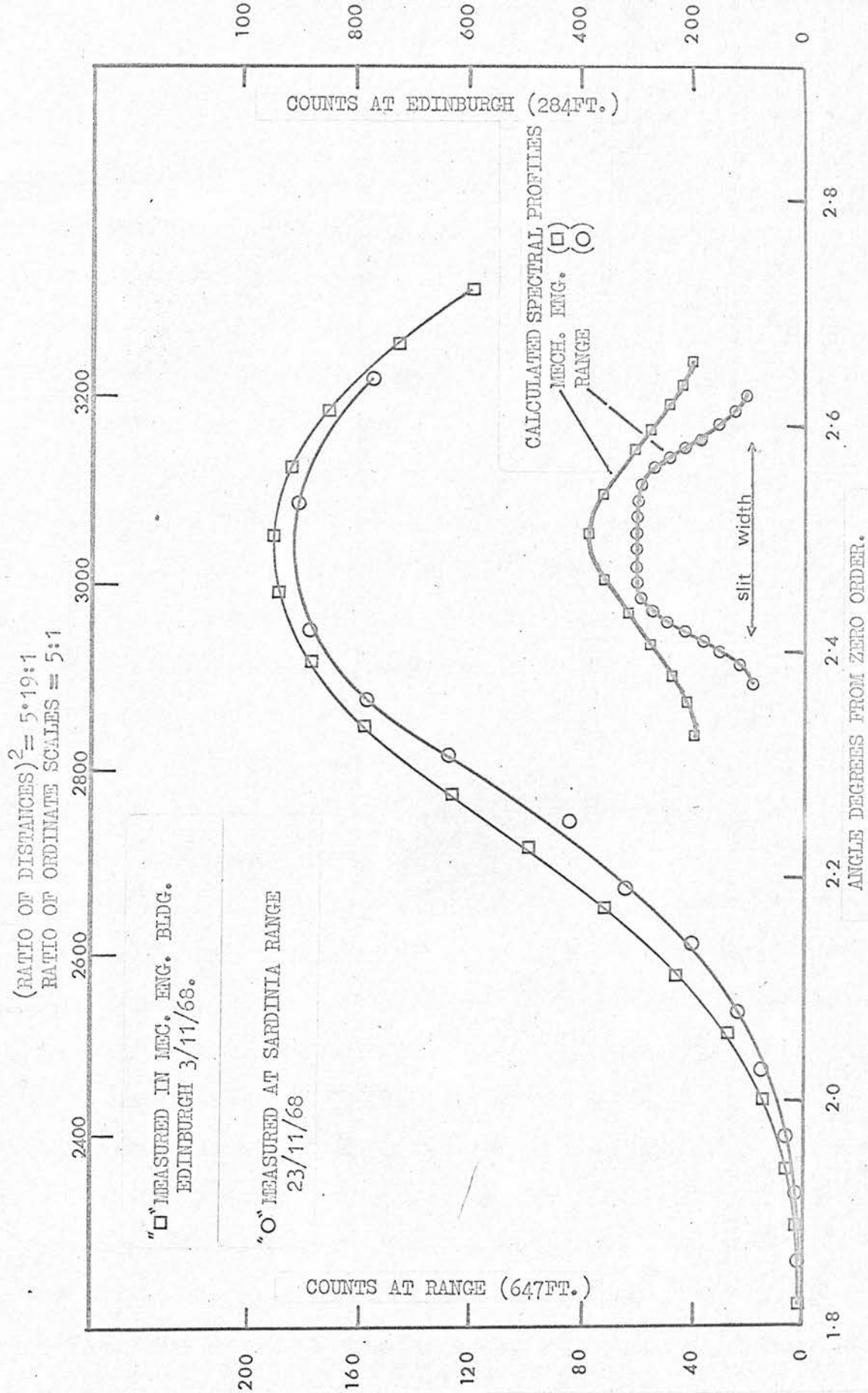


FIG 8 OUTPUT OF PULSE COUNTING SPECTRO PHOTOMETER WHEN CALIBRATED WITH RIBBON LAMP.

in the calibration is such as to make it difficult to assess the total error which may exist. Comparison of my pre-flight ribbon lamp calibration and the calibration through Stecher's and my β Tauri measurement (also shown in Fig. 7) shows a discrepancy of about 10% around 2800A, where the sources of systematic error are likely to be least, while the departure appears to be up to a factor of two near the useful limit of the ribbon lamp measurements (2400-2500A). Within the limitations of uncertainty of the low-pressure mercury lamp readings the departure is similar and again in the expected direction. i.e. the sensitivity of the instrument appears underestimated. A further discussion of the error situation is connected with the discussion of the reduction in section 4. 4. but the basis for the reduction has been the calibration based on the Stecher β Tauri data comparison, since he has stated his relative calibration to be accurate to "a few per cent". but modified by the ribbon lamp curve. In so far as the data can be of use in differential reddening and spectral typing investigations the actual calibration used is of no importance provided it bears some relation to reality. However Section 4. 4. shows that the calibration reference used is far from being the only substantial source of error.

3. 3. Payload Integration and Test

The pattern of payload integration and test was broadly similar for the three rounds, the operations which take place at the payload authority (i.e. ESTEC) or their contractors being briefly as follows:-

- (a) A preliminary integration involving a prototype instrument in which major mechanical and electrical/electronic incompatibilities are identified and solved.
- (b) A prototype vibration test, involving realistic components where these are novel or open to doubt, and mass dummies otherwise. This enables weak points to be identified as well as ascertaining the general payload behaviour and resonance values. It is carried out at 1.5 or 2 times the "flight acceptance" level and is intended thereby to contain 99% of the actual in-flight vibration envelope area. It is carried out in both sine and random modes.
- (c) Flight payload integration, when acceptance flight simulation runs are made, all troublesome interference being eliminated.
- (d) Flight acceptance vibration, which takes place with the payload in flight condition and telemetry running.

- (e) Range (preparation hall) integration, where final checks, calibrations and flight simulation runs are made, including transmissions for record at the range telemetry station.
- (f) Pre-launch checkout in the launcher, which is a more limited version of (e), and includes the use of the launcher land lines.

In 1965 and 1966 the laboratory calibration was carried out between stages (d) and (e), i.e. directly before despatch to the range, but improved confidence and the general shortening of the flight integration and check-out procedures with experience has led to it being done before (c), with final "distant light" checks being repeated at the range before (e).

3.4. Flight Performance

As has been indicated earlier and elsewhere, the flight of R63 in payload S05/1 in August 1965 did yield stellar signals which can now be clearly identified as zero order and spectral scans of good strength and signal quality. However, two on-board faults in the payload systems for which ESRO was responsible (partial loss of telemetry due to weak signal following corona breakdown of the transmitter and a faulty lunar aspect sensor amplifier), allied with the "flat spin" rocket motion which is peculiarly difficult to reconstruct, meant that, in spite of effort spanning over a year by P. Becker at ESOC, no sensible solution to the attitude problem was obtained. Since, with hindsight, the few observations would probably have been very difficult to identify with stars, and wavelength calibrate, the scientific loss is not very substantial though, at the time, most unfortunate.

The lack of scientifically useful data from the otherwise successful S05/2 flight of May 1967 is more difficult to explain. This instrument was, of course, basically that which had served during the abortive 1965 and 1966 preparations of this payload. The mechanical construction, which was less robust than the later R65(2) design, had begun to suffer from corrosion and general wear and tear due to the handling

and to readjustment of sealant locked threads. The mirror, Kanigenon-aluminium, which had been supplied at favourable rates and short notice by Grubb Parsons, was the only one used which was not plate glass; it had also deteriorated, from the initial poorer finish characteristic of this material, due to stripping and recoating after the delay. The diffraction grating and lithium fluoride lens were also over two years old; calcium fluoride, which is more resistant to atmospheric attack, has been used for subsequent Fabry lenses. However, a simple loss of optical transmission of the instrument is not adequate explanation in view of the high background light level and the strong horizon crossing signals. The quite exceptionally strong aurora which occurred that night was observed by the accompanying photometer instrument as a brightening on the N.W. horizon, but even if this accounted for the background, it remains to account for the low signal levels. The poor amplifier frequency response was a first idea; playback with a "frequency compensating" amplifier failed to improve the signal/noise significantly. Therefore, the most likely explanation, now, would seem to have been a deterioration of optical quality, due to movement of an optical element or, as mentioned earlier, heating of the replica grating plastic due to kinetic air ingress through the hatch. Modifications were made in the latter shortly before

the S27/1 flight to avoid such ingress. One other plausible notion, already mentioned, is that a fluorescing contaminant (e.g. grease or oil) on the optical surfaces would cause a general "glow" while spoiling specular reflection; certainly there was also a loss of efficiency of the accompanying "spare" instrument.

By contrast, the most remarkable feature of the S27/1 flight, especially in respect of the pulse-counting channel, was the very low and stable background counts in favourable parts of the sky, falling to the "zero" level (< 1000 counts/sec) on occasion. In fact the background light distribution has now been fully analysed and certain deductions drawn (Sudbury and Ingham, 1970, loc. cit., and Section 5).

Every check which has been made (e.g. fluctuation noise, count distribution, continuity over the dynamic range) has indicated that the pulse counting instrument functioned efficiently and perfectly in this flight. The D.C. channel also gave good signals, the usual "cathode high potential" noise spikes not being present in troublesome quantity or amplitude, although the signal:noise is clearly inferior to that of the counting channel and the exact conversion to true signal levels much more subject to inaccuracy. Reduction of data from this instrument was assisted by one minor incorrect

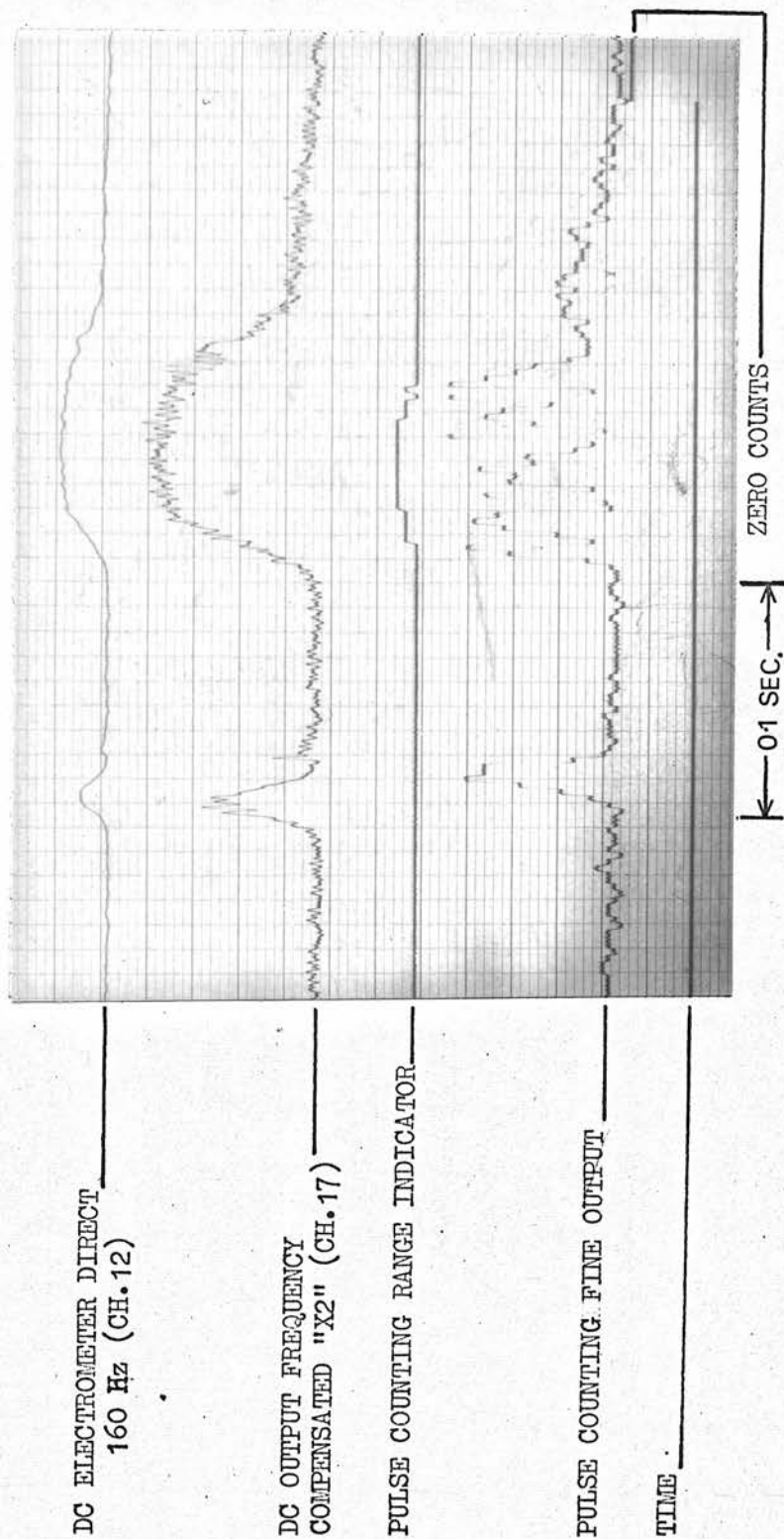


FIG 9 SECTION OF S27-1 TELEMETRY RECORD
SHOWING SIGNALS DUE TO STAR & CEPHEI.

function of the payload; the roll-control unit, set for $18^{\circ}/\text{sec}$, actually achieved $\sim 15^{\circ}/\text{sec}$, thereby making the "direct" amplifier output, transmitted through the low-bandpass channel 12 (160Hz), the equivalent of some 100A movement for this instrument - just adequate for the 190A slit width.

Also apparent from inspection of the record is the accuracy of in-flight alignment between the two spectrophotometers. The "counting" zero order lags about 9ms on the D.C. zero order. Since the phase lag of the frequency-compensated D.C. channel is very small while the pulse-counting has a built-in sample hold delay of nearly 3ms, the true offset is about 6ms or less than 0.1 degrees. The field width of the D.C. spectrophotometer is about 5% (0.15°) less than that of the pulse-counting instrument (due to its longer focal length) and this is apparent in that a number of spectra appear in the pulse-counting channel and not at all or at obviously reduced intensity in the D.C. channel while the converse does not happen. In addition to providing evidence on the "grazing" stars in the counting channel, this shows that the offset across the field was less than $\pm 0.075^{\circ}$. This indicates the value of the careful alignment between the instruments' optical and mechanical axes before flight and shows that the total subsequent relative displacement must certainly have been less than about 0.25mm in the typical

distances and radii involved. If all this movement did take place and occurred solely at one primary mirror edge, the resulting loss of focus would be around 30A of resolution. Clearly, unless by good fortune the errors compensated, the expected defocus is much less. By way of contrast, the misalignment in track centres with the R100 photometer also on board (no effort at relative alignments having been made) was greater than 1° , only about 0.6° of which is accountable by precessional motion in the 0.4 seconds of time offset between the experiments. As a consequence, only a small number of stars were common to the two types of instruments.

IV DATA REDUCTION AND ANALYSIS.

4. 1. The Nature of the Data.

At this stage it is perhaps worth clarifying the exact nature of the data to be reduced. For the pulse counting instrument, we can state clearly that each point of the data represents the measured number of counts, received through a slit width corresponding to 210A, with a spectral movement during the count integration interval of slightly less than 50A. If we include the relatively small amount of blurring due to the image size and aberrations (10A at 2500A), the instrument profile during one integration period (i.e. represented by one data point) is a trapezium of base around 270A and upper side 150A, the "Half-width" (full width at half maximum) being still 210A. Fig.10 shows how this profile differs from the "static" profile normally obtained during point-by-point ground calibration, though clearly it can be approximated and reconstructed from the static profile calibration curve by a convolution process. Over the counting range 0 -252 each value has a maximum uncertainty of $\pm 1\frac{1}{2}$ counts by reason of the four count resolution steps and should also be represented by the mean of the possible counts which

STATIC BANDPASS
(PRE FLIGHT CALIBRATION)

DYNAMIC BANDPASS
(SCANNING STARS AT
 $15^\circ/\text{SEC.}$)

SMOOTHED BANDPASS
WEIGHT(1,2,1)
(INPUT FOR POLYNOMIAL FIT)

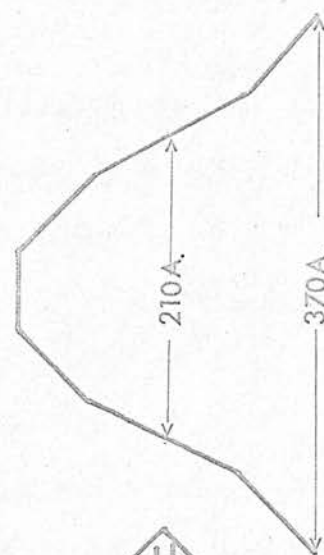
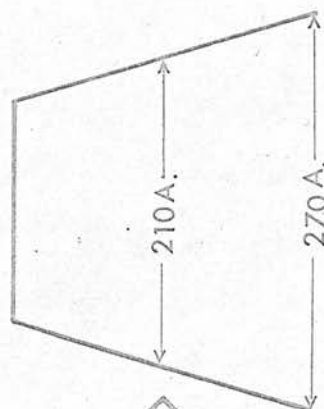
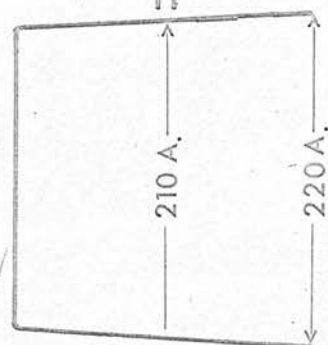


FIG. 10 EFFECTIVE BANDPASS UNDER VARIOUS CONDITIONS FOR R65(2) COUNTING CHANNEL

can produce this value e.g. the first level is 1.5 counts ± 1.5 maximum error (Beattie & Paterson 1970 loc cit). However within the range 0-252 this correction is only significant for the scientific and quantitative consideration of the background light level (Sudbury & Ingham 1970 loc cit). The stellar signal points always require the subtraction of a background "noise" level and hence the constant 1.5 counts disappears. (This process also converts the rectangular instrumental error probability distribution characteristic of an absolute count level on such a counting system into a triangular form with a base maximum error of ± 3 counts and a $62\frac{1}{2}\%$ probability of ± 1 count). Because of the increased step heights for counts exceeding 255, a failure to use the "Mean values" results in under-estimates of successively two counts to 504, four to 1016 etc. As these errors are always less than 1% of the respective values, the correction has not in fact been applied. The one-sigma probable error of each individual data point, is, of course, dominated (as a design criterion) by the stochastic error of $(\text{counts})^{\frac{1}{2}}$. The brightest stars gave counts around 10^3 and hence stochastic errors of $\pm 3\%$ (i.e. 30 counts); for the majority, individual counts were in the 30-100 counts range, with backgrounds of <10 to (at worst) ~ 50 , so

individual data point errors were \pm 10-30% (5-15 counts).

Among the disadvantages of the D.C. system is the much less obvious nature of the effective instrumental profile when this is band-limited. Although in this instance, the 190A slit-width does not allow the presence of information at higher resolution than 95A or 170 Hz, the problem remains, for the low frequency (160Hz) telemetry channel and uncompensated output, that the slit profile is "smeared" in a frequency dependent fashion (due to the phase lag around the nominal cutoff frequency) and thus the finer spectral detail will suffer a wavelength shift with respect to the slower changes. It therefore seems safer to use the wide-band-pass (500Hz) data from the frequency compensated amplifier and smooth this with a "σ-smoothed" Fourier formula (Lanczos 1957 p 267) corresponding to a bandpass beyond the spectral resolution frequency. The author has, in fact, chosen to match the smoothed digitised data to correspond in its sampling characteristics to the "raw" counting data; bearing in mind the higher dispersion of the D.C. instrument, this results in a 3db point around 330Hz. The data is then treated by the same programme (Section 4. 3. 4.).

4. 2. Attitude Solution.

Preliminary attitude data is computed by the European Space Operations Centre (E.S.O.C.) applying rigid body dynamics to the rotations of the rocket to provide a best linear fit to the signals given by the on-board aspect sensors (three axis magnetometer and four moon-sensor units). Because of the fundamental resolution limitations and insufficiently known offsets of these sensors, the first solution is likely to have errors around five degrees. When flying stellar instruments, however, a first check on the solution can be made from the horizon crossing signals (which should obviously be symmetric and depressed a calculable amount in topocentric coordinates). With confidence from such a check, good instrumental data can then allow the identification of a few of the brightest stars reasonably unambiguously, either because they are found in an otherwise "bare" area of the sky or, with luck, by sliding the predicted track to make a local "fit" to the transit times. The accurate offsets thus derived are then fed back to ESOC who interpolate and extrapolate revised solution still by reference primarily to the aspect sensors. This solution, being accurate to some 2° - 3° or better during the greater part of the

flight above 80km, was adequate for the unambiguous identification of the great majority of the 75 or so stars observed in December 1968, although the process is somewhat laborious and very time consuming; it involves plotting all the tracks and observed signal times on transparencies across large scale star maps (the Skalnate Pleso Atlas Coeli was used), sliding these around over a reasonable error ellipse, until a fit sequence is found, and identifying all the stars so fitting in the Bright Star catalogue, in addition, of course, to checking that all other bright stars found within the track are of late enough type to explain their absence in the record, and that the relative signal intensities, at least of the more "normal" stars, are broadly within expected limits.

However, for the present study the above procedure was found insufficient for the following reasons:-

- (1) The rate of scan in roll across the sky, which is a non-linear function of time, was clearly not predicted with sufficient accuracy for wavelength identifications. An error of $\pm 1\%$ which was $\pm 30\text{\AA}$ at 3000\AA , caused very substantial anomalies in applying the steeply falling sensitivity curve at this end of the spectrum

- (2) Certain of the more isolated and less bright stars, on scans containing perhaps 2 - 4 stars, could not be "fitted" with sufficient precision to give unambiguous identification; the opposite type of problem occurred in one or two very crowded regions (e.g. Cygnus).
- (3) It was desirable to have some supporting information on "grazes"- or, equally, which stars were clearly well centered in the slit length.
- (4) It was unsatisfying not to know if the identification solution was dynamically possible.
- (5) Recognition of faint star signals was desirable for the background light studies.
- (6) In the event, it was found that, for the usual human reasons, a significant number of errors, mostly in time reading but occasionally in cross-referencing or because of zero order identification problems, had found their way into the lists. The improved solution clearly demonstrated the large residuals of such objects.

At the author's request the derivation of this improved solution was kindly undertaken by W. Muller-Breitkreutz and A. Sesma at ESOC who were able to

carry it out using entirely the R65(2) stellar signals. Sesma finally produced r.m.s. residuals of only $\pm 0.085^\circ$ in the critical roll (spectrum scanning) direction, while the lateral fit (along slit) is shown in Fig. 11 (r.m.s. residual 0.825°) which demonstrates the high degree of final confidence achievable by such a solution.

In addition to more than fulfilling the above primary purposes including allowing the scan rate to be defined to an error less than 0.3% (10A at 3000A), such an accurate solution avoids the lingering doubt that some feasible locally satisfactory fits of the signal sequence might have been ignored because one or more of the objects in the track had not been expected to give a high U.V. output e.g. an anomalous late-type star. In fact, from the list of stars observed (table 2) it will be seen that no stars later than A5 were identified. The final distribution of stars against Spectral type is

0	4	B0-2	10	B3-5	21
B6-9	19	A0-2	16	A3-5 or Ap/Am	10

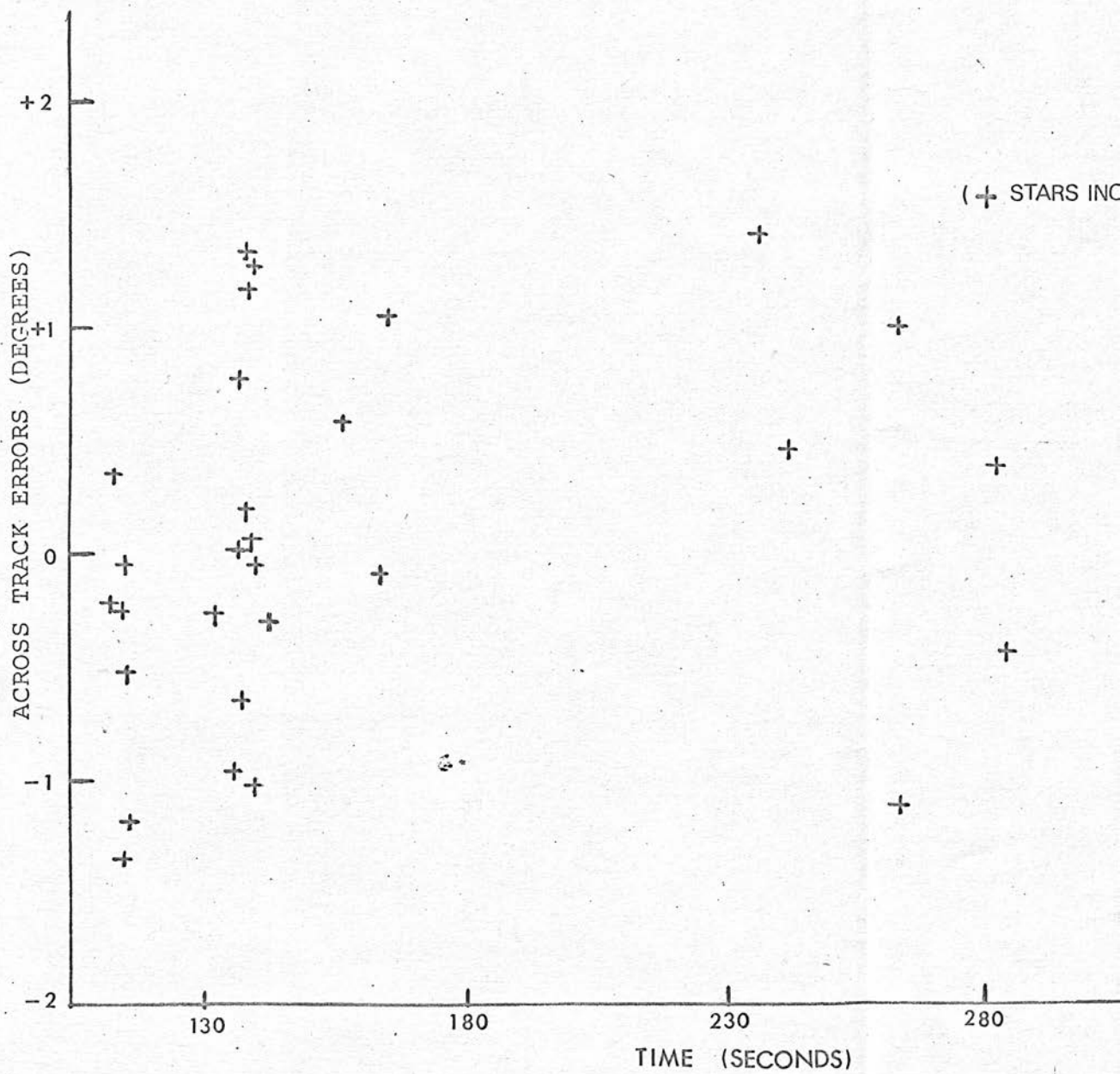


FIG.II ACROSS SLIT RESIDUAL PLOT S27/I ATTITUDE SOLUTION.

4. 3. Reduction of Data.

To reduce the data into usable form the following steps are necessary:-

- (1) Measurement of the output at a sufficient number of points in the neighbourhood of the stellar signal.
- (2) Averaging of the background at suitable points.
- (3) Identification and accurate timing of the net zero order signal.
- (4) Subtraction of the background from the counts in the region of the spectrum.
- (5) Smoothing and curve fitting the spectrum.
- (6) Interpolating the spectrum to fixed wavelengths. (Identified from the zero order, roll rate and dispersion).
- (7) Multiplying the interpolated measures by the appropriate calibration factors.
- (8) Normalisation to $V = 0$.
- (9) Correction for reddening using the $B - V$ colour excesses and a nominal reddening function.

Brief comments on some details of these processes follow.

4. 3. 1. Measurement.

This process is quite distinct for the pulse counting and D.C. measurement channels. The D.C. output was digitised (by ESOC) direct from the telemetry tape record at 1000 samples/sec. (from 790Hz and 160Hz channels) and supplied on an I.B.M. compatible FORTRAN coded tape. This had to be edited (by the Edinburgh Regional Computing Centre) to suit the Observatory Elliott 4130 magnetic tape procedure. The 790Hz data is then smoothed in the computer by a Fourier smoothing formula as mentioned (Section 4.1.) at 333 samples/sec for points in the neighbourhood of the stellar signals subsequent to being multiplied by the amplifier and telemetry calibration curves and the resulting figures printed out. From this print-out and by comparison with the UV paper record suitable background regions could be identified and computer subtracted. Otherwise the processing follows the same pattern as the pulse counting Channel.

Although the pulse counting data is in a much more precise and sophisticated form, it is not possible to use the digitising process as the 600Hz channel is being used very near to its bandwidth limit and there is no way of synchronising the

digitiser readings to the counter integration period. (such problems may be averted in the future by ESRO's proposed use of the more sophisticated digital telemetry transmission system). Therefore these data had to be reduced by hand from the high speed (500mm/sec) paper record; at some 100 readings per star this is a laborious and tedious process. At the same time comparison is made between the two telemetry channels containing the pulse-counter outputs to allow the "range" to be taken into account in evaluating the "fine output" data i.e. the values are listed directly as counts.

4. 3. 2. Background Evaluation.

The regions chosen for evaluation of the background were in general some 30ms on either side of the zero order; these correspond to wavelengths not transmitted by the optical system (or, probably by interstellar space). The region following the spectrum, which ideally should be used also, is likely to be contaminated, especially for brighter stars, by second order UV and "leaked" visible response, and similarly points preceding the zero order by more than about 70ms may contain positive order responses. Averages of ten successive readings

were used (as in general background study (Sudbury & Ingham 1970 loc cit)). In overcrowded regions or for blended stars some ad hoc modifications had to be made to the above principles using judgement of the nearest available "undisturbed" background.

4. 3. 3. The Zero Order.

It has been already noted as a feature of this instrument that the zero order is attenuated to an amplitude very near that of the spectral output - slightly less as Fig 9 shows - so that it can be used as the zero wavelength reference for the spectrum. The zero order image is in fact slightly defocussed when the spectrum is in focus; in any case, since its total width is going to be at least twice that of the slit-width resolution, the problem arises of what characteristics to use as a reference. In laboratory setting up the mean of the two half-maximum-height points was found to lie accurately at the zero of the (linear) dispersion. However, the stochastic noise and the asynchronism of the pulse counting sample times with respect to the zero order make this method unreliable to apply to the observations, especially of the fainter stars, and

therefore the alternative and nearly equivalent technique of using the centroid as the reference was used. The centroid technique has the merit of involving all the readings in the zero order as contributing to the final result and Kirsopp (private communication) has shown that for "bright" stars (i.e. large signal/noise) the error does not exceed about $\pm 10\%$ of the sample time i.e. $\pm 0.3\text{ms}$ in our case. The other technique investigated was that of convoluting the array of values around the zero order with a "model" zero order array. Except for some of the fainter A-type stars which had very weak zero orders, the methods gave results which lay within a range of one millisecond ($\sim 20\text{A}$). In all cases the mean background was subtracted before the above processing.

4. 3. 4. Smoothing and Curve Fitting.

The process of smoothing has already been mentioned for the D.C. channels. As there was some (although considerably less) redundancy in the pulse counting values, a simple smoothing formula was also applied to this using weights $(\frac{1}{4}, \frac{1}{2}, \frac{1}{4})$. The effect of this smoothing formula is that the bandpass half-width is unaltered but the whole width is, of course,

increased (Fig. 10) by some 18%; the random error is reduced by $\frac{1}{\sqrt{2}}$ or nearly 30%. The smoothed data was fitted with an orthogonal polynomial using G.I.

Thompson's ALGOL program ORTHPOLY from the Observatory's Elliott 4130 computer library. The weighting function for the values was $\frac{N}{\sqrt{N+Z}}$ where N is the net count and Z the noise background. The fixed wavelengths were interpolated by the corresponding library program OPY. The Smoothering, Interpolation, Normalisation and Reddening correction are combined into a single ALGOL program SNORE.

Although the time taken to devise, debug and prove these programmes and to type all the stellar pulse counting data on punched tape was certainly comparable with the time it would have taken to reduce all the data by hand, the computer method has these advantages:-

- (a) Subject to the punched data (which is readily checked) being correct, it is essentially error free.
- (b) It provides a totally impersonal fit to the fluctuating data, of a degree which is consistent with the slit-width resolution. This fit was 12th order for the best spectra, diminishing to 8th order for the poorest spectra if less than thirty "points" were

involved. The ORTHPOLY program has criteria for rejecting points with excessive deviation, and otherwise makes no more of the data than is justified.

- (c) The interpolation to fixed wavelengths is also carried out consistently and accurately.
- (d) It is only a few minutes work to try the effect of alternative calibrations or reddening correction curves, or to correct the effect of input data errors.
- (e) The program is immediately available for the D.C. data reduction and for any future similar flight results.
- (f) The output is also made on punched tape for re-input to any future processing e.g. graph plotting.
- (g) The results are directly available in printed form without typing errors.

The printed-out data included the residuals of the polynomial at each data point; the tabulated brightness data is only printed for wavelengths between input points 1 and N-1 where the data runs from 0 to N, thereby avoiding substantial spurious end-effects in the polynomial fitting at points of low weight. The weighted RMS deviation is printed as part of the ORTHPOLY procedure and this is listed in Table 3 as SIG.

4. 3. 5. Reddening Correction.

For the reddening correction, three external items of information had to be introduced:- the intrinsic colour, the colour excess, and the assumed extinction function. Intrinsic colours were obtained from the table of Fitzgerald (1967) using a spectral type derived from the Photoelectric Catalogue (Blanco et al 1968); where more than one spectral type was quoted, a "majority verdict" was taken unless there was substantial extrinsic evidence to prefer otherwise e.g. for α Scl where Heintze (1969 loc cit) has shown that the B 5 typing is the correct one. Similar criteria were applied for the B - V data; here the intrinsic accuracy and scatter of the listed measures are a real problem, since two or three hundredths of a magnitude scatter in B - V, which is quite typical, leads to scatter of one or two tenths of a magnitude in the reddening corrected values around 2400A. (The resolution of spectral typing for the intrinsic colour purposes leads to comparable scatter). Where several values were listed an "estimated mean" was used, i.e. values departing greatly from the mean were omitted, the mean itself being rounded to the nearest 0.01 mag. Finally, as a preliminary correction, the B - V excesses were applied to a reddening function

consisting of three straight lines on a scale of magnitude vs reciprocal wavelength in microns:-
 $E(\lambda) = 2.05(\frac{1}{\lambda})$ which is normalised to $E_{B-V} = 1$,
 $E(\lambda) = \frac{-7}{11}(\frac{1}{\lambda}) + 8.5$, and $E(\lambda) = 1.88(\frac{1}{\lambda}) - 5.572$,
which can be applied to the E vs $(\frac{1}{\lambda})$ diagram of Stecher (1965) within the error bars. The extrapolated A_V for the initial line is 4.0 mags., which is a reasonable compromise of measured values from 3 to 6 (e.g. Spitzer 1968 p.69) and is a surprisingly good straight line fit through all the ground based observations given by Boggess & Borgman (1964). The problem of deriving an "improved" reddening curve from the observations in this thesis, in the light of the variation of reddening in this wavelength region indicated by Bless & Code (1970) in different parts of the sky is discussed in Section 5.

4. 4. Sources and Amounts of Errors.

4. 4. 1. The Counting Channel.

The ensuing discussion is specific to the situation of the counting channel where the problem is best defined and most points studied. At the time of writing some of the details apply in principle to the D C reduction from the digitised tape, discussed briefly in section 4.4.2.

4. 4. 1. 1. Gross Errors.

(a) Identification. The process of attitude solution has already been described in Section 4.2. and gives a high level of confidence that rechecking after the accurate star-based solution has eliminated remaining errors of identification, except where the possibility is indicated in the list of stars. The problem of possible intensity errors through blending, perhaps with stars on the edge of the field, is more complex but I believe that the presence of all "contaminating" stars brighter than $V = 6.5$, and within at worst $2\frac{1}{2}$ magnitudes visual brightness of the star, has been indicated correctly.

(b) Reduction. In the process of reading nearly

10,000 data points by hand, some errors inevitably occurred, the principal type detected being the complete omission of one reading, which can have the effect of causing wavelength misidentification and consequential substantial intensity errors (Sec.4.4.2.) All the spectral data have therefore been rechecked against the paper record, two or three value errors also having been detected in the process. Initially the spectral calibration was determined by reading times at the zero order and at the beginning of the spectrum using a Gerber Variable Scale. Subsequently, realising that the use of the sample repetition interval itself was in fact a more accurate method I compared reference intervals obtained by the two methods and checked again, with the paper record, any values differing by more than one millisecond; in only one case was a missing point detected. Zero order centroids were checked and recalculated at the same time. In view of the proportion of the above errors initially, it would seem very unlikely that after the checking more than, at most, one case of such an error could remain in the listed data. On a few faint stars the actual location or extent of the zero order in the presence of random or background fluctuations or blending is a matter of judgement; where significant doubt remains this has been indicated.

4. 4. 1. 2. Random and Systematic Errors.

Individual input points have a random error corresponding to the signal to noise and signal strength (i.e. the value of $(N^{\frac{1}{2}} + Z^{\frac{1}{2}})/N$ at and around the point); because the order of the polynomial fit allows for substantial overdetermination, the "true N" value to be ascribed to a particular print-out point is clearly not the smoothed counts in one 50A interval but the weighted sum of adjacent points. The background fluctuation error is also correspondingly reduced. In the tabulation the weight given for each point is the value of $N/(N^{\frac{1}{2}} + Z^{\frac{1}{2}})$ nearest to the interpolated point. By the foregoing argument the fractional r.m.s. stochastic error will be about one third of the reciprocal of this. Additional to, but clearly not independent of the random error, is the accuracy of the polynomial fit. Although there might be some significance in printing the "running r.m.s. residuals" local to the tabulated point, for simplicity the r.m.s. over the entire tabulated range has been given.

The systematic error of individual points will, in general, be small compared to the above and following errors; the origin is the mis-estimation of background which may be due to:-

(a) the random error in obtaining the background --since the background value is the average of two sets of ten points this error is certainly relatively small ($<30\%$ of the signal error when $N/Z \div 1$) and

(b) the error introduced by (in general) extrapolating the spectrum background from the values before and after the zero order (to avoid the second order contamination). This error is peculiar to each star, depending on its location in the sky with respect to the horizon and the moon (predominantly) as well as the ecliptic and the Milky Way. Because of the crowding of early type stars there, the Milky Way is the most troublesome area, as the problem of finding an "undisturbed background" is greatest just where this background is generally changing the most rapidly. The estimate of the resulting error, which is non-uniform in the spectrum (i.e. proportional to the net count at each point), must unfortunately be subjective. Where it is significant it has been indicated by '+' after the NZ value. It is quite apparent, from the steady background between zero-order and spectrum signals of bright stars, that the small angle scattered light remained very low in flight - certainly less than 1%. The laboratory value was less than 0.1%, though such a large ratio is difficult to measure exactly with the normal

laboratory optical collimator set-up without spurious effects, and some deterioration may be expected due to aging of, and dust collected on, optical surfaces during payload integration.

The more significant errors, for the brighter stars, are the relative-with-wavelength and the fixed-wavelength relative-star-to-star errors. The first of these has two primary components.

- (a) the accuracy of the calibration from original comparison with Stecher's β Tauri and
- (b) the error in assigning the wavelength scale.

4. 4. 1. 3. Calibration Error.

The calibration itself has the following error chain:-

- (a) Accuracy of assigning wavelength scale to my β Tauri measure.
- (b) Effective wavelength and bandpass of this measure at a given wavelength vs, Stecher's corresponding values.
- (c) Accuracy of Stecher's Beta Tauri observation and reduction.
- (d) Accuracy of Stecher's calibration.

Stecher indicates his relative calibration to be "a few per cent"; Allowing for changes in

calibration in flight, and cathode non-uniformities (Stecher did not use a Fabry lens) we may say around 10%. Stecher does not indicate the accuracy of his observation. With dispersion six times greater, offset perhaps by lower throughput and certainly twice the slit-width resolution, we may assess his overall statistical accuracy over 100A as comparable with my own for this star, - better than $\pm 3\%$ r.m.s. or say 8% limit (3-sigma) near maximum. We should, from our own experience, perhaps allow another 10% for rate-meter amplifier, reading, and wavelength errors. Hence Stecher's relative error, summing r.m.s. wise, may be around $\pm 15\%$ limit per spectral point.

Our statistical error, as already stated, will be around $\pm 8\%$ limit at the maximum of sensitivity. The wavelength scale error is the most difficult to assess, especially as its effect varies with wavelength for two reasons. The minor effect (for β Tau) is likely to be the actual roll-rate error ($\pm 10A$ at 3000A for 0.3% error). The zero-order/spectrum relative positioning errors are $\pm 0.25 \text{ ms} \equiv \pm 5A$ for the well-defined zero order of this star. The dispersion is also known to a similar accuracy so there is a combined limit error of about $\pm 17A$. Now the true β Tau spectrum itself has a gradient of about 10%/100A so on a "flat" part of the calibration

curve we might be a mere $\pm 2\%$ out from this cause. Unfortunately, around 1700 and 2800A the calibration curve changes by as much as $1\%/A$, so the error in these regions may be $\pm 17\%$ additionally.

Combining all errors, we may thus expect a relative error in our calibration to be around $\pm 20\%$ in the best regions and perhaps 25-30% where the calibration curve has a steep slope. In these regions there is, further, a very substantial difference between the effective wavelength $\lambda(\text{eff})$ and the observed $\lambda(\text{obs})^*$, amounting at most to 40A (Fig. 7). The higher resolution and triangular shape of his effective bandpass makes $\lambda(\text{obs}) - \lambda(\text{eff})$ much smaller ($\sim 10A$) for Stecher. A correction has therefore been applied by determining, with the use of a preliminary calibration curve and the nominal profile, a $\lambda(\text{obs})$ having a $\lambda(\text{eff})$ corresponding to the tabulated wavelengths within $\pm 10A$. A fresh calibration curve (that given in Fig. 7) was then prepared from this. With a worst error of perhaps $\pm 10A$ on the determination of the appropriate $\lambda(\text{eff}) - \lambda(\text{obs})$ we may expect a worst error of $\pm 10\%$ from this cause.

The form of the calibration curve longwards of 2800A has been derived entirely from the tungsten ribbon lamp calibration; this has been corrected for input effective wavelength as already described

* $\lambda(\text{obs})$ here being the central wavelength as given by zero order, roll rate, and dispersion.

(Section 3.2.1) and the steadily improving agreement between the relative-to-Stecker and ribbon-lamp calibrations at longer wavelengths suggests that the relative errors around 2800A should be less than 20%. Between 2400 and 2800A the calibration based entirely on the comparison with Stecker's β Tauri produced a depression in all the spectra of some 0.5 magnitude maximum. Since this was clearly anomalous, the calibration curve ultimately used in this region was obtained by taking the mean of the ribbon lamp and β Tauri calibrations from 2600 - 2800A and joining this smoothly to the β Tauri calibrations by 2350A. As already remarked, for the purposes of the self-consistent photometry providing the main emphasis of the Section V. discussion, the exact calibration curve is unimportant although coincidence on an absolute scale is pleasing.

4.4.1.4. Tabulated Star Errors.

When it comes to applying the given calibration curve to the spectra, some of the errors directly correspond to those already considered for the derivation of the calibration curve i.e. the errors arise independently from stochastic fluctuations within the spectra and from wavelength identification

errors. For fainter stars, the probable error due to the zero order time derivation increases due to the increased fluctuation errors and, ultimately, becomes an identification problem which could lead to a gross error (Section 4.4.1.1.). Otherwise an estimate of the maximum error in wavelength from stochastic fluctuations in the zero order may be obtained by consideration of an ideal zero order model signal consisting of three values of say, 10 counts each on a mean background of 10 counts. Then the r.m.s. fluctuation of each value is approximately six counts. Hence we have a 10% probability that the nominal sequence (10,10,10) becomes (4,10,16), which would cause a centroid shift of 0.4 interval or 20A. Such signal:noise ratios occur with stars having peak spectrum weights around 3 or 4 for early and 5 or 6 for later type stars.

4. 4. 2. D.C. System Errors.

Delays of several months in processing the D.C. digitised data into a form compatible with the 4130 computer Algol software have prevented analysis of these data at the time of writing and cause the ensuing discussion to be incomplete. The following error chain can be identified:-

- (a) D.C. amplifier calibration was by a switched L.T. battery-high resistor combination, checked against Keithley laboratory electrometers (which were also used in the tungsten ribbon lamp calibrations). The likely error here is $\pm 5\%$ relative (i.e. through the scale) and another $\pm 5\%$ absolute.
- (b) D.C. amplifier and E.H.T. drift. The latter is believed to be only a few volts; measurement problems make it difficult to monitor at 2-2.5KV but this value is based on experience with digital voltmeter measures at lower voltages. The resultant gain variation will be $\pm 2\%$ at most. D.C. amplifier offset drift is only a few mV but there are sensitivity drifts due to ageing and temperature of the main feedback resistor (say $\pm 5\%$ of reading), while temperature can also alter the diode conducting point determining the sensitivity change, but only by one or two per cent (on the amplifier 10V scale).

The above represent systematic errors; for individual points greater error arises from the random noise of the input resistor (on the lower ranges) and the photocurrent fluctuations - indeed Pao et al (1966 loc cit) have shown that more information may

be obtainable, at similar light levels, by squaring the broad-band photocurrent/^{fluctuation} noise than by measuring the current. Topp et al (1969) have discussed the detected noise using a D.C. system; their final expression (Equn 12) can be simplified for our CsTe Ascop where dark, dynode and leakage currents are negligible and stage gain ~ 2.5 , to obtain

$$\text{Signal/Noise} = \left[\frac{N_S}{4f_c (1 + N_B/N_S + \langle I_{NL}^2 \rangle_{AV}) / 4e^2 G^2} \right]^{\frac{1}{2}}$$

where f_c is the cutoff frequency, G the overall tube gain, e the electronic charge N_B the background and N_S the source counts, and $\langle I_{NL}^2 \rangle_{AV}$ the r.m.s. load resistor noise. For an input resistor of $150M\Omega$, $f_c \sim 200Hz$ and overall gain of 3×10^6 , the final term in the denominator is 0.1 (i.e. the shot noise becomes negligible, showing the importance of high tube gain) and the fractional noise becomes

$$\frac{N}{S} \sim \left[\frac{I_S}{4f_c \cdot G \cdot e (1 + I_B/I_S)} \right]^{-\frac{1}{2}}$$

where I_S , I_B , are the signal and background currents.

Using the same values as earlier, we obtain

$$\frac{N}{S} \sim 1.7 \times 10^{-5} (I_B + I_S)^{\frac{1}{2}} / I_S$$

and we find, for example, that with $I_S \sim 10^{-9}$ amps,

$$I_B \sim 5 \times 10^{-10} \text{ amps,}$$

$$\frac{N}{S} \sim 0.65$$

while for $I_S \gg I_B$, $\frac{N}{S} \sim 1.7 \times 10^{-5} (I_S)^{-\frac{1}{2}}$ and hence,

$$\text{e.g. at } I_S = 10^{-8} \text{ amps, } N/S \sim 0.17$$

For weighting purposes in the polynomial fitting the more complex expression (with the numerical factor rounded up to 2×10^{-5}) will be used if $I_S < 10 I_B$.

It is apparent that the characteristic intrinsic errors of the D.C. system, analogous with the $N^{\frac{1}{2}}$ of the pulse counting, are some $\pm 25\text{-}30\%$ for the strongest signals, $\sim 10^{-8}$ amps, and may be $\pm 75\%$ for signals around 10^{-9} amps and twice the background. The "cathode high" spikes (Section 2.5) give an extra risk of local errors of a gross nature, not present in the counting data.

V. RESULTS AND DISCUSSION.

5. 1. Presentation of the Data.

The background brightness data have been discussed in the attached paper by Sudbury & Ingham, but some additional detail is given in Section 5. 4.

The stellar data from the counting channels are presented in Tables 4 - 1 to 4 - 43 representing the final Punch (4) print statement of the Algol program SNORE B, (Appendix 4) for all the stars listed in Table 3. The processes leading up to the output have been described in Section 4, while Section 5. 2. and 5. 3. discuss the data.

As mentioned, the D.C. digitised data have not become available in time to present them with this thesis but Appendix 4 includes the Algol program COMT, which extracts chosen sections of the digitised telemetry data from the magnetic tape, converts them into photomultiplier current (by reference to arrays polynomial-interpolated from the calibration curves of the amplifier and the telemetry) and assembles them into continuous arrays. From this point the procedure is identical to that described for the counting data, with the procedure SMTHFN replaced by a Fourier convolution procedure; the general program

FOLGEN, developed from WMESCAN (Section 3.11) for carrying out such processes, appears also in Appendix 4. Figs 12(a) to (d) give the relationships of the various spectral indices from the reddening-corrected columns of Table 4 which are now discussed.

5. 2. The Stellar Data.

The consistently near-linear relationship between the ultraviolet colour index and the spectral type is the most notable feature of Figures 12(a)-(d). The slope increases slightly from about 0.3 to about 0.4 mags per spectral subtype from 2500A through to 1850A, with indication that types earlier than B3 lie above the line.

A particular topical application of these diagrams has been to the fluxes tabulated by Blondelot (1970). His tabulation was derived by applying observations from a number of sources, but especially that of Viton (1970) to the published models. Since the intention was primarily to provide data for predictions of the observed brightnesses of stars for identification purposes he has also included interstellar reddening but the plot of Fig. 13 uses the $m_v = 0$ data where reddening is negligible. Such a plot based on a pre-distribution of the Communication gave



FIG.12b. RELATION BETWEEN SPECTRAL TYPE AND NORMALISED BRIGHTNESS FOR 2000 A.

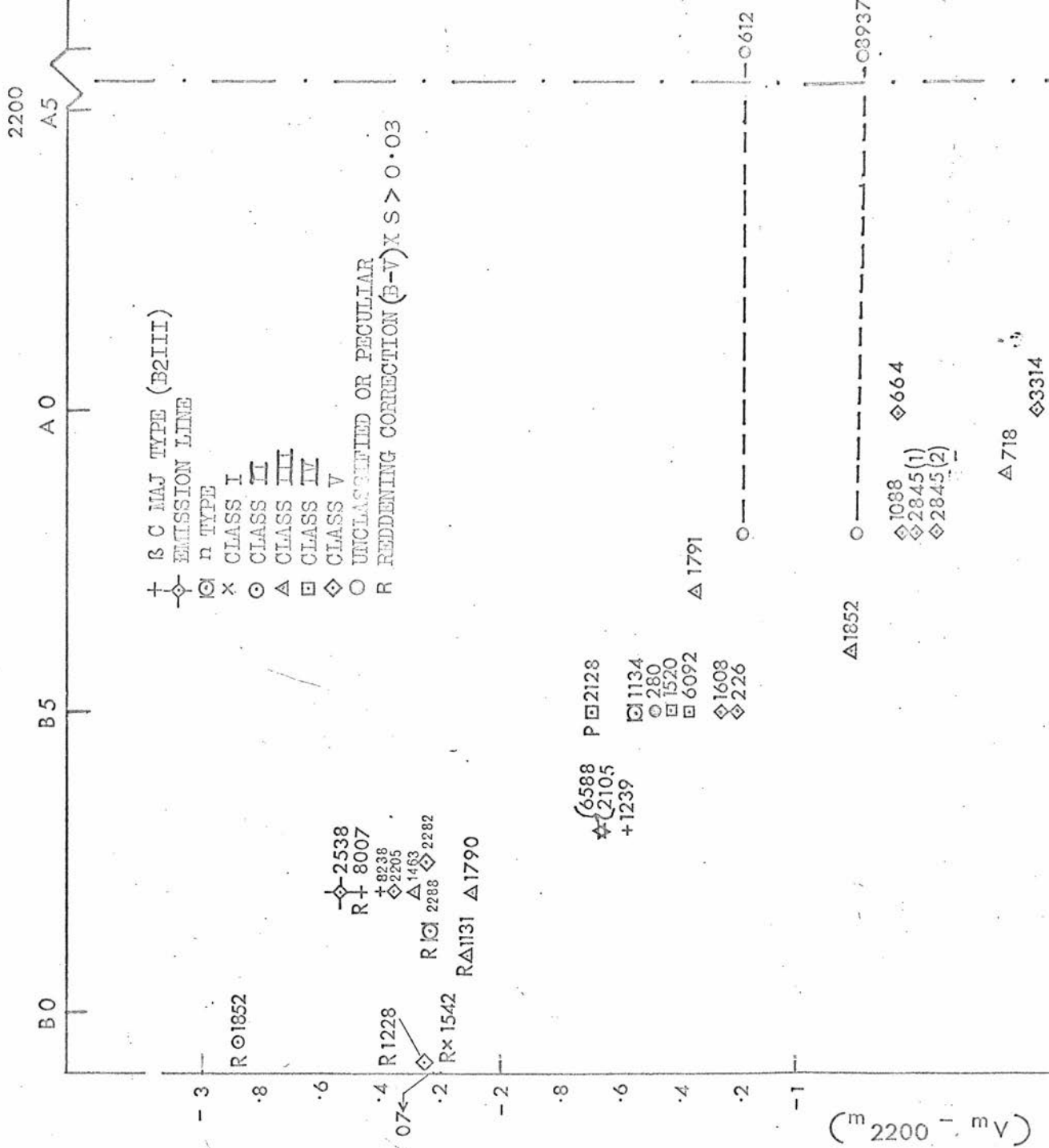


FIG. I2c RELATION BETWEEN SPECTRAL TYPE AND NORMALISED BRIGHTNESS FOR 2200 Å.

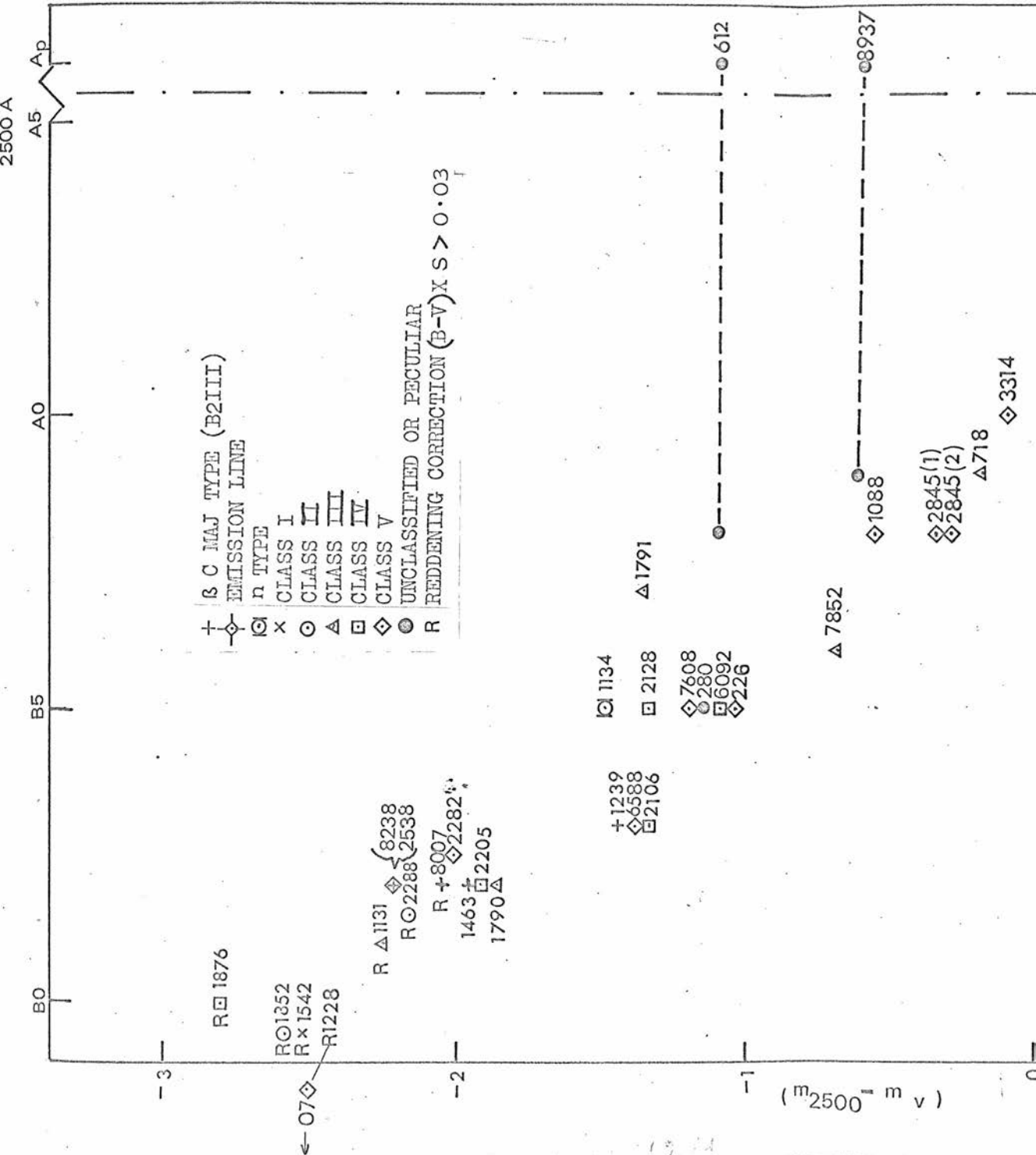


FIG.12d. RELATION BETWEEN SPECTRAL TYPE AND NORMALISED BRIGHTNESS FOR 2500 Å.

a fit which, while remarkably close in position as well as slope for the earlier type stars (B1 - B5), produced a rapidly increasing discrepancy for later types, tabulations for A types being some four magnitudes below my data points; indeed, had the stars really given these fluxes they would not have been observable at all by the S27-1 instruments. Since it was highly improbable that the aspect solution had only found A-stars having several magnitudes of UV excess (apart from the astrophysical implications of such anomalies) and as my findings were in accord with those of Bless et al and Stecher, intimation of this to Blondelot helped him to locate a computational error; the revised data (as plotted) not having these dramatic effects and corresponding well in trend with the least-squares fit to main sequence stars.

The plots confirm the excess flux reported by Bless et al for β Scl and currently by Campbell (in press) for other peculiar stars if classified as A-stars. In fact BS 8937 (β Scl) fits well enough if accorded Osawa's (1965) He-Balmer classification as shown. Of the other two peculiar stars, some blending of BS 612 (∇ For) may account for the excess if placed as B8. BS 3894 is 30 ϕ U Ma but is not the star (BS 4072) incorrectly listed by Osawa and his references as 30 ϕ U Ma, a mistake which presumably originates from careless use of the Boss

Catalogue reference. BS 3894 is listed in some references as A3s and this idiosyncrasy may be associated with the excess. Other abnormal stars having apparently significant excess fluxes relative to the dwarf sequence are BS 2538 (~~X~~C Ma) B2 V e and BS 1134 (δ For) B5ne.

The three β Canis Majoris (β Cephei) type stars, β Cep, (BS 8238), γ Eri (BS 1463) and BW Vul (BS 8007), all B2 III, appear to be unexceptional in their UV fluxes; these stars all have low rotational velocity (Stothers & Simm 1969) whereas high rotational velocity may be one characteristic leading to UV excess (Campbell, in press). Hill (1967) has shown that the visible region fluxes are also normal.

BS 8781 (α Peg) is anomalously faint with respect to my own main sequence and to Stecher's spectrum and this may be associated with the possible variability noted in the Yale Bright Star Catalogue, since by criteria both of attitude solution and comparison with the DC data this star was well within the pulse-counting instruments' field. Of the two other anomalies, BS 664 is blended with BS 655, but the excess of the "reference star" β Tau (BS 1791) is more puzzling. Possible blends are several magnitudes fainter, so adjacent nebulosity may explain the excess at 2000Å and longer. Babcock has quoted a B9p classification for this star which may make it an unfortunate "reference".

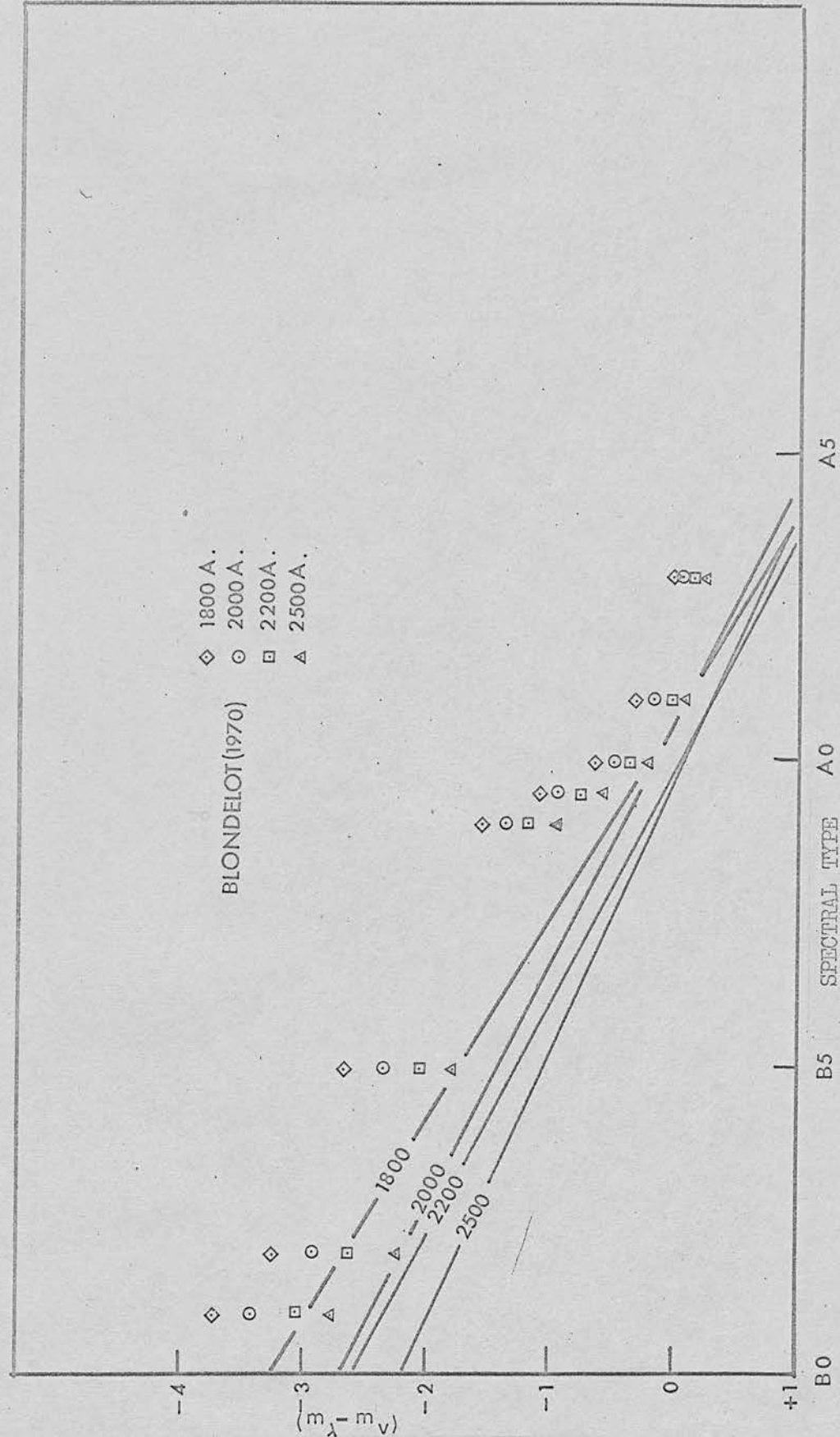


FIG 13 MAIN SEQUENCE DATA
COMPARED TO VALUES BY BLONDELOT

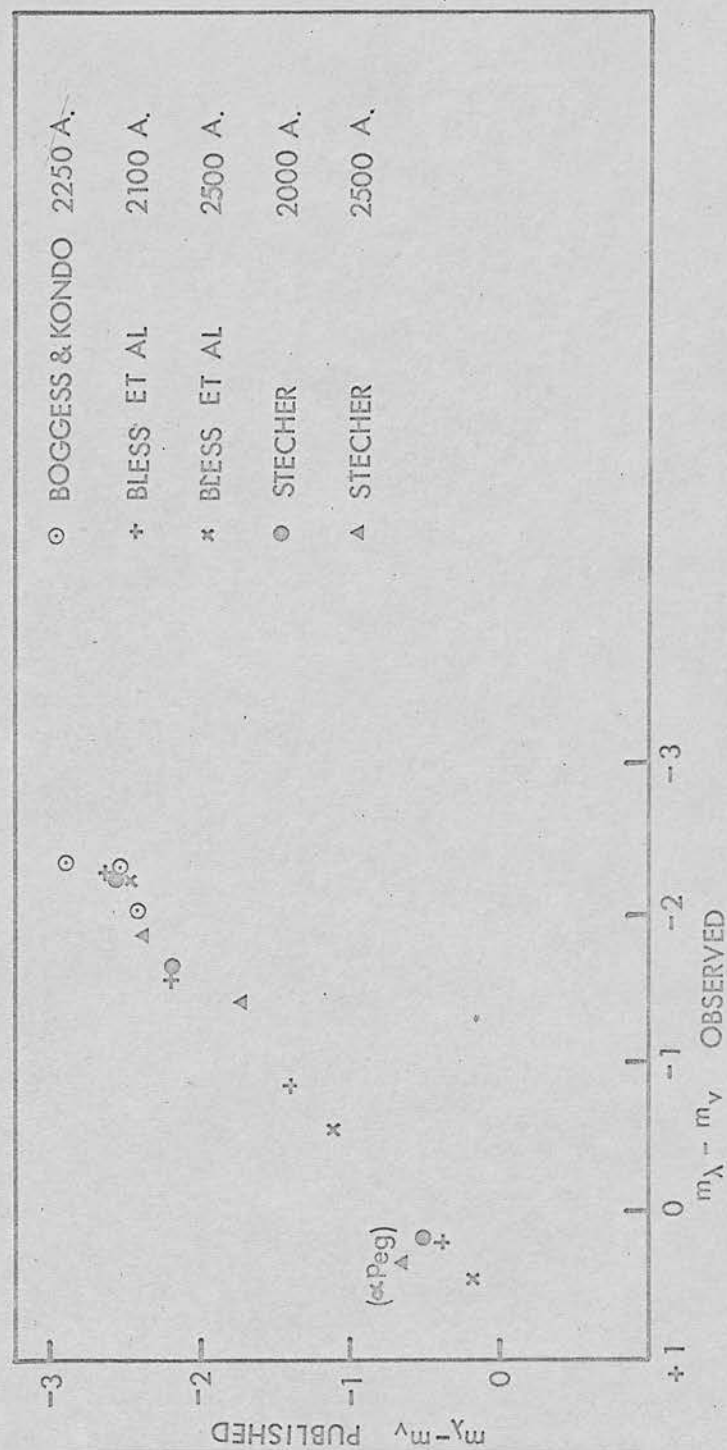


FIG 14 COMPARISON OF PRESENT OBSERVATIONS AND PUBLISHED DATA.

FIG 15a. PLOTS OF SPECTRAL DISTRIBUTION FOR 30 STARS.

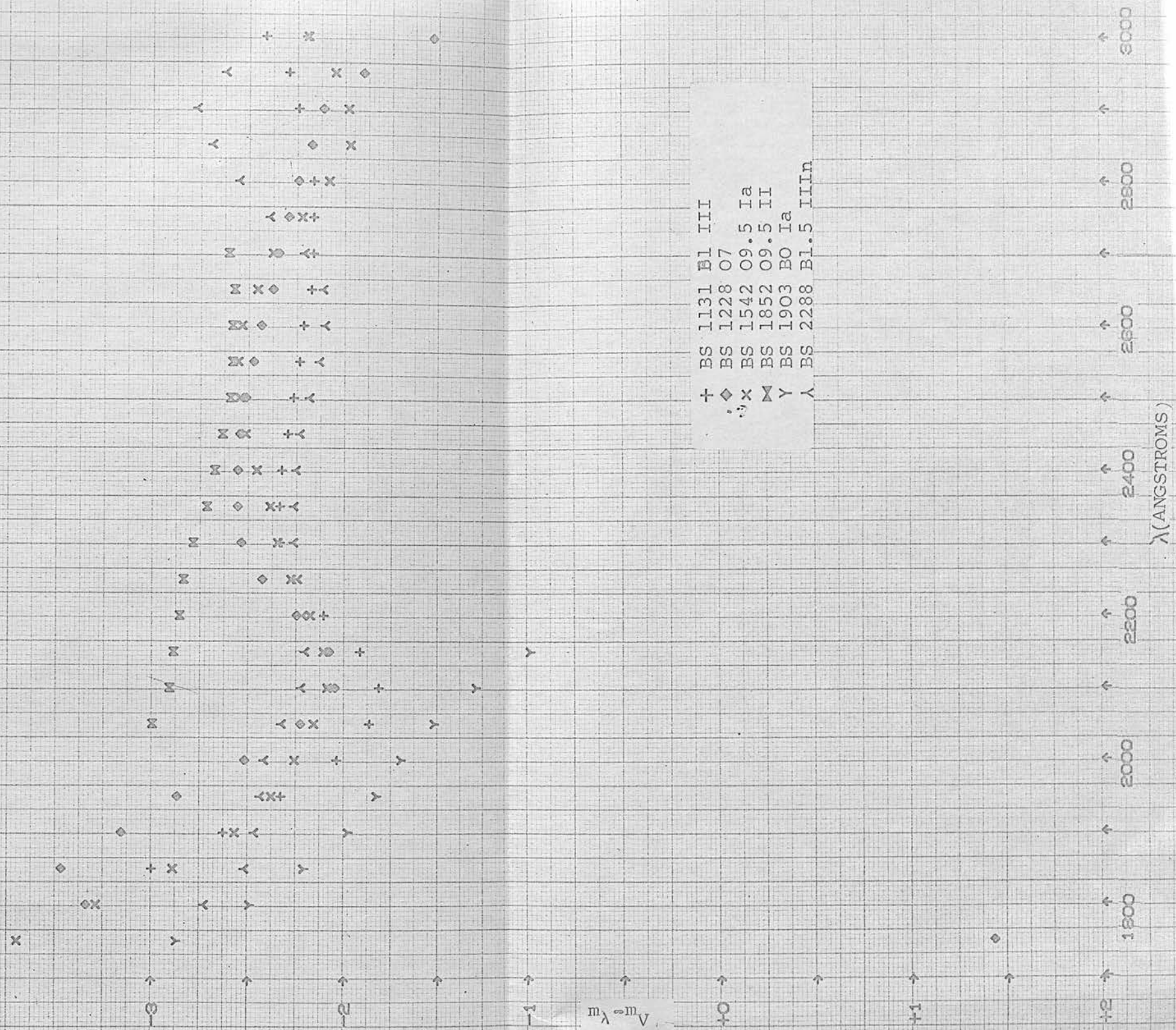


FIG 15a. PLOTS OF SPECTRAL DISTRIBUTION FOR 36 STARS.

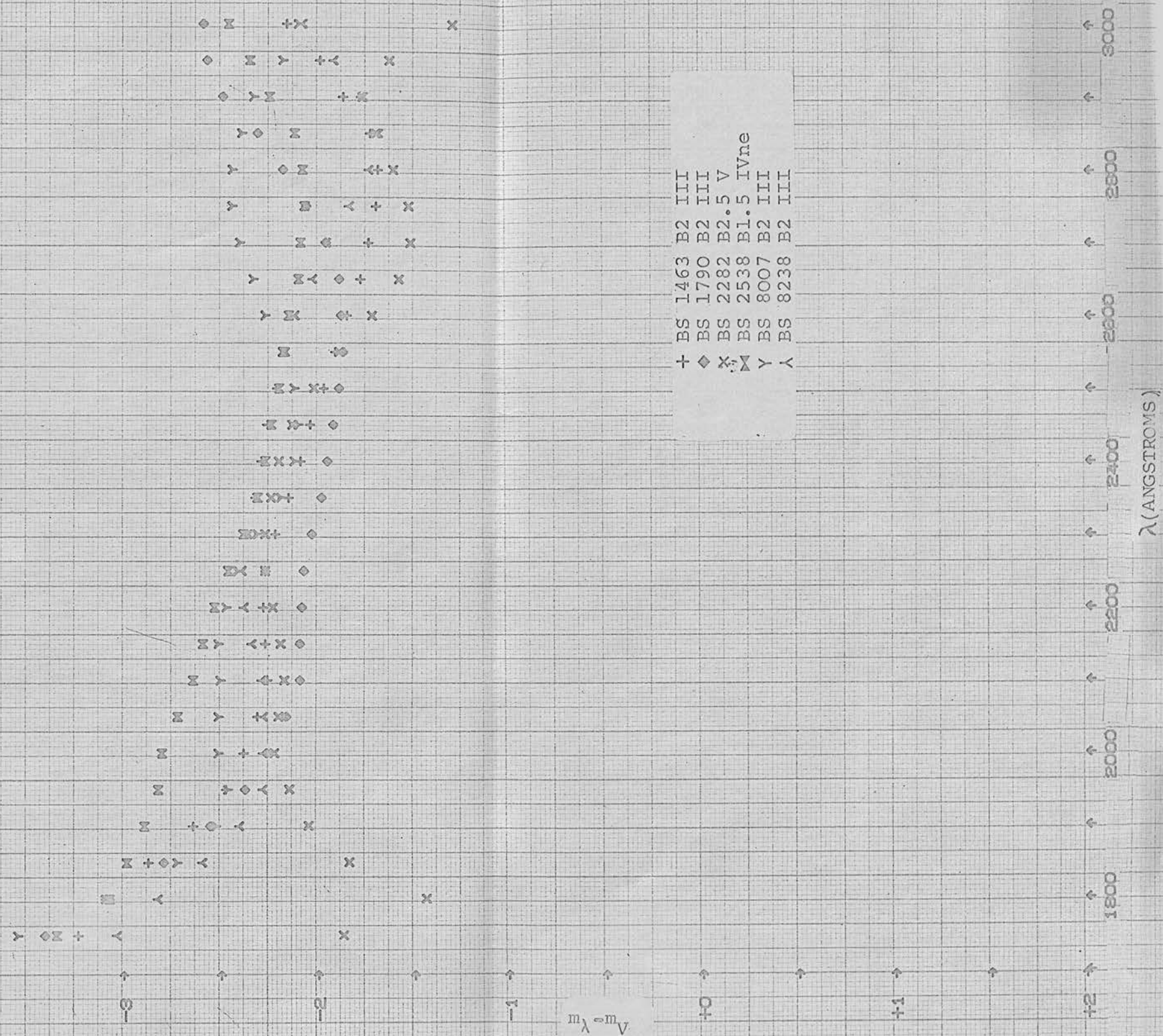


FIG. I5b. PLOTS OF SPECTRAL DISTRIBUTION FOR 36 STARS.

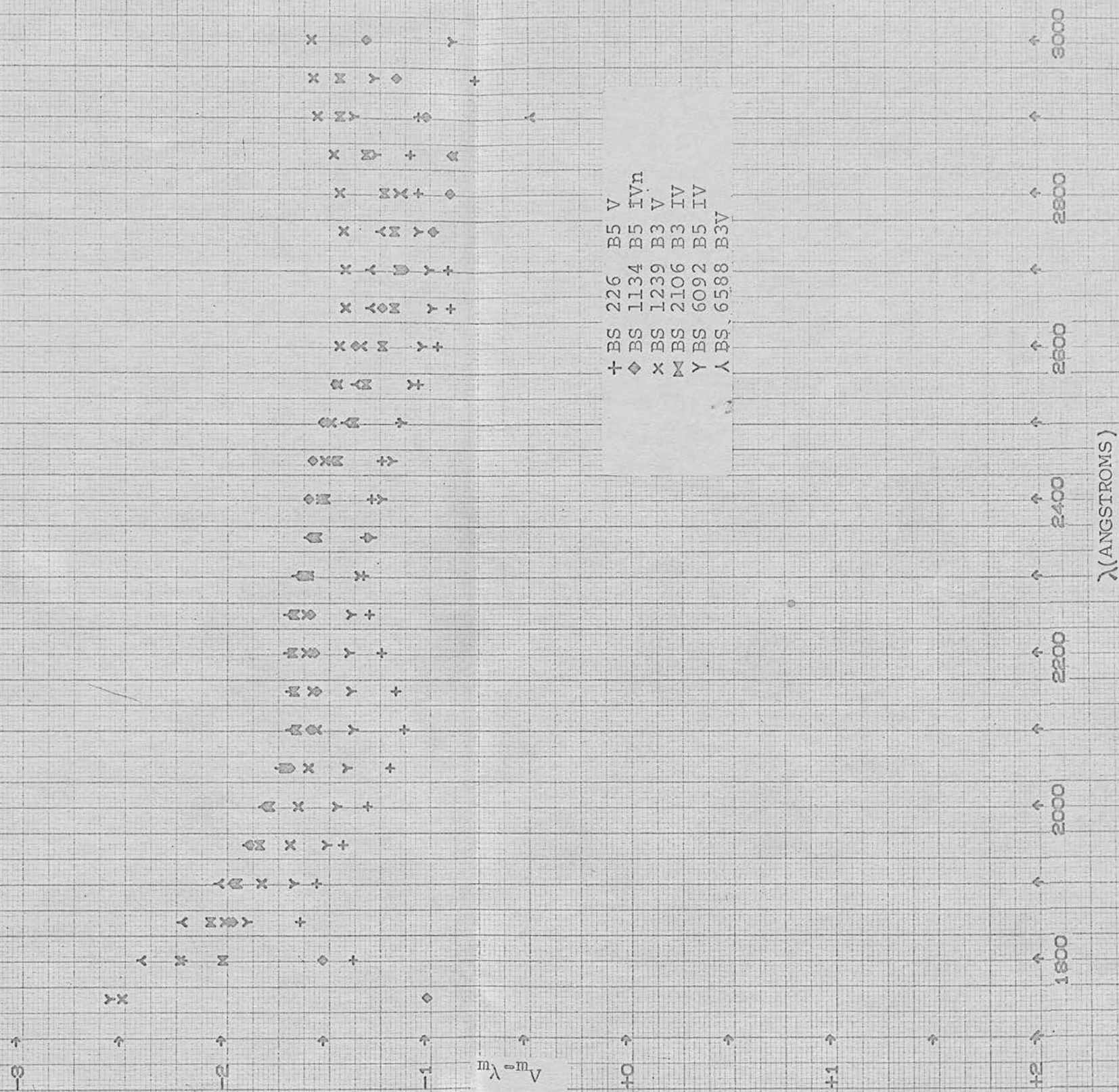


FIG.15c. PLOTS OF SPECTRAL DISTRIBUTION FOR 36 STARS.

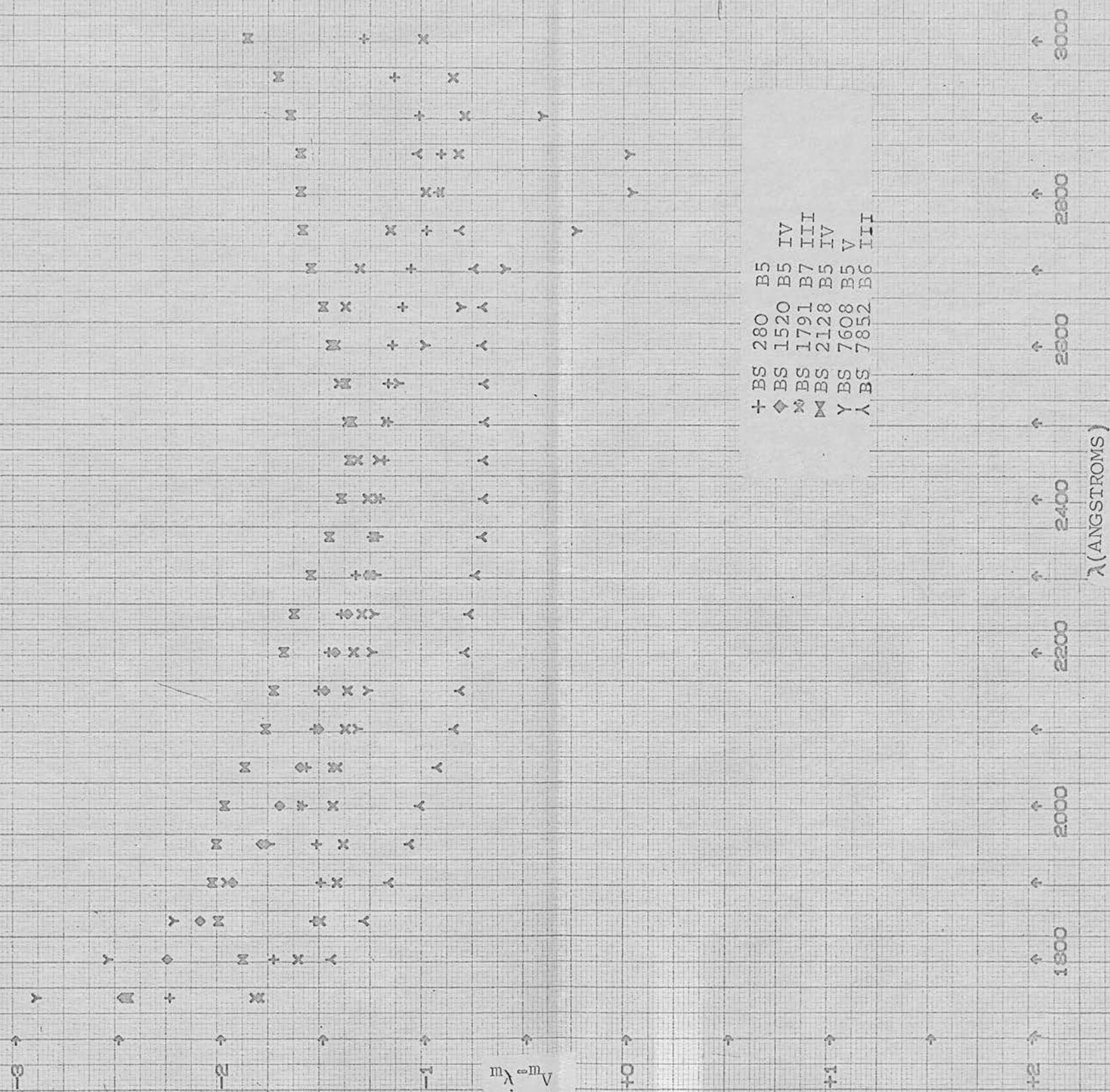


FIG. I5d. PLOTS OF SPECTRAL DISTRIBUTION FOR 36 STARS.

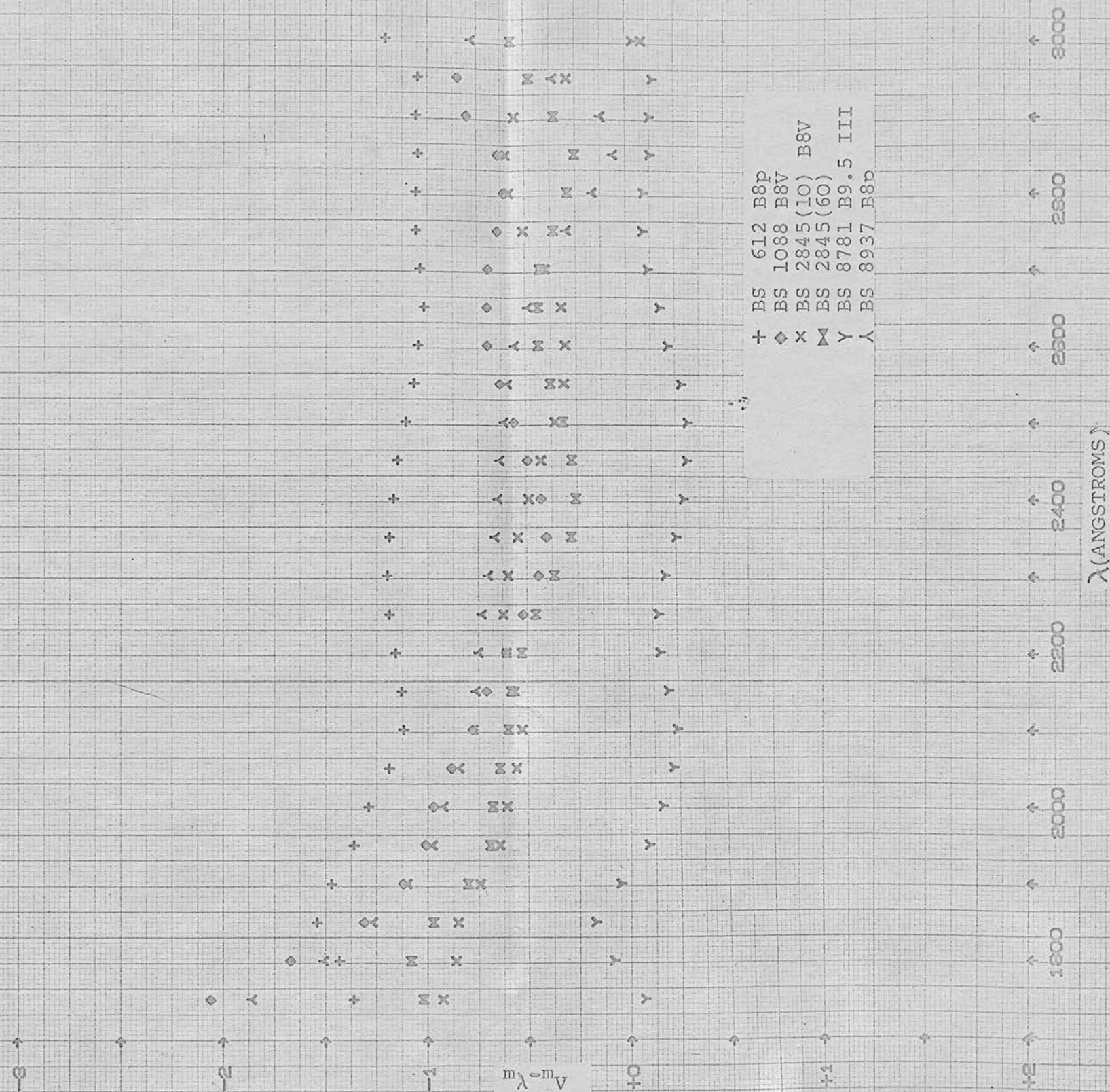


FIG 15e PLOTS OF SPECTRAL DISTRIBUTION FOR 36 STARS.

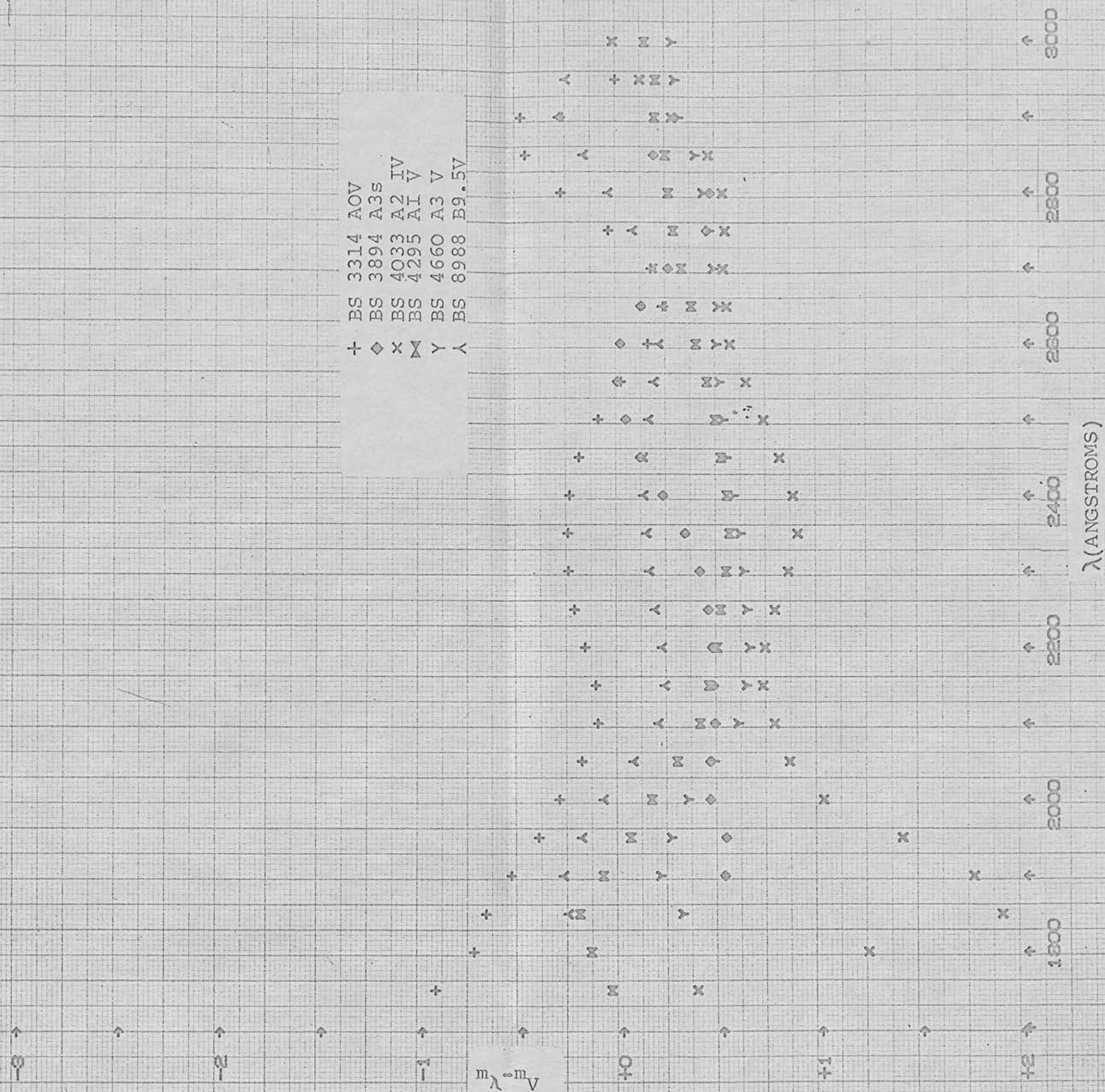


FIG.I5f. PLOTS OF SPECTRAL DISTRIBUTION FOR 36 STARS.

β CMi (BS 2845) which was well observed twice, is variously classified from B7 III to B8 V. The earlier classification would make the star under-luminous and the B8 V classification, which fits well, has been used. The consistency between the two sets of observations (near the beginning and the end of the useful observation period) supports the conclusions of error situation assessment in Section 4.4.

Heintze (1969 loc. cit.) has pointed out that α Scl (BS 280) is wrongly classified as B9 by his criteria and must be B5; this is in complete accord with my observations, which tentatively suggest B5 III.

Comparison with other published observations where these exist at 2100Å and 2500Å is given in Fig. 14 and indicate about 0.6 mag. zero-point departure, in accord with the comparison of Fig. 13.

It should be possible to check and compare the validity of the various measures around 2800Å by comparing to narrow-band ground-based measurements around 3300Å (i.e. shortwards of the Balmer jump but not too near the atmospheric cutoff). Unfortunately, of the very few measures made in this region on bright stars and in usable form, the most extensive and relevant, those of Kharitonov (1963) and Bahner (1963) show differential mean errors of nearly 0.1 magnitude and scatter of similar amount, when normalised to 4030Å. In an endeavour to cast some light on

these discrepancies start was made on a series of narrow band measurements, using filters at 3300Å and 4000Å, on the Royal Observatory twin photoelectric telescope in the Spring of 1970. Eleven stars have been measured, several on more than one night but further measurements, in the Autumn observing season, are believed to be required to ascertain the atmospheric extinction and its variation at Edinburgh.

5. 3. Interstellar Reddening.

It is clear that the Stecher-derived reddening correction has generally been adequate within the scatter, intrinsic and experimental, of the data, and it would be presumptuous to propose any modified law on the basis of these observations. Individually, one may suggest that BS 1903 (ξ Ori) may be under-corrected, although the absence of any comparison supergiant must make this tentative. BS 2128 would appear to be slightly over-corrected in the 2000-2200Å region with reference to the longer and shorter wave-lengths; the presence of an Am star (although these are of "late" type (Ferrer et al 1970)) of comparable visual magnitude again makes any deduction dubious. BS 1542 (α Cam) and BS 1852 (δ Ori), the two most heavily reddened objects in the list, show good agreement at 2500Å, but BS 1542 is either relatively sub-luminous or more reddened at 2200Å.

The dozen or so usable but poorer quality spectra

on fainter stars, not included herewith, may yield some statistically useful data on reddening; however, as these are largely of later types, their mean extinction is not large.

To deduce small adjustments in the interstellar reddening curve on the basis of a small random sample would be particularly dubious with the growing body of evidence that the extinction properties are spatially very variable both in the ultraviolet (Code & Bless 1969) and in the visible (Gottlieb & Upson 1969, Peters 1970).

5. 4. The Galactic and Extragalactic Background.

The data obtained on the background radiation has been described by Sudbury & Ingham (1970 loc.cit.) Reported here is some additional information which was omitted from the reference for the purposes of brevity.

The action of the spectrophotometer as a photometer when viewing background radiation is not quite obvious. A sensor placed behind the slit in fact "sees" the sky as a kind of ultraviolet "rainbow", the lateral extent of the 3° long background field being seen in the various ultraviolet wavelengths corresponding to those which would be received from a star in such a position. The full width half maximum

extent of the field of view is the product of the inverse dispersion with the spectral response f.w.h.m.; hence, for the pulse counting spectrophotometer ($1^\circ = 1216\text{\AA}$) the 770\text{\AA} response embraces a 0.63° field. However, since each element of the field can only contribute 210\text{\AA} (the slit-width) to the detector, the effective field (i.e. the sky area) which corresponds to the full spectral response is only a product of slit height by slit width in field terms i.e. $(2.9^\circ \times 210\text{\AA}) / 1216\text{\AA} \text{ deg}^{-1} = 0.500 \text{ deg}^2$. (by chance!).

The instrument scans approximately 0.4° during the 27.5 m.s. over which the average for each value was taken and so the half-height response of each value is approximately 1° in the scanning direction; the fortunate circumstance of the nodes of the instrument scan pattern on the sky being near the galactic poles enabled this resolution to be exploited in scanning through the galactic plane. It is much greater than, for example, that of Lillie (1968), (about 3°) and although our 0.25 sec. sampling points (except where disturbed by stars) give a similar resolution in the subsequent plot, Lillie has an additional problem due to the stray light from scattering in the quartz lens. We have also the zero order response displaced 2° on the preceding side of the main field which may be expected to have an

(uncalibrated) spectral response determined primarily by the photomultiplier and probably, therefore, somewhat wider than that of the main spectral sensitivity. the relative intensity of the response is assessed by comparing the total counts received in the spectrum and zero order of β Tauri: these amount to 956 and 13,191 respectively. Hence the zero order response intensity is some 7% that of the spectrum response. As the contrast ratio of the sky brightness maps only amount to some 4 : 1, we are justified in neglecting it.

More complete comparison with the calculations of Habing (1968) and the observations of Lillie is possible by summing the counts received from all the observed stars. The sum of the mean counts (per integration interval) for 36 of the spectra of individual stars amounts to 4129. We may allow perhaps another 25% for stars unreduced because of blending, grazing, or faint zero orders, say 5000 counts in all. The twelve useful scans of the sky covered a total area of some 6250 deg²; so, if our sample is typical, the entire 41,250 deg² of sky would yield about 33,000 counts from resolved stars. Using the mean sensitivity of 190×10^9 counts/erg/cm²/sec/Å the total area flux from such sources is 1.7×10^{-7} ergs/cm²/sec/Å or a volume flux of 0.58×10^{-17} ergs/cm³/Å. This is roughly one-third

of the flux obtained by extrapolation of the measured background brightness from the four scans, as published.

It must be noted that over 40% of the measured counts arise from only two sources, γ and δ Ori (which values are also somewhat over estimated due to blending problems), while only 484 counts arise from 24 stars having mean counts of 40 or less. Hence this result would be subject to a very substantial sampling error even if the sampled population were random. Nevertheless, major anisotropy or a dramatic reduction in the total flux would seem to be needed to arrive at the 3:1 ratio in the opposite sense required by the calculation of Habing.

The total flux ($\approx 2.2 \times 10^{-17}$ ergs/cm²/Å) is about half that adopted for the same wavelength region by Lillie from the Aerobee photometer data but substantially nearer to his "Aerobee flight calibration" points; the zero point difference can amount for the residual.

M.F. Ingham provided all the expertise and computations for the zodiacal light reduction in respect of the foregoing work and assembled the published contour map.

5. 5. Conclusions and Prospects.

The data from this project, although plainly diminished in value by the time elapsed from its beginnings, have given both unexpected results in a field little explored, but for which the instrument was not designed, and corroborative data on stellar brightness. In addition to the pre-flight experience of the practical problems of this research, unique in Europe, the subsequent reduction of the data has helped to clarify ideas regarding the reduction of the S2/68 satellite data, whereby the process of scanning a spectrum with the motion of a star image across a (wide) spectrophotometer entrance slot generates output having a close relationship to the rocket data. The consistency of the data has re-emphasised that relative pulse-counting photometry above the atmosphere gives a potential accuracy limited only by photon statistics.

However, in a current context of existing and imminent stabilised satellite and rocket experiments, the remaining potential of the instrument must plainly be questioned. In its present form, a repeat flight of the instrument, which can readily be adapted to second order working at the more interesting wavelengths shortwards of 1700A, could produce a similar

amount of low resolution data at a cost of some £500 per spectrum. If the instrument is properly and absolutely pre-flight calibrated as would now be possible with the Edinburgh satellite facilities, the short lead time to firing of an unstabilised experiment could make this a worthwhile exercise in current scientific terms. Pressed near to its optical limit, with a slit width of some $30\overset{\circ}{\text{A}}$, it could also valuably be used "synoptically" as an adjunct to an objective dispersion photographic experiment. This would enable an extensive net of well (photoelectrically) calibrated photographic spectra to be set up, apart from the several line spectra which the spectrophotometer itself would provide.

The resulting cost per useful data point from the flight, as well as the usefulness of the data itself, would be two or three times more favourable and very similar therefore to that of satellite data (£200-£400 per spectrum), apart from satisfying a current need for the stellar references which satellites, because of the pre-launch procedure, cannot provide.

REFERENCES.

- Alfano, R.P. and Ockman, N. (1968)
J. Opt. Soc. Amer. 58, 90.
- Adams, T.F. and Morton, D.C. (1968)
Astrophys. J. 152, 195.
- Alexander, J.D.H., Bowen, F.J. and Heddle, D.W.O.
(1963) Space Research III, 1068
(ed. Priester) North-Holland Pub.
- Bahner, K. (1963). Astrophys. J. 138, 1314.
- Baker, M. and Laurenson, L. (1966) Vacuum 16, 633.
- Beattie, D.H. and Paterson, C.M. (1970)
J.I.E.R.E. (in press)
- Blanco, V.M., Demers, S., Douglass, C.G. and
Fitzgerald, M.P. (1968) Photoelectric
Catalogue. Pubs. U.S. Naval Obs. 2nd Ser. Vol.21
- Bless, R.C. and Code, A. (1970). Proc. I.A.U. Symp.
No. 36 (in press) North-Holland Pub.
- Bless, R.C., Code, A.D. and Houck. T.E. (1968)
Astrophys. J. 153, 561.
- Bless, R.C., Code, A.D. and Schroeder, D.J. (1968)
Astrophys. J. 153, 545.
- Blondelot, E. (1970) Comunicacion No.12.
Dept. D'Astrophysique, Univ. de Mons
- Boggess, A. and Borgman, J. (1964)
Astrophys. J. 140, 1638.
- Boggess, A.E. and Dunkelman, J. (1958)
Astron. J. 63, 303.
- Boggess, A.E. and Kondi, Y. (1968)
Astrophys. J. 151, 15.
- Campbell, J.W. Absolute Stellar Photometry in the
Region 1900-3000A (in press)
- Cavanaggia, R. and Pecker, J.C. (1953).
Ann. D'astrophys. 16, 47.
- Cayrel, R. (1958) Suppl. Ann. d'Astrophys. No.6.
- Chater, W.T. (1969). Rev. Sci. Instr. 40, 529.

REFERENCES (2)

- Childs, C.B. (1962) Applied Optics 1, 711.
- Chubb, T.A. and Byram, E.T. (1963)
Astrophys. J. 138, 617.
- Code, A.D. (1960) in Stellar Atmospheres p.50.
(ed. Greenstein)
- Code, A.D. and Bless, R.C. (1969)
Publ. Astron. Soc. Pacific 81, 475.
- Davis, J. and Webb, R.J. (1970) Astrophys. J. 159, 551.
- Elst, E.W. (1967) Bull. Astr. Inst. Netherlands 19, 90.
- Fastie, W.G. (1963) J. Quant. Spectrosc. & Radiat. Transfer 3, 507.
- Ferrer, O., Jaschek, M. and Jaschek, C. (1970)
Astron. & Astrophys. 5, 318.
- Fischer, G. (1965). Le Vide 120, 443.
- Fitzgerald, M.P. (1967) Interstellar Reddening in the Environs of the Sun. Thesis. Case Western Reserve University,
- Gottlieb, D.M. and Upson, W.L. (1969)
Astrophys. J. 157, 611.
- Habing, H.J. (1968) Bull. Astr. Inst. Netherlands 19, 421.
- Hayes, D.S. (1970) Astrophys. J. 159, 165.
- Heintze, J.R.W. (1969) Bull. Astr. Inst. Netherlands. 20, 154.
- Hill, G. (1967) Astrophys. J. Suppl. No. 130, 263.
- Hiltner, W.A., Garrison, R.F. and Schild, R.E. (1969)
Astrophys. J. 157, 313.
- de Jager, C. and Neven, L. (1957)
Rech. Astron. Obs. Utrecht. 13, No. 4.
- Kharitonov, A.V. (1963) Sov. Astron. -A.J. 7, 258.
- Kreff, H., Rossler, F., and Ruttenauer, A. (1937)
Zeit. f. Techn. Phys. 18, 20.

REFERENCES (3)

- Kodaira, K. (1970) *Astrophys. J.* 159, 931.
- Kupperian, J.E., Boggess, A.E. and Milligan, J.E.
(1958) *Astrophys. J.* 128, 453.
- Lillie, C.F. (1968) An Empirical Determination of the
Interstellar Radiation Field. Thesis,
Univ. of Wisconsin.
- Lanczos, C. (1957) Applied Analysis. Pitman.
- Mihalas, D.M. (1966) *Astrophys. J. Suppl.* 13, 1.
- Mihalas, D.M. and Morton, D.C. (1965)
Astrophys. J. 142, 253.
- Morton, D.M. and Adams, T.F. (1968)
Astrophys. J. 151, 614.
- Muraca, R.F. (1965) Report on the Telescope Contamin-
ation Problem. Stanford Research Inst.
Aug. 9, 1965 (unpublished).
- Murty, M.V.R.K. (1962) *J. Opt Soc Amer.* 52, 768.
- Oke, J.B. and Schild, R. (1970)
Proc. I.A.U. Symp. No. 36 (in press)
- Osawa, K. (1965) *Ann. Tokyo Astr. Obs. 2nd Series* 9,
No. 3. 123.
- Pao, Y-H., Zitter, R.N. and Griffiths, J.E. (1966)
J. Opt. Soc. Amer. 56, 1133.
- Peters, G. (1970) *Astron. & Astrophys.* 4, 134.
- Peters, G.J. and Aller, L.H. (1970)
Astrophys. J. 159, 525.
- Quinn, T.J. and Barber, C.R. (1967) *Metrologia* 3, 19.
- Saito, S. (1954, 1956) *Contrib. Inst. Astrophys.*
Kyoto, Nos. 48 & 69.
- Samson, J.A.R. (1964) *J. Opt. Soc. Amer.* 54, 6.
- Samson, J.A.R. (1967) Techniques of Vacuum Ultraviolet
Spectroscopy. Wiley.
- Schurer, K. (1968) *Optik*, 1, 44.

REFERENCES (4).

- Smith, A.M. (1967) *Astrophys. J.* 147, 158.
- Spitzer jr., L (1968) Diffuse Matter in Space,
Interscience (Wiley)
- Stecher, T.P. (1965) *Astrophys. J.* 142, 1683
(1969) *Astron. J.* 74, 98.
- Stecher, T.P. and Milligan, J.E. (1962)
Astrophys. J. 136, 1.
- Stothers, R. and Simon, N.R. (1969)
Astrophys. J. 157, 673.
- Sudbury, G.C. (1969) *Appl. Opt.* 8, 2013.
- Sudbury, G.C. and Ingham, M.F. (1970) *Nature* 226, 526.
- Topp, J.A., Schrotter, H.W., Hacker, H., and
Brandmuller, J. (1969). *Rev. Sci. Instr.*
40, 1164.
- Underhill, A.B. (1950, 1956, 1960, 1961, 1962)
Pubs. Dominion Astrophys. Obs. 8, 10, 11.
- Underhill, A.B. (1963) *Space Sci. Rev.* 1, 749.
- Viton, M. (1970) *Proc. I.A.U. Symp. No. 36*, 120.
- Warneck, P. (1965) *J. Opt. Soc. Amer.* 55, 921.
- Wickramasinghe, N.C. (1967)
Interstellar Grains. Chapman & Hall.
- Willstrop, R.V. (1958, 1960)
Monthly Not. Astron. Soc. S. Africa 17, 40.
Monthly Not. Roy. Astron. Soc. 121, 17.
- Wilson, R. (1968) *Ultraviolet Astronomy: Observational
Aspects in Electromagnetic Radiation in Space*
ed. Emming. D. Reidel
- Young, A.T. (1968) *The Observatory* 88, 151.

ACKNOWLEDGEMENTS.

The Introduction has already indicated my extensive indebtedness to the contributions of others in the process of obtaining and reducing this data.

At the Royal Observatory Edinburgh the following were particularly involved in the ways indicated:-

J. Fletcher devised mechanical layouts to solve the R 63 redesign problems, carried out much of the early wiring and testing, and assisted in many day-to-day progressing operations; C.H. Patterson turned the counting system into logic and hardware; D.H. Beattie spent many long hours debugging this and other systems and was a tower of strength in the final calibration, integration and checkout operations and crises on the R 65 (2) instruments; J.H.J. McKemmie manufactured virtually all the mechanical parts of the payloads, turning many outline schemes into mechanical reality with skill, hard work and imagination; J. Clark built much and devised part (J.Clark & G.C. Sudbury 1967)* of the calibration apparatus, assisted with great versatility in its operation, and kept the Space Research Division workshop running smoothly and cheerfully under great pressure of work; J.W. Campbell originated the electronics layouts used in the R 63 instruments; Dr. H.E. Butler gave the initial practical impetus, continued advice as needed, and soothing encouragement and supervision; and Professor H.A. Bruck, as my principal Supervisor, ~~who~~ supported my starting and restarting

* J. Sci. Instrum. 44 , 400.

this part-time course, and ~~who~~ had the imagination and foresight to permit the initiation of ultraviolet astronomy at the Observatory in the infancy of the subject. Mrs D.E. Bashford, G.M. Carstairs and Mrs R.M. Tittensor assisted with many of the tedious plotting, indexing, chart reading, and data typing and editing tasks required to bring the data to usable form.

In external organisations, among many who were involved, Dr. K. Schroeter (ESTEC payload team leader), P. Colson (payload engineer and hatch ejection system designer), E.J. Miller (ESTEC payload contract engineer), R. Hobbs and all his British Aircraft Corporation payload team, S.J. Pooley (range campaign manager), G. Scoon (telemetry engineer), and ESLAB project scientists D.D. Clark, Dr. J. van Boeckel and R. Meiner, are particularly remembered for their endeavours to seek the best solution at all times and in the face of many varied human and technical problems. The co-operation of the European Space Operations Centre and the high quality of the final attitude solution computed by A. Sesma were essential to the successful completion. My father voluntarily undertook the labour of draft and final typing of this thesis and pointed out some stylistic errors; my wife suffered the frequent additional domestic dislocation necessitated by this Project.

All these, and many others who have made perhaps less extensive but still vital contributions, truly deserve

to share the dedication of this thesis.

Since 1965, financial approval of this work has been due to the recommendation of the Astronomy, Space and Radio Board of the Science Research Council, who own the rights in Figures 2 and 3. Figure 4 is by permission of the British Aircraft Corporation. I also thank the Computing Science Department of the Heriot-Watt University for use of their computer graph-plotting facilities for Figure 15. I am indebted to J. Clark for making most of the other diagrams presentable and Miss J. Hardie for additional typing. E.M.I. Electronics Ltd. were generous in the arrangements for the supply of their D104 tube.

APPENDIX I.

DESIGN AIMS OF EXPERIMENT R 63.

(Note:- This Appendix is reproduced exactly as written in 1963 and therefore truly represents the design aim of the instrument as conceived).

Theoretical Assessment of a Convergent Light Scanning Spectrophotometer to be fired in a Skylark Rocket.

(1) The Skylark rocket is at present not roll rate controlled. Rates as high as $100^{\circ}/\text{sec.}$ may be experienced, but improved alignment of fins may reduce this and perhaps the lowest limit, at which roll stability may be lost, is $10^{\circ}/\text{sec.}$ It is necessary to assess the performance of a scanning device at these different rates, and three exemplary values will be chosen, $100^{\circ}/\text{sec.}$ $25^{\circ}/\text{sec.}$ and $10^{\circ}/\text{sec.}$

The nature of the present design of Spectrophotometer is such that it scans through $1000\text{A}/\text{degree}$ of roll. We take a typical slit width as 100A , so that this is scanned by $1/10^{\circ}$ of roll motion. The other parameter we shall assume is of $2\frac{1}{2}\%$ overall quantum efficiency, perhaps composed of 25% optical efficiency and 10% phototube counting efficiency. The effective collecting area is taken as 200 sq. cms.

(2) For a typical star we shall assume a B 0 type

star having the same brightness at 2000A as at 5465, the V filter effective wavelength. Such an $m_v = 0.00$ star will then give, at 2000A, approximately 4×10^{-9} erg/sq cm/sec/A ^② or 4×10^2 quanta/sq cm/sec/A. Hence 2×10^5 quanta/sec will be detected by our instrument from an $m_v = 0.00$ B.O. type star.

The number of quanta actually recorded/100A will be

- (a) At $100^\circ/\text{sec.}$ 2×10^2
- (b) At $25^\circ/\text{sec.}$ 8×10^2
- (c) At $10^\circ/\text{sec.}$ 2×10^3

If we assume a minimum of 10 quanta must be detected to be statistically meaningful, then we can detect B O type stars at the following magnitudes:-

- (a) $m_v = 3$
- (b) $m_v = 4.5$
- (c) $m_v = 5.7$

The output current in each case is about 10^{-8} amps assuming a gain of 10^6 .

② Allen Astrophys Quantities, 1st. Ed. p.24.

Addendum 1970:- The 1968 instruments flew with 200A resolution and $15^\circ/\text{sec.}$ roll rate (i.e. 30% better light collection than the possibility (c)) and stars were detected to magnitude 6.5. The faintest 'normal' star reduced, BS 2288 B 1.5V, magnitude 5.51, gave approximately 80 counts during a scan motion of 100A

near 2500A, or three times the predicted value above.

It was also shown at design stage that, statistically, the total number of stars observed above the threshold level, in a flight, is maximised around 15-30° /sec. roll rate.)

APPENDIX II

Approximate Cost Breakdown of one Spectrophotometer.

(1969 Prices & Exchange Rates are used.)

	£
Primary Mirror manufacture	125
do. do. coating & overcoating	90
Diffraction Grating overcoated	100
Fabry Lens (assuming CaF ₂)	30
E H T inverter	100
L T inverter	100
Stabilisers, smoothing components	50
Externally manufactured boxes, aluminium alloy, castings (including part cost of patterns)	say 100
Miscellaneous electronics, relays, connectors, PTFE wire, encapsulants	say 150
	<hr/> 845

ADD

Either

Ascop photomultiplier	850	
D.C. Amplifiers	<u>50</u>	
	900	
	TOTAL	<u>£1,745.</u>

Or

OR

Select one from three		
E.M.I. photomultipliers		
@ £100 each	300	
Pulse counting & logic	<u>150</u>	
	450	
	TOTAL	<u>£1,295.</u>

APPENDIX III

The Sky Background Experiment (R.O.E.-D.)

This experiment had for the Division two main objectives:-

- (1) The determination of the U.V. background brightness by day and by night for astrophysical and technical purposes,
- and (2) The development and proving of the techniques and instrumentation required for subsequent experiments.

Although the daytime determination was of some interest for the Division's already initiated involvement in the S1/2/68 telescope, it was necessitated in this case by the fact that the pair of rounds on which suitable space was available at short notice was due to have a night and a day firing for the benefit of the primary experimenter. The instrument was conceived simply as a photomultiplier of the solar-blind type (a CBS CL 1064 with rubidium telluride cathode and quartz window in fact) viewing the sky through a set of concentric rectangular apertures in a baffle system, so as to provide a field of some one hundred square degrees ($12^{\circ} \times 8^{\circ}$ in fact). The rectangular shape was dictated by the rectangular (25mm X 10mm) opaque photocathode. A Ledex-driven wheel, which stepped successively in the light path to the photocathode a clear aperture, an OX-10 glass filter (bandpass 2500 - 4000Å approximately) and an opaque segment, giving some indication of the

spectral distribution and the essential knowledge of the dark current plus amplifier drift. For the daytime flight a photodiode actuated a Ledex holding a shutter arm so as to protect the photomultiplier when the field of view came near the sun.

The power supply was a special one based off the R.A.E. (Farnborough) GW 10 inverter which fed both the twin LT stabiliser boards for the amplifier and an EHT transformer, the rectified output (3KV maximum) of which was stabilised by "corona" tubes. Much trouble was experienced due to the breakdown of the high voltage at low pressures, in spite of the silicone rubber encapsulation. Nevertheless it was essentially this unit which, with rebuilt EHT, successfully provided supplies for the spectrophotometer flown in the S-05/1 instrument while for the S-05/2 the same system was divided to give a separate EHT unit for easier servicing. The practice, followed in all subsequent R.O.E. experiments, of having the EHT off during ascent until the corona region is passed, was initiated (by the author) as a modification on the R.O.E.-D. experiment following corona experienced during testing. With the design of corona tube (G.E.C.) available at that time it did require some thirty seconds for the EHT output to settle from a value about 50 volts above the final value (by the flight of S.05/2 the use of Victoreen tubes had eliminated this problem).

The D.C. amplifier was a discrete transistor P.C.B.

unit based on the design of Fastie (1963) but without the range extension by means of diode shunting of the feedback resistor described by Fastie (see also section 2.5.1.3.). Instead, use was made of the six available filter wheel positions to allow three of them to operate on lower sensitivity. This change was initiated by a cam on the wheel.

An extensive monitoring system (E.H.T., L.Ts., wheel position, amplifier sensitivity, solar shutter) was employed. This showed that on the successful daytime round (SL 141) all systems functioned correctly. When a correct attitude solution was eventually received in 1966, it showed that the output was saturated when it viewed earth or nearer than 70° to the sun but at other points the output fell to quite low levels. There appeared however to have been a substantial change in the absolute calibration between laboratory and range measurements, and some corona breakdown also seems to have occurred in flight due to inadequate venting of the photomultiplier base, for a short period after E.H.T. switch-on (recurring at re-entry). The data is thus only of qualitative value in implying the relative darkness of the sky, (now known from satellite measurements to be plenty low enough for stellar observations) when the line of sight is sufficiently far away from the sun to prevent sunlight falling on the baffle system.

J.W. Campbell had prime responsibility for the

electronics design and detector mount of this instrument and J.M. Fletcher played a major part on the mechanical design. My own activities were primarily on the electromechanical systems (filter wheel and shutter) optical baffle design, and angular and spectral response. However there was close group liason on all aspects of the design and many of the ideas developed jointly.

APPENDIX IV

Computer Programmes Developed for Spectral Reduction

SNORE B4.

SPLOT 5B.

AMPL 4.

COMT 4.

FOLGEN.

```

SNORE B4;
"BEGIN"
  "INTEGER" BS, N, J, K, M;
  "REAL" NZ;
  "ARRAY" CRIT 1[1:24];
  M:=26;
  "FOR" K:=1 "STEP" 1 "UNTIL" 24 "DO" "READ" CRIT 1[K];
    "BEGIN" "COMMENT" CALCOR READIN;

  "REAL" "ARRAY" CAL[1:2,0:M], L[0:M], REDCOR[0:M];
  "FOR" K:=0 "STEP" 1 "UNTIL" M "DO"
    "BEGIN"
    "READ" CAL[1,K], CAL[2,K], REDCOR[K];
    L[K]:=CAL[1,K];
    "END" OF K-CYCLE;
  PUNCH(4);
  "COMMENT" N+1 IS THE NO. OF DATA,
  J IS MAXIMUM DEGREE OF FIT WANTED
  M+1 IS THE NO OF INTERPOLATION POINTS;
  B:WAIT;
  "READ"BS, N, J;
  "IF" J=-8 "THEN"
    "BEGIN""IF" N>34 "THEN" J:=-12 "ELSE"
    "BEGIN" "IF" N>30 "THEN" J:=-10;
    "END";
  "END" OF J-SWOP;

  "BEGIN"
  "ARRAY" X, Y, WT[0:N], W[0:2, -1:(ENTIER(ABS(J)+0.05))],
  Z, YY[0:M], RAW[-1:N+1], SPEC[1:2,0:M];
  "INTEGER" J1, PRT, I;
  "REAL" SIG;
  "REAL""PROCEDURE" SMTHFN(J, A);
  "VALUE" J;
  "INTEGER" J;
  "REAL" "ARRAY" A;
  "BEGIN" "REAL" B;
  B:=A[J-1]+2*A[J]+A[J+1];
  B:=B/4;
  "PRINT" ALIGNED (5,1), (A[J]), "'S6'", SAMELINE, (B), "'L'";
  SMTHFN:=B;
  "END" SMTHFN;

  "REAL" "PROCEDURE" SUMMIT (BOT, TOP, I, EL);
  "VALUE" BOT, TOP;
  "INTEGER" BOT, TOP, I;
  "ARRAY" EL;
  "BEGIN" "REAL" TOT; TOT:=0;
  "FOR" I:=BOT "STEP" 1 "UNTIL" TOP "DO"
    TOT:= TOT + EL[I];
    SUMMIT:= TOT;
  "END" SUMMIT;
  "LIBRARY" OPY, ORTHPOLY;

```

"COMMENT" SNORE B4 PAGE 2;

"FOR" K:=-1 "STEP" 1 "UNTIL" N+1 "DO"

"READ" RAW[K];

"READ" NZ;

NZ:=SQRT(NZ);

"PRINT" 'BS',DIGITS(4),BS,'L2', 'S2' A[J] 'S8' B[J] 'L2';

"FOR" K:=0 "STEP" 1 "UNTIL" N "DO"

"BEGIN"

Y[K]:=SMTHFN(K,RAW);

WT[K]:=(Y[K])/(SQRT(Y[K])+NZ);

X[K]:=K;

"END" OF K - CYCLE;

"PRINT" 'L' MEAN COUNTS', SAMELINE,

ALIGNED(5,0), SUMMIT(0,N,K,Y)/N,

' MEAN WT ',ALIGNED(2,1),((SUMMIT(0,N,K,WT))/N);

PRT:=1;

ORTHPOLY (X,Y,WT,N,J,W,K,J1,SIG,PRT);

"BEGIN"

"COMMENT" INTERPOL PROGRAM;

"INTEGER" C,A,H;

"REAL"INT,DEL,PE,D,R;

"INTEGER" "ARRAY" RESULT [1:10];

F: "BEGIN"

"COMMENT" INNER BLOCK;

"BEGIN"

"READ" D,INT, DEL,PE;

R:=INT+DEL;

"PRINT" PUNCH(4),'L',

FREEPOINT(4),'R ',R,' D ',D,' NZ ', (NZ*NZ),'L';

"END";

PUNCH(4);

A:=1;

INSTRING (RESULT,A);

A:=1;

OUTSTRING (RESULT,A);

PUNCH(3); "PRINT" 'L',DIGITS(4), BS;

PUNCH(4);

"END" OF INNER BLOCK;

"PRINT" 'L2';

PUNCH(1); "PRINT" 'RLQ'BS', DIGITS(4), BS, 'UL'; PUNCH(4);

"FOR" I:=0 "STEP" 1 "UNTIL" M "DO"

"BEGIN"Z[I]:=(L[I])/D-R;

YY[I]:=OPY(W,J1,Z[I]);

"PRINT"PREFIX('S2'), ALIGNED (4,0), (L[I]),

ALIGNED (4,1), (YY[I]),ALIGNED (2,3), (Z[I]), 'L';

"PRINT" PUNCH(1),(L[I]),(YY[I]);

"END";


```

"COMMENT" SNORE B4 PAGE 3;
"PRINT" 'L2S6`N`S4`Y[I]`S4`WT[I]`S2``, SAMELINE,
'Y[I]-OPY`S2` WT[I]/(Y[I]-OPY) `L``;
"FOR" I:=0"STEP" 1 "UNTIL" N "DO" "BEGIN"
"PRINT" I, PREFIX('S2`'), ALIGNED(4,0),(Y[I]), WT[I],
ALIGNED (4,0),(Y[I]-OPY(W,J1,X[I])),
ALIGNED (4,2),(WT[I]/(Y[I]-OPY(W,J1,X[I]))), 'L``;
"END";

```

```

"END" OF INTERPOL PROGRAMME;
"BEGIN" "COMMENT" THIS IS THE CALCOR TREATMENT;
"REAL" MAG,BVX,RAY,SW;
"REAL" "ARRAY" TEMP[0:M];
"READ" MAG,BVX;
RAY:=EXP(0.9211*MAG);
SW:=210.0;

```

```

"PRINT" 'L` MAG `,MAG,` BVX `,BVX,` RAY `,RAY;
"PRINT"
'FLS8`BS`, DIGITS(4), BS`,` V=`,
ALIGNED(1,2), MAG,` (B-V)XS `,BVX,`LS7Q``,
'FLUXES AND MAGS. NORMALISED TO V=0 (3.8*10-9 CGS/A)

```

```

LAMBDA FLUX RDCRFLX MAG RDCRMAG WT RECIP-MU
[NM] [(CGS/A)*10-9] `UL``;
"PRINT" PUNCH(1), 'L6``;

```

```

"FOR" K:=1 "STEP" 1 "UNTIL" M "DO"
"BEGIN"
"IF" Z[K]<1 "THEN" "GOTO" CYC;
"IF" Z[K]>(N-1) "THEN" "GOTO" CYC;

```

```

"BEGIN"
"REAL" LUVMAG;
SPEC[1,K]:=CAL[1,0]/10 + 5.0*K;
SPEC[2,K]:=YY[K]*CAL[2,K];
LUVMAG:= -(LN((SPEC[2,K])/(3.8*SW)))/0.9211;
TEMP[K]:=SPEC[2,K]*RAY*(EXP(0.9211*REDCOR[K]*BVX))/SW;
"PRINT" PREFIX('S2`'), ALIGNED(8,0), (SPEC[1,K]),
ALIGNED(2,2), '`,`(SPEC[2,K]*RAY/SW), (TEMP[K]),
ALIGNED (1,2), (LUVMAG - MAG), (LUVMAG-MAG-BVX*REDCOR[K]),
ALIGNED(2,0), WT[ENTIER(Z[K]+0.5)], ALIGNED(1,2),
'`,`((103)/(SPEC[1,K])), 'L2``;

```

```

"PRINT" PUNCH(1),(SPEC[1,K]),
(LUVMAG-MAG), (LUVMAG-MAG-BVX*REDCOR[K]);

```

```

"END";

```

```

CYC:

```

```

"END" OF K-CYCLE;

```

```

"PRINT" PUNCH(1), 'L``,10000,'R``;

```

```

"END" OF CALCOR;

```

```

"PRINT" 'F``;

```

```

PUNCH(3);

```

```

"PRINT" 'L`LOAD NEW DATA`;

```

```

PUNCH(4);

```

```

"END" OF OUTER BLOCK; "GOTO" B;

```

```

"END";

```

```

"END" OF PROGRAMME;

```

```

SPLOT 5B;
"COMMENT" PLOTS SIX OUTPUTS FROM SNORE B PUNCH(1);
"BEGIN"
  "INTEGER" K,A,COUNT;
  "REAL" SPEC, TEMP, LUVMAG;
  COUNT:=1; SETORIGIN(250,0);
  "FOR" K:=-250 "STEP" 125 "UNTIL" 750 "DO"
    "BEGIN" MOVEPEN(0,K);
      CENCHARACTER(9);
    "END" OF Y(MAG) SCALE;
  "FOR" K:=0 "STEP" 150 "UNTIL" 1950 "DO"
    "BEGIN" MOVEPEN (K,-250);
      CENCHARACTER (10);
    "END" OF SCALE MARKING;

DATIN: WAIT;
"BEGIN"
  "INTEGER" "ARRAY" RESULT[1:10];
  A:=1;
  INSTRING(RESET,A);
  PUNCH(3);
  "PRINT" 'L';
  A:=1; OUTSTRING(RESET,A);
  "FOR" K:=0 "STEP" 1 "UNTIL"26 "DO"
    "READ" SPEC, TEMP;
    "COMMENT" THESE RE REDUNDANT ELEMENTS;
    "FOR" K:=0 "STEP" 1 "UNTIL" 50 "DO"
      "BEGIN"
        "READ" SPEC;
        "IF" SPEC>3000 "THEN"
          "BEGIN" COUNT:=COUNT+1; "GOTO"KEY;
          "END"
        "ELSE" "BEGIN"
          "READ" TEMP,LUVMAG;
          MOVEPEN ((15*(SPEC-170)),(-250*LUVMAG));
          CENCHARACTER(COUNT);
        "END";
      "END" OF K-CYCLE;

KEY:
  MOVEPEN(1500,(750-50*(COUNT-1)));
  CENCHARACTER(COUNT+1);
  MOVEPEN(1550,(740-50*COUNT));
  PUNCH(5); WAY(0,5));
  A:=1; OUTSTRING(RESET,A);
  "IF" COUNT>6 "THEN"
    "BEGIN"
      "PRINT" PUNCH(3), 'L' FRESH PAPER RESTART PROGRAM PLEASE
    "END"
    "ELSE" "BEGIN"
      "PRINT" PUNCH(3), 'L' MORE DATA PLEASE;
      "GOTO" DATIN;
    "END"
  "END" OF PLOT SEQUENCE;
"END" OF SPLOT;

```

AMPL1;

"COMMENT" CONVERTS AMPLIFIER CALIBRATION TO ARRAY
FOR THE DIGITISED TAPE VIA A LINEAR/POLYNOMIAL FIT;
"BEGIN"

"INTEGER" K,L,M,N,J;

"REAL" "ARRAY" X,Y,WT[0:200], CRIT1[1:24], TITLE[1:10];

"FOR" K:=1 "STEP" 1 "UNTIL" 24 "DO"

"READ" CRIT1[K];

"READ" J;

K:=1;

INSTRING(TITLE,K);

"FOR" K:=0 "STEP" 1 "UNTIL" 200 "DO"

"BEGIN"

"READ"X[K]; "IF"X[K]<-9999 "THEN"

"BEGIN" N:=K-1;

"GOTO" NEWBIT;

"END" "ELSE" "READ" Y[K];

"END";

NEWBIT: "READ" L;

"IF" L=0 "THEN" "GOTO" EVWT;

"IF" L=-1 "THEN" "GOTO" RTWT;

"IF" L=1 "THEN" "GOTO" RDWT;

EVWT: "FOR" K:=0 "STEP" 1 "UNTIL" N "DO"

WT[K]:=1.0;

"GOTO" POLBEG;

RTWT: "FOR" K:=0 "STEP" 1 "UNTIL" N "DO"

WT[K]:=SQRT(N);

"GOTO" POLBEG;

RDWT: "FOR" K:=0 "STEP" 1 "UNTIL" N "DO"

"READ" WT[K];

POLBEG:

"BEGIN"

"ARRAY" W[0:2,-1:J],YY[0:200];

"INTEGER" J1,PRT,I;

"REAL" SIG;

"LIBRARY" OPY,ORTHPOLY;

PUNCH (4);

PRT:=1;

ORTHPOLY(X,Y,WT,N,J,W,K,J1,SIG,PRT);

PUNCH (1);

"PRINT" '^RL^';

K:=1;

OUTSTRING(TITLE,K);

"PRINT" '^L^';

"FOR" K:=-1 "STEP" 1 "UNTIL" J "DO"

"BEGIN" "FOR" L:=0 "STEP" 1 "UNTIL" 2 "DO"

"PRINT" W[L,K];

"PRINT" '^L^';

"END"

"PRINT" '^L2R^';

"COMMENT" AMPL1 PAGE 2;

CURCAL:

"BEGIN" "COMMENT" THIS BLOCK IS SPECIAL FOR THE DC TAPE;

"REAL"VOLTS, NAMPS;

PUNCH (4);

"PRINT" 'L';

K:=1;

OUTSTRING(TITLE,K);

"PRINT" 'L2`NANOAMPS`L';

PUNCH (1);

"PRINT" `NANOAMPS`L';

"FOR" K:= -128 "STEP" 8 "UNTIL" 119 "DO"

"BEGIN" "FOR" L:=K "STEP" 1 "UNTIL" K+7 "DO"

"BEGIN"

"READ" VOLTS;

"IF" VOLTS>1250 "THEN"NAMPS:=OPY(W,J,VOLTS)

"ELSE"

NAMPS:=VOLTS/180;

"PRINT" NAMPS;

"PRINT" PUNCH(4), ALIGNED(3,2), NAMPS;

"END" OF L-CYCLE;

"PRINT" 'L'; "PRINT" PUNCH(4), 'L';

"END" OF K-CYCLE;

"PRINT" 'R';

"END" OF CURCAL;

"END" OF POLBEG;

"END" OF GENPOLY;

"COMMENT" AMPL1 IS AN ADAPTETION OF A GENPOLY FIT
PROGRAMME;

COMT4;

"COMMENT" PROGRAM FOR EXTRACTING DATA BETWEEN TWO TIMMES
TIMBEG AND TIMEND ON MAG TAPE AND ASSEMBLING INTO A
SINGLE ARRAY TAPINT WHICH IS CONVERTED TO CURRENT
READINGS AS STAMPS (STELLAR AMPS);

"BEGIN"

"INTEGER" K,L,M,I,J,MYBLOK,SAMPLE;

"INTEGER" "ARRAY" TAPINT[1:1000],

DUMP[-1:512], TINT[1:4];

"BOOLEAN" WUNBLOK;

"REAL" TIMBEG,TIMEND;

"REAL" "ARRAY" TEBLOK[1:2], STAMPS[1:1000], NAMPS[-128:
128];

"FOR" I:=-128 "STEP" 1 "UNTIL" 119 "DO" "READ" NAMPS[I];

"COMMENT" NAMPS IS THE TELY*AMP CONVERSION ARRAY;

MORE:

"BEGIN"

"READ" TIMBEG,TIMEND;

"IF" TIMEND<TIMBEG "THEN" "GOTO" END;

M:=1;

MTSOURCE(4,'RCC062ES');

"FOR" K:=1 "STEP" 1 "UNTIL" 4 "DO"

MTREAD(4,TINT,1,1);

NUBLOC:

MTREAD(4,TINT,1,2);

TEBLOK[1]:= TINT[1]+ 0.001*TINT[2];

WUNBLOK:="FALSE";

"IF" TEBLOK[1]>TIMEND "THEN" WUNBLOK:="TRUE";

"IF" TEBLOK[1]>TIMBEG

"THEN" "BEGIN"MYBLOK:=M-1;

MTBACK(4);

MTBACK(4);

MTREAD(4,TINT,3,2); MTBACK(4);

TEBLOK[2]:= TINT[3]+0.001*TINT[4];

"GOTO" GOTIT;

"END"

"ELSE" "BEGIN" M:=M+1;

"GOTO" NUBLOC;

"END";

GOTIT: "BEGIN"

MTREAD (4,DUMP,-1,511);

"PRINT" PUNCH(4),'L', PREFIX(' '), 'MYBLOK', MYBLOK,

' MTCOND', MTCOND(4), ' TIMBEG', TIMBEG,

' TEBLOK', TEBLOK[1],

TEBLOK[2], 'L', DUMP -1,0), (DUMP[-1]), DUMP[0], 'L';

"FOR" L:=1 "STEP" 8 "UNTIL" 505 "DO"

"BEGIN"

"FOR" K:=L "STEP" 1 "UNTIL" L+7 "DO"

"PRINT" PUNCH(4), PREFIX(' '), DIGITS(3), DUMP[K];

"PRINT" PUNCH(4), 'L';

"END" OF L-CYCLE;

X: "END" OF DUMP SEQUENCE;

"END" OF TIMBEG FIND;


```

"COMMENT" COMT4 PAGE2;
"BEGIN" "COMMENT" TRANSFER AND CONVERSION BLOCK;
  "REAL" TEDIF1,TEDIF2;
  "INTEGER" ELBEG,ELEND,TAPTOT;
  TEDIF1:=TIMBEG-TEBLOK[2];
  TEDIF1:=1000*TEDIF1-0.9;
  ELBEG:=ENTIER(TEDIF1);
  "FOR" I:=ELBEG+1 "STEP" 1 "UNTIL" 509 "DO"
    "BEGIN" K:=I-ELBEG;
    TAPINT[K]:=DUMP[I];
    "END";
  K:=509-ELBEG;
  "COMMENT" K IS NOW NO. OF ELEMENTS OF TAPINT FILLED FROM
  DUMP;

  "IF" WUNBLOK "THEN"
    TEDIF2:=TIMEND-TEBLOK[2]
  "ELSE" "BEGIN"
    TEDIF2:=TIMEND-TEBLOK[1];
    MTREAD(4,DUMP,-1,511);
    "END";
    TEDIF2:=1000*TEDIF2;
    ELEND:=ENTIER(TEDIF2-0.9);
    "IF" WUNBLOK "THEN" "GOTO" ENUF "ELSE"
      "FOR" I:=1 "STEP" 1 "UNTIL" ELEND "DO"
        TAPINT[K+I]:=DUMP[I];
  ENUF:
  "PRINT" PUNCH(4),DIGITS(4), 'ELS',ELBEG,ELEND,
  ALIGNED(4,1), 'TEDS',TEDIF1,TEDIF2, 'L';

  TAPTOT:=K+ELEND;
  "PRINT" PUNCH(4),DIGITS(4), 'TAPTOT',TAPTOT, 'L';

  "FOR" I:=1 "STEP" 5 "UNTIL" TAPTOT-4 "DO"
    "BEGIN""PRINT" PUNCH(4), 'L', DIGITS(4), I, 'S2';
    "FOR" K:=I "STEP" 1 "UNTIL" I+4 "DO"
      "BEGIN"
        "PRINT"PUNCH(4),SAMELINE, DIGITS(4), TAPINT[K];
        J:=TAPINT[K];
        STAMPS[K]:=NAMPS[J];
        "PRINT"PUNCH(4),SAMELINE, ALIGNED(4,2),(STAMPS[K]);
      "END" OF K-CYCLE;
    "PRINT"PUNCH(4), 'L', DIGITS(4), I, 'S2';
  "END" OF I-CYCLE;
  "END" OF T/F & CONV BLOCK;
END: "END" OF COMT;

```

FOLGEN;

"COMMENT" FOLDS A WITH SYMMETRICAL C POINT BY POINT;

"BEGIN" "INTEGER" I,J,K,RANUM; "REAL" NORM,FACTOR;
"REAL" "ARRAY" A,B,UNORM[0:100];

"REAL" "PROCEDURE" SUMMIT (BOT,TOP,I,EL);
"VALUE" BOT,TOP;
"INTEGER" BOT,TOP,I;
"ARRAY" EL;
"BEGIN" "REAL" TOT; TOT:=0;
"FOR" I:=BOT "STEP" 1 "UNTIL" TOP "DO"
TOT:= TOT + EL[I];
SUMMIT:= TOT;
"END" SUMMIT;

"FOR" I:=0 "STEP" 1 "UNTIL" 100 "DO"
"BEGIN" "READ" A[I];
"IF" A[I]=-1 "THEN" K:=I-1;
"IF" A[I]=-1 "THEN" "GOTO" X;
"END";

X:

"READ" RANUM,FACTOR;
"BEGIN" "REAL" "ARRAY" C,D[-RANUM:RANUM];
"FOR" I:=0 "STEP" 1 "UNTIL" RANUM "DO" "READ" C[I];
"FOR" I:=-RANUM "STEP" 1 "UNTIL" -1 "DO" C[I]:=C[-I];

NORM:= SUMMIT(-RANUM,RANUM,I,C);

NORM:=NORM*FACTOR;

"PRINT" PUNCH (4), 'NORM', NORM, 'L',
'B[J]', SAMELINE, 'S6', 'A[J]', 'L';

"FOR" J:=RANUM "STEP" 1 "UNTIL" K-RANUM "DO"

"BEGIN" "INTEGER" S,L;

"FOR" S:=-RANUM "STEP" 1 "UNTIL" RANUM "DO"

"BEGIN" L:=J-S;

D[S]:= C[(S)]*A[L];

"END" OF S-CYCLE;

UNORM[J]:= SUMMIT(-RANUM,RANUM,S,D);

B[J]:=UNORM[J]/NORM;

"PRINT" PUNCH(4), ALIGNED(4,1), PREFIX('S3'), (B[J]), (A[J]),
UNORM[J], 'L';

"END" OF J-CYCLE;

"END" OF FOLD;

"END";

A Rocket-Borne Photoelectric Spectrophotometer Using Convergent Beam Dispersion to Observe Far Ultraviolet Stellar Spectra

G. C. Sudbury

**COMMUNICATION FROM THE
ROYAL OBSERVATORY, EDINBURGH
No. 73**

a reprint from **Applied Optics**
volume 8, number 10, October 1969

A Rocket-Borne Photoelectric Spectrophotometer Using Convergent Beam Dispersion to Observe Far Ultraviolet Stellar Spectra

G. C. Sudbury

The advantages of the Monk-Gillieson dispersion system using a plane grating off axis in the convergent beam from a paraboloidal collecting mirror have been applied to obtain low resolution photoelectric spectra of over forty bright stars in the 1500–3000 Å region. Techniques of construction, alignment, calibration, and dc and pulse counting output data handling are described. The flight performance, in unstabilized Skylark rockets, is discussed.

I. Introduction

It has been known for a long time that a dispersive element may be used in the convergent beam of a focusing system, if high spectral resolution over an extended wavelength region is not required.^{1,2} However the particular application described here was inspired by a paper by Murty,³ in which is illustrated and analyzed the method of using a paraboloid to collect parallel light and a plane grating placed off axis to the mirror to produce dispersed images, which at one wavelength are acomaatic as well as anastigmatic. This paper describes how one form of Murty's scheme has been applied in the construction, at the Royal Observatory, Edinburgh, of a series of rocket-borne scanning monochromators. Flight data are also presented which demonstrate the performance of these instruments in measuring far uv stellar continuous spectra at low resolution.

At the time Murty's paper appeared the Space Research Group of the Royal Observatory, Edinburgh, was in process of formation and the then recent success and unexpected results of the NASA Goddard Space Flight Center-Institute of Optics-Naval Research Labora-

tory rocket-borne uv stellar spectrophotometer^{4,5} underlined the potential of that line of work. In Europe, as in the U.S.A., at that time only unstabilized rocket vehicles were available for stellar work. Therefore, the same principle of a random sky scan had to be employed, by which the vehicle roll motion causes the spectra of stars within the field to be swept across the measuring slit. For our purposes, though, the convergent beam dispersion type of spectrometer seemed preferable to the more conventional incident beam dispersion system of Ref. 4 (referred to as BMHS), for a number of reasons:

(1) One less reflecting surface is required, given that beam-folding is necessary to fit the large aperture optics within the rocket diameter; the improvement in transmission efficiency and reduction in scattered light are particularly worthwhile for stellar work in the far uv.

(2) Since the zero order is heavily vignetted (by a factor of about ten) at the grating stop, the use of a *visual blind* photocathode (e.g., cesium telluride) provides sufficient further reduction of sky light to make venetian blind type sky baffles unnecessary; besides increasing the transmission, especially near the limits of the wavelength range, the possibility of spurious responses by baffle *glints* is also reduced.

(3) A substantial advantage at European finance levels lies in the relative cheapness of the optical elements; in particular only one quite small grating is needed, compared with the mosaic of four 104-mm square gratings for a smaller collecting area in the BMHS system.

(4) The optical mounting problems and weight for an instrument of similar aperture are obviously less than in the BMHS instrument.

The author is with the Royal Observatory, Edinburgh 9, Scotland, U. K.

Received 5 March 1969.

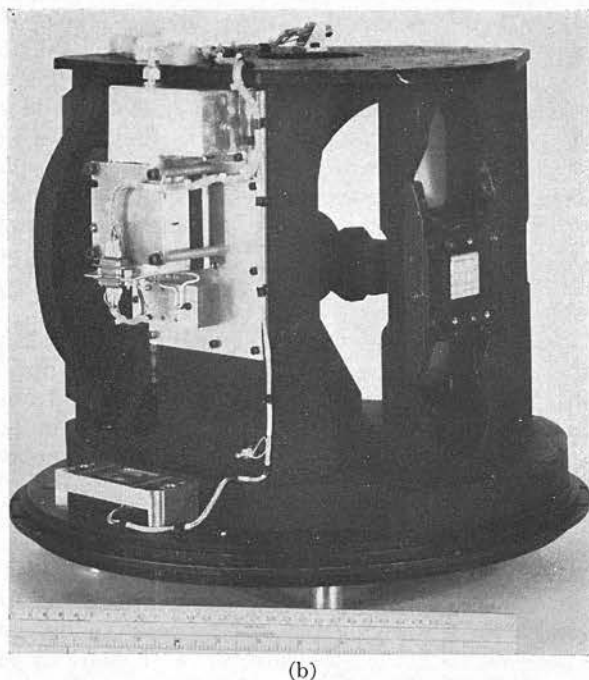
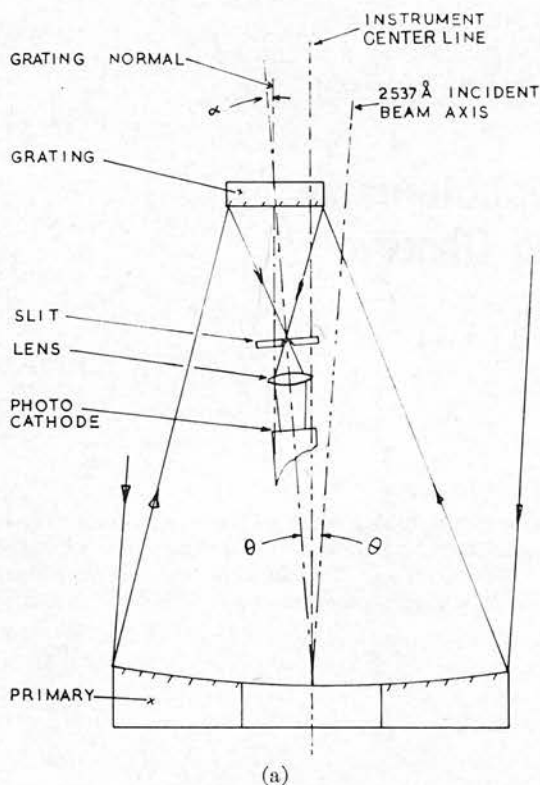


Fig. 1. (a) Optical layout of spectrophotometer. (b) see Spectrophotometer in flight configuration.

At the same time three superficial disadvantages of the convergent beam system were not of any substantial account in our application:

(1) Using a 21.5-cm diam collecting mirror, which is nearly as large as the aperture available in the standard Skylark sounding rocket section, a beam approaching $f/2$ can be accommodated; the convergence of the beam is then sufficiently low that the loss of resolution away from the optimum wavelength is unimportant compared with the limitations on slitwidth resolution of photon noise statistics, imposed by the short available scanning time for each star.

(2) Since the angular dispersion is a function of the grating-to-focal-plane distance, it is low—about one-fifth of a BMHS system of similar dimensions. As only the completely uncontrolled Skylark was available to the group when design was begun, a low dispersion reduced the chances of spectra being truncated due to the precession rate (which might be large relative to the roll-rate) carrying the dispersed image off the end of the measuring slit; given the nonrandom spatial distribution of bright early type stars, the likelihood of blending of the spectra of nearby stars is also reduced.

(3) As pointed out by Murty,⁶ a substantial amount of convergence on to the plane grating *spreads* the blaze efficiency as a function of wavelength when compared with its variation in a collimated incident beam. The net loss is not great for an instrument required to work usefully over an entire octave of frequency; in fact without this spreading the combination of blaze efficiency with vignetting and photocathode/window cutoffs might produce an undesirably peaky response.

II. The Instrument: Optical Details

The optical layout of the spectrophotometer is shown in Fig. 1 (a). The optical specification of the latest form of the instrument is as follows:

Primary mirror: Paraboloid, over-all diameter 8.5-in. (215-mm), focal length 15.5 in. (394 mm) approximately, material plate glass, manufactured by G. A. Hole and Son, Brighton, England. Aluminized and overcoated with MgF_2 by Pilkington-Perkin-Elmer, St. Asaph, Wales.

Grating: Plane 58-mm square blank, 52-mm square rulings, 600 lines/mm, replica on fused silica blank, 2000 Å blaze, manufactured, aluminized, and overcoated by Bausch & Lomb Inc., Rochester, U.S.A.

Lens: biconvex symmetrical, 1.25-in. (31.5-mm) radius of curvature, material—calcium fluoride, manufacturer—West Instruments, Brighton, England.

Photomultiplier: Either cesium telluride photocathode on 2.54-cm diam sapphire window, venetian blind dynodes, manufactured by EMR Inc., Sarasota (Ascop type 541F 05-M 14) used in direct current mode or cesium telluride photocathode on 2.54-cm diam fused silica window, box and grid dynodes with internal dynode chain (2 MΩ), manufactured by EMI Electronics, Ltd., Hayes (type D104 QB development model), used in pulse-counting mode.

The mirror-grating spacing is approximately 280 mm and the grating vertical center line is positioned 4.25° off axis with respect to the primary mirror. The

photomultiplier and lens axes lie along the mirror-grating pole line.

Dispersion is typically between 1000 Å and 1250 Å per degree of rotation depending on the exact primary focal length; the field perpendicular to the dispersion direction is 3°.

III. Mechanical Construction

Figure 1(b) shows the instrument in its current form. The members carrying the optical parts are screwed to the machined face of a cast magnesium alloy (type ZRE1) baseplate which itself is screwed to a standard bulkhead of the rocket payload section. The structure is given rigidity to withstand vibration without loss of adjustment by the entrance baffle, which is a central box-shaped magnesium alloy casting, and by an aluminum alloy top plate linking the grating mount and mirror and baffle castings.

The primary mirror cell is an L-section magnesium alloy cast ring with removable back-plate, retention and adjustment of the mirror being by means of three sets of three steel grub screws having nylon pads inserted in the ends which bear on the mirror. Flats are ground in the circumference on front face of the mirror where the screws are to bear.

The two main components of the grating mount are milled from solid aluminum alloy bar. The grating is retained in its cell in similar fashion to the mirror, with two additional screws for lateral restraint. The cell is detachable from the grating post for storage and can be remounted without loss of adjustment.

The photomultiplier is mounted in silicone rubber rings within the PM block, which is made in two fitted halves. A nose piece on the front end of this block contains the Fabry (field) lens, held between nylon washers, and also provides a fixing for the slit plate. A rectangular baffle on the slit plate and the method of mounting the grating behind the grating post make it impossible for sky light to enter the slit directly. Focusing is achieved by sliding the entire PM assembly on guides milled into the magnesium alloy mount.

For flight, the instrument is mounted via the bulkhead in a special 33-cm high Skylark parallel body section. This body section contains an aperture about 23 cm square, the cover of which is ejected at about 80 km by a leaf spring after an explosive squib latch release.

IV. Electronics

For the dc measurements commercial FET-input operational amplifiers are now used. A semilogarithmic characteristic over the upper part of the output range is obtained by means of biased-off diodes successively shunting in lower value feedback resistors as the output rises.

Since the large main feedback resistor (200 MΩ), coupled with stray line capacitance, starts to give substantial loss of frequency response above 100 Hz, the output from this amplifier, in addition to being telemetered directly, is fed to another amplifier connected

as an active filter, giving frequency compensation to 500 Hz and a dc gain of two; this output is fed to a separate telemetry channel.

Details of the photon pulse-counting system are to be published elsewhere⁷ and it suffices to say here that after the usual amplifying, shaping, and discriminating processes, the pulses pass to a twelve-stage binary counter. The counter states are processed by parallel i.c. logic and digital-to-analogue circuitry so as to produce two analogue outputs. One has a stepwise resolution interval of one part in thirty-two on successive scale of 0–128, 128–256, 256–512, etc., counts (maximum 4096). The other output indicates the scale in use. The count is accumulated and displayed for 2.25 msec, the sample/reset time being a further 0.25 msec. The choice of scale is such as to maintain the photon statistical fluctuation fairly constant at between two and four steps of the histogram display, throughout a counting range of 500:1.

The EMI photomultiplier flown was found to have a very distinct and stable threshold between signal and noise pulses when run with 1800 V overall. Under these conditions, the dark count was negligible with a discriminator level which passed over 90% of signal pulses.

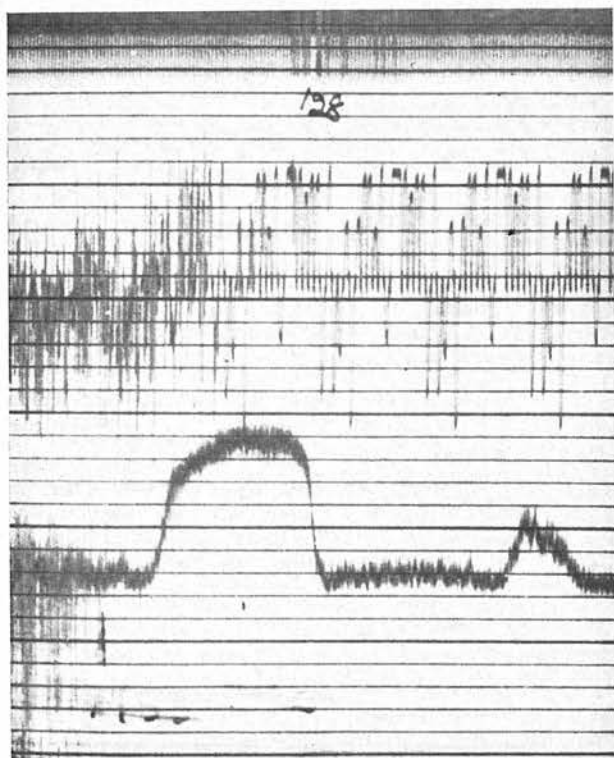
Commercially available EHT inverters are now used but substantial additional input and output smoothing is found to be essential with these to avoid spurious counts at the inverter frequency. All high voltage parts are encapsulated in silicone rubber. The EHT units and the pulse counting preamplifier are mounted on the respective instruments, but the remaining electronics are separately mounted (on antivibration feet) under the rocket nose cone.

V. Optical Adjustment and Calibration

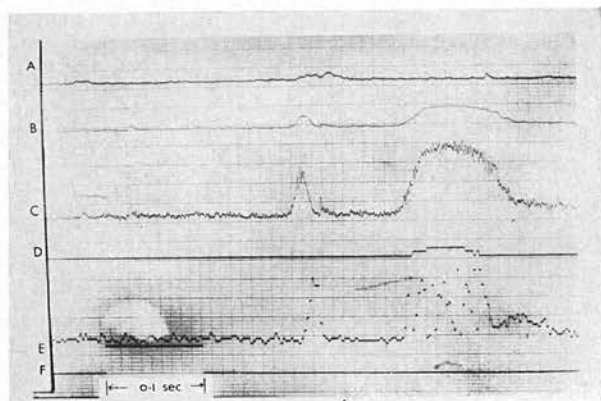
Because of the skew nature of the optics, the large aperture ratio of the system, and the fact that it is only corrected for the uv, the setting up of the system is a relatively lengthy process. In fact, a special rotary table was designed and built to aid the operation.⁸

It is necessary first to square the grating to the experiment mechanical center line (which is accurately related to the rocket axes). This was done by autocollimation of the zero-order reflection in the beam of artificial star collimator; without the PM block fitted, sufficient light passed through the hole in the primary mirror for this purpose. The instrument was then rotated through 180° and the mirror adjusted so as to bring the zero-order image to a point at the right height and directly above the experiment center line. The mirror and grating were then square to each other, which satisfies Murty's Eq. (20),³ because in our case the radius of the illuminated area on the grating is just about one-quarter of the mirror radius and so (in Murty's notation) $\tan \vartheta = \tan \alpha$, where ϑ and α are the angles of the mirror axis and grating normal, respectively, to the coma-balanced incident beam axis. [Fig. 1(a).]

The bright Hanovia mercury arc source used for the collimator illumination in the preceding adjustments



(a)



(b)

Fig. 2. (a) Section of telemetry record of August 1965 flight showing uv spectrum and zero-order signal of unidentified star. (b) Section of telemetry record of 3 December 1968 flight. Channel A is a photometric channel measuring in the 1300–1700 Å region. The same star (Beta Cephei) is scanned by the two spectrophotometers. The sharp zero-order signal seen on channels B, C, and E is followed about 0.1 sec later by the spectral scan readily visible on channels B and C. Channel B is the FET-amplifier dc output direct, while channel C is frequency compensated and has a dc gain of two from Channel B; both outputs are derived from an Ascop photomultiplier. Channels D and E are the display of the integrated counts from an EMI photomultiplier, E being the high resolution scale, while levels on D indicate the range being used. The smallest changes displayed on Channel E correspond to four counts when using the most sensitive range. Trace F is IRIG B time.

was then replaced by a Pen-Ray capillary low pressure mercury lamp focused on to a quartz scatter plate behind the collimator slit. The PM-slit assembly was now fitted but using a narrow slit, giving a few Åstroms resolution. The instrument could then be focused on the sharp 2537 Å line by scanning photoelectrically through the dispersed image and bringing into coincidence the profiles formed by the left and right hand sides of the incoming beam. For this process high accuracy and freedom from backlash of the telescope table were particularly necessary.

Because of the blaze spreading problem mentioned earlier and the fact that the aperture stop of the optical system changes for differing wavelengths, the meaningful calibration which could be carried out was with the optical system as a whole. One absolute calibration was at 2537 Å by means of a Pen-Ray lamp set up at a distance of over 100 m and monitored by an International light photometer, itself checked in various ways. An independent calibration at wavelengths longwards of 2500 Å was made against a Philips ribbon filament lamp, also at a distance, calibrated for visible output and color temperature by British National Physical Laboratory. The tables of de Vos⁹ were used for extrapolation to the uv. A relative calibration at shorter wavelengths was carried out in the vacuum chamber using dc or microwave discharge source monochromator using the Wadsworth principle (independently devised, but as subsequently described by Schroeder¹⁰) and a cassegrain collimator, to feed the instrument. The reference for this relative calibration was a simple photometer using a salicylated detector and a collecting mirror of known reflectivity, simultaneous obstructions being introduced into the beam.

VI. Flight Results

All the flights of this instrument have been from the Italian military range at Salto di Quirra, Sardinia, in the European Space Research Organisation program. The first flight was on ESRO Skylark SO5/1 in August 1967. Because of a partial failure of the on-board telemetry, over one-third of the relevant record was lost. Furthermore, there was a fault in the attitude sensing system, and pitch-yaw lock-in caused a large precession and slow roll. Consequently no attitude solution was obtainable, although comparison of Figs. 2(a) and 2(b) shows that (unidentifiable) spectra were obtained on this flight, the difference in scale being due to the roll rate on the earlier flight. (The direction of the record is reversed.)

Various factors delayed firing of the second roll rate pair (SO5/2) until 26 May 1967. For this flight the Space General roll rate control unit was supplied by ESRO; the only instrumental change was the use of kanigenized aluminum primary mirror supplied by Grubb Parsons.

Although all systems functioned technically correctly on this flight, for reasons which remain obscure the background was a fairly high background and only three stellar objects were observed on the trace; the signal/noise

was too poor to make interpretation possible. Most likely explanations for the poor quality of the data are loss of focus and deterioration of the replica grating due to ingress of kinetically heated air.

These flights each involved only a single spectrophotometer with dc output from an Ascop photomultiplier. The launch which took place on 3 December 1968 at 21.39 UT (Skylark S27/1) used two parallel instruments, having, respectively, the dc and counting outputs described in Sec. IV. This flight reached an apogee of 199 km and was entirely successful for these instruments. A section of the telemetry record is shown in Fig. 2(b). The roll rate was controlled to $14.3^\circ/\text{sec}$ so the dispersion gives a spectral scan rate of about $15 \text{ \AA}/\text{msec}$. The frequency response of the channels is thus high enough to make possible deconvolution of the 190 \AA slit width resolution to give about 100 \AA spectral resolution.

Sixty-five stars were observed on both the channels, all these spectra being accompanied by zero-order signals. Of the spectra, twenty-two were rated as very good or good, having accuracy limited by photon statistics with rms deviation 10%, eighteen rated as fair (10–30% accuracy), and the remaining twenty-five were poor, probably being usable only to refine aspect data. Particularly notable is the low level of background light, about $2 \times 10^{-10} \text{ erg cm}^{-2} \text{ sec}^{-1}$ per angstrom of resolution—less than the input from a fifth magnitude AO star—obtained without angular baffling of the incoming beam but using visual blind detectors.

A further flight is planned (Payload S27/2) using similar instrumentation but extending measurements to 1200 \AA on one channel.

VII. Conclusions

The advantages in simplicity, efficiency, compactness, and economy of the short focal length objective dispersion convergent beam monochromator have been demonstrated in obtaining far uv stellar observations.

Like most space projects, the successful construction and flight of these instruments has required the assistance and cooperation of numerous individuals and organizations. In particular, at the Royal Observatory, Edinburgh, much is owed to the initial impetus and continued support of H. E. Butler, to the extensive redesign work of J. Fletcher, the tireless fabrication of J. H. J. McKemmie, and the development and production of the pulse-counting system by C. M. Paterson and D. H. Beattie. This work has been under the auspices of the Science Research Council since 1965. Testing, integration, and launch were carried out by European Space Technology Center and British Aircraft Corporation personnel under the scientific supervision of the European Space Laboratory.

References

1. G. S. Monk, *J. Opt. Soc. Amer.* **17**, 358 (1928).
2. A. C. H. P. Gillieson, *J. Sci. Instrum.* **26**, 335 (1949).
3. M. V. R. K. Murty, *J. Opt. Soc. Amer.* **52**, 768 (1962).
4. R. M. Blakney, M. V. R. K. Murty, N. Hochgraf, and W. Staudenmaier, in *Proceedings of the Conference on Optical Instruments and Techniques*, K. J. Habell, Ed. (Chapman and Hall, London, 1962), p. 279.
5. T. P. Stecher and J. E. Milligan, *Astrophys. J.* **136**, 1 (1962).
6. M. V. R. K. Murty, Spectroscopy Div., BARC, Mod. Lab., Trombay, private communication.
7. D. H. Beattie and C. M. Paterson, Royal Observatory Edinburgh (in preparation).
8. J. Clark and G. C. Sudbury, *J. Sci. Instrum.* **44**, 400 (1967).
9. J. C. de Vos, *Physica* **20**, 690 (1954).
10. D. J. Schroeder, *Appl. Opt.* **5**, 545 (1966).

Table 2. . . . Identified Stellar Signals.

Time	Time in seconds from launch (0 secs is 20h 38m 49.5s UT on 1968 Dec. 12)
Ref No	Sequence number of observation
271-	
BS/HR	Yale University Bright Star Catalogue Number
B/F	Bayer-Flamsteed designation
m _v	Visual magnitude
Sp. Type	MKK classification
B-V	Colour excess
Elevation	Degrees above zenith normal plane
Remarks	bl blended with another object z.o. zero order recognition problem gr believed grazing observation * See Notes at end of table.

<u>Time</u>	<u>Ref.No.</u> <u>271-</u>	<u>BS/HR</u>	<u>B/F</u>	<u>mV</u>	<u>Sp.Type</u>	<u>B-V</u>	<u>Elevn.</u>	<u>Remarks</u>
89.888	01	2282	ζ C Ma	3.02	B2.5IV		1.4°	*
108.31	02	8937	β Sc1	4.37	B8p	- 0.10	3.4°	gr
111.66	03	1134	δ For	4.99	B5IV n	- 0.17	16°	*
113.07	04	1621		4.90	B9	- 0.06	19°	gr
113.36	05	1731/ 1753/4		6.48 6.17/6.36	B3 B8		19.5°	Sp.bl. with z.o. of 1792
114.21	06	2108 2128	2 Mon 3 Mon	5.02 4.95	Am B5IV	+ 0.20 - 0.11	20°	*
114.51	07	2205		5.06	B2V	- 0.22	20°	
114.80	08	2325 2344	10 Mon	6.14 5.06	B3 B2V	- 0.14 - 0.18	19°	*
115.00	09	2395		5.09	B6V	- 0.15	19°	gr
115.2	09A1	2461		5.78	B8III	- 0.10	19°	gr
115.35	09A2	2517		6.14	B8II-III	- 0.14	19°	gr
116.10	10	2845	β C Min	2.84	B8V(B7A)	- 0.10	17°	*
132.24	11	8937	β Sc1	4.37	B8p	- 0.10	2.5°	*
134.15	12	612	ν For	4.68	B8Sip	- 0.17	19°	*
136.025	13	1100	20 Eri	5.22	A0si	- 0.14	30°	
137.01	13A	1363	d Eri	5.84	B5III	- 0.15	35°	

<u>Time</u>	<u>Ref.No.</u> <u>271-</u>	<u>BS/HR</u>	<u>B/F</u>	<u>m_v</u>	<u>Sp.Type</u>	<u>B-V</u>	<u>Elevn</u>	<u>Remarks</u>
137.39	14	1463	ν Eri	4.12	B2III	- 0.21	36°	*
137.51	15	1520	μ Eri	4.02	B5IV	- 0.15	37°	gr
137.60	15A	1567	π ⁵ Ori	3.72	B2III	- 0.19	37°	gr
138.49	16	1790	γ Ori 32 Ori	1.64 4.21	B2III B5IV	-0.23 - 0.15	37°	bl.
138.70	17	1879/80	λ Ori φ Ori	3.66/5.66 4.41	O8/Oe5 BOIV	- 0.17	36°	bl.
139.00	17A	2010	134 Tau	4.90	B9IV	- 0.07	38°	gr
139.32	18	2159	ζ ^γ Ori	4.42R	B3.V	- 0.27	35°	
139.356	19	2199	70 ⁷⁰ ξ Ori	4.45	B3V	- 0.19	35°	
139.432	19A	2198	69 Ori	4.90	B5V.17	- 0.17	35°	*
139.81	19B	2343	18 ν Gem	4.15	B7Ive	- 0.11	33°	gr
142.52	20	3690	38 Lyn	3.78	A3V	+ 0.06	15°	
156.42	21	8937	β Scl	4.37	B8p	- 0.10	0.5°	
157.45	22	280	α Scl.	4.30	B5	- 0.16	15°	
159.53	23	708	72 ρ Cet	4.88	B9V		35°	gr
161.356	24	1153	29 Tau	5.36	B3V	- 0.12	50°	
161.74		1243		5.68	B8	+ 0.02	52°	bl. with z.o. 1239
161.837	25	1239	λ 35 Tau	5.40	B3V		54°	*

<u>Time</u>	<u>Ref.No.</u> <u>271-</u>	<u>BS/HR</u>	<u>B/F</u>	<u>m_v</u>	<u>Sp.Type</u>	<u>B-V</u>	<u>Elevn.</u>	<u>Remarks</u>
162.35	25A	1389	68 Tau	4.23	A2IV	+ 0.05	54°	*
163.57	26	1791	β Tau	1.65	B7III	- 0.13	52°	
164.84	26A	2420	52 Aur	5.26	B8III	- 0.07	45°	
167.57	27	4033	λ U Ma	3.45	A2IV	+ 0.03	12°	
168.0	27A	4248	ω U Ma	4.75	A1V			
185.02	27A1	718	ξ 2 Cet	4.34	B9III	- 0.05	66°	gr
185.65	27A2	847	σ Ari	5.46	B7V	- 0.09	70°	*
187.05	27A3	1131	ο Per	3.83	B1	+ 0.06	71°	*
187.38	28	1228	ξ Per	4.03	O7	+ 0.01	70°	
191.51	28A	3894	30φUMa	4.54	A2/35	+ 0.03	38°	*
207.81	28B	317	28 Cet	5.59	AOIV	0.00		
209.98	28C	545/6	γ Ari	4.83/4.75	Asi/B9V	- 0.02	68°	*
210.09	29	553	6βAri	2.65	A5V	+ 0.13	68°	*
211.05	30	664	γ Tri	4.08R	AO(p)	+ 0.02	81°	z.o.v. faint
213.31	31	1204		4.87R	B9V	- 0.04	65°	
213.78	32	1542	α Cam	4.29	O9.5Ia	+ 0.04	58°	

<u>Time</u>	<u>Ref.No.</u> <u>271-</u>	<u>BS/HR</u>	<u>B/F</u>	<u>m_v</u>	<u>Sp.Type</u>	<u>B-V</u>	<u>Elevn.</u>	<u>Remarks</u>
216.596	33	4295	β U Ma	2.36	AIV	- 0.02	17°	
235.94	34	226	ν And	4.53	B5V	- 0.15	74°	*
239.09	35	1289		5.44R	B5V		47°	
241.58	36	4660	δ U Ma	3.32	A3V	+ 0.08	12°	
263.20	37	8338	β Cep	3.18	B2III	- 0.25	44°	
263.81	38	7750	χ Cep	4.38R	B9III	- 0.05	38°	gr
264.70	39	6079 6116	19 U Mi 21 U Mi	5.48 4.56	B8 Ap	- 0.15 + 0.01	29°	*
281.855	40	9098	2 Cet	4.54	B9IV	- 0.05	27°	
284.34	41	8781	α Peg	2.49	B9.5III	- 0.05	40°	
287.36	41A	8040		5.55(B)	B8	- 0.13	35°	*
288.0	41B	7740	33 Cyg	4.27R	A3IV-V			
288.2025	42	7608	23 Cyg	5.08	B5V	- 0.13	30°	*
288.73	42A1	7210		5.24	B3n		25°	*
291.41	42A2	5329/5350	17/21 B ₀₀	4.54 Var 4.78VAR	A7		1°	bl. 5329
305.76	43	280	α Scul	4.39	B5	- 0.16	16°	
306.97	44	9098	2 Cet	4.54	B9IV	- 0.05	23°	

<u>Time</u>	<u>Ref.No.</u> <u>271-</u>	<u>BS/HR</u>	<u>B/F</u>	<u>mV</u>	<u>Sp.Type</u>	<u>B-V</u>	<u>Elevn.</u>	<u>Remarks</u>
307.34	45	8989	ω^2 Aqr	4.48	B9.5V	- 0.04	25°	
311.50	45A	8007	BW Vul	6.44	B2III	- 0.13	24°	
312.37	46	7708	28 Cyg	4.98	B3Ve	- 0.16	19°	*
312.48	47	7647	25 Cyg	5.20	B3Ve	- 0.17	18°	*
312.60	47A	7613	22 Cyg	4.93	B6III	- 0.09	18°	*
313.265	47A1	7258		6.21	B3			
314.41	48	6558	i Her	3.80	B3V	- 0.18	6.5°	
315.58	49	6092	τ Her	3.89	B5IV	- 0.15	0°	
325.84	50	2538	χ C.Ma	3.96	B1.5IIIne	- 0.24	-6°	*
326.14	51	2361	λ C.Ma	4.47	B4V	- 0.18=	-4°	gr
326.39	52	2279		5.77	B9	- 0.09	-3°	bl.
326.62	53	2288		5.51VAR	B1.5IIIn	- 0.20		
		2469	γ Col	5.72	A1	+ 0.02	-1.5°	*
		2106		4.35	B3IV	- 0.18		
328.42	53A	1189		5.42	B9+B8	- 0.02	9.5°	*
		1190		4.86				
332.13	54	9098	2 Cet	4.54	B9IV	- 0.05	20°	gr
332.54	54A	8968		5.00	A5	+ 0.24	21°	gr
334.46	55	8402	o Agr	4.79	B8Ve	- 0.09	19°	

<u>Time</u>	<u>Ref.No.</u> <u>271-</u>	<u>BS/HR</u>	<u>B/F</u>	<u>m_v</u>	<u>Sp.Type</u>	<u>B-V</u>	<u>Elevn.</u>	<u>Remarks</u>
336.29	56	7852	ξ Del	4.04	B6III	- 0.02	11°	
337.04	56A1	7622	11 Sgr	5.33	B9IV	- 0.04	6°	
337.46	56A2	7437	9 Vul	5.08	B7V	- 0.13	2.2°	
337.77	56A3	7306	1 Vul	4.59	B3IV	- 0.06		bl. with 7301
348.82	57	3314		3.90	AOV	- 0.02	-5°	
353.915	58	1088	19τ ⁵ Eri	4.26	B8V	- 0.10	24°	
357.73	58A	8998	106Aqr	5.24	B8V	- 0.09	22°	*
359.34	59	8452	38Aqr	5.46	B6III	- 0.12	13°	
374.03	59A	3163	8 Cnc	5.11R	AOIV	+ 0.00	5°	gr
374.84	60	2845	β C Mi	2.84	B8V(B7)	- 0.10	12°	
376.0	60A	2298/9	8 Mon	4.48	A5IV		22°	*
376.89	61	1903	ε Ori	1.70	B0Ia	- 0.05	28°	
376.94	62	1852	δ Ori	2.20	O9.5I1	- 0.21	28°	
377.05	62A1	1788	28 Ori	3.44	B0.5V	- 0.19	29°	
377.23		1765	22 Ori	4.73	B2IV	- 0.17		
377.74	63	1520	μ Eri	4.02	B5IV	- 0.15	30°	

<u>Time</u>	<u>Ref.No.</u> <u>271-</u>	<u>BS/HR</u>	<u>B/F</u>	<u>m_v</u>	<u>Sp.Type</u>	<u>B-V</u>	<u>Elevn.</u>	<u>Remarks</u>
377.93	64	1463	ν Eri	4.12	B2III	- 0.21	34°	
380.32	64A	708	ρ Cet	4.90	AO			
382.75	65	9098	2 Cet	4.62	AO			
383.06	66	9031	108 Aqr	5.00	B8/9p	- 0.17		

COMMENTS FOR TABLE 2

271-01	Sp. Type from Hiltner et al (1969)
02	Also 271-11, -21, and -60.
03	Sp. Type from Hiltner et al
05	Sp. bl. with z.o. of BS 1792 5.64 A0
06	2128 grazed
08	2344 grazed?
10	Also -60
11	See -02
12	Some blending with BS 652 (5.27 AI V?)
14	Also -64
15	Also -63
19A	Bl. with BS 2223 (5.28, B9)
24A	Sp. bl. with z.o. of BS 1239
25A	Near gr.
27A2	High background stray light from Moon
27A3	As -27A2 - also possibly some light from ζ Per 2.91 Bl.
28A	<u>Not</u> HD 89822, BS 4072!
28A1	z.o. v. faint
29	z.o. bl. with sp. of -28A2
30	z.o. very faint
34	Near M31.
39	BS 6034 (5.53, A0) also present.
40	Also -44, -65.

- 271-41A bl. with gr. of BS 7929 (51 Cyg, 5.38, B2V)
- 42 Shorter wavelengths bl. with sp. of BS 7634 (6.09, A2)
- 42A2 5329 gr.
- 46 With 7736, (29 Cyg, 4.89, A2p)
- 47 z.o. bl with sp of -46
Also bl with 7620, 6.00 B3
- 47A Note proximity of BS 7543
z.o. bl. with sp. of -47.
- 50 Spectral type from Hiltner et al.
Followed by BS 2492 (10 C.Ma 5.16, B3p)
- 52 Spectral type of 2288 from Hiltner et al.
z.o. bl. with sp. of 51
- 56A3 With BS 7301 (5.55, A1)
- 58A Telemetry fading
- 60A z.o. confused
- 62A1 Some blended stars with z.o.s in sp. of 61, 62.

Table 3. List of Reduced Stellar Spectra.

BS/HR	Yale University Observatory Bright Star Catalogue Number.
B/F	Bayer-Flamsteed Name
271-	Sequence number of observation (Refer to Table 2).
S.T.	Spectral Type (M.K.K.)
BVX	Colour excess $(B-V) - (B-V)$ (see Table 2 for colour excesses).
NZ	Noise background counts/interval of polynomial fit
SIG	Weighted RMS deviation
NOTES	The following abbreviations apply bl blended with another object z.o. zero order very weak or dubious in location gr believed to be a grazing observation var variable * refer to comments at end of table or of Table 2.

<u>BS/HR</u>	<u>B/F</u>	<u>271-</u>	<u>S.T.</u>	<u>BVX</u>	<u>NZ</u>	<u>SIG</u>	<u>Notes</u>
226	v And	34	B5V	0.01	12	6.41	
280	α Scl	22	B5	0.00	9	5.07	
612	v For	12	B8p	0.00	10	6.77	
664	γ Tri	30	AOV(p)	0.03	25	6.45	bl z.o.
718	ξ 2Cet	27A1	B9III	0.02	35	3.45	gr
1088	τ 5Eri	58	B8V	0.01	9	5.00	
1131	o Per	27	B1 III	0.32	65 +	11.9	*
1134	δ For	03	B5IVn	0.00	14	5.27	
1189/90		53A	B9+B8	0.00	12	5.78	z.o. *
1228	ξ Per	28	Q7	0.33	68 +	8.82	var
1239	λ Tau	25	B3V	0.00	60	7.69	var
1463	v Eri	64	B2III	0.03	28	11.5	*
1520	μ Eri	63	B5IV	0.01	28	6.78	gr *
1542	α Cam	32	O 9.5Ia	0.30	15	5.93	
1790	γ Ori	16	B2III	0.01	38	94.5	*
1791	β Tau	26	B7III	0.00	46	90.0	
1852	δ Ori	62	O 9.5II	0.09	50	71.9	bl *

<u>BS/HR</u>	<u>B/F</u>	<u>271-</u>	<u>S.T.</u>	<u>BVX</u>	<u>NZ</u>	<u>SIG</u>	<u>Notes</u>
1876/9/80	ϕ/λ Ori	17	BOIV/O8+Oe5	0.14	55 \pm <u>1</u>	65.4	
1903	ϕ Ori	61	BOIa	0.19	34	58.6	*
2106	γ Col	53	B3IV	0.02	36	8.24	
2128 (O8)	2 (3) Mon	06	B5IV (+Am)	0.05	27	6.48	b1
2205		07	B3IV	0.00	29	5.71	
2282	ζ Cma	01	B2.5V	0.02	142 \pm <u>1</u>	67.1	*
2288		52	B1.5IIIn	0.06	41	5.79	zo
2538	K Cma	50	B1.5 IV ne	0.00	56 \pm <u>1</u>	53.9	
2845	β CMi	10 60	B8V	0.01	26 23	10.0 5.89	
3314		57	AOV	0.00	37	3.61	
3690	38 Lyn	20	A3V	0.00	11	2.02	zo
3894	ϕ UMa	28A	A2 or A3s	0.00	6	1.47	
4033	λ UMa	27	A2IV	0.00	10	2.91	*
4295	β UMa	33	A1V	0.00	6	8.93	*
4660	δ UMa	36	A3V	0.00	7	5.64	
6092	τ Her	49	B5IV	0.00	24	10.8	
6588	i Her	48	B3V	0.02	15	12.3	

<u>BS/HR</u>	<u>B/F</u>	<u>271-</u>	<u>S.T.</u>	<u>BVX</u>	<u>NE</u>	<u>SIG</u>	<u>Notes</u>
7608	23 Cyg	42	B5V	0.03	13	5.57	*
7852	ε Del	56	B6III	0.01	15	8.89	*
8007	BW Vul	45A	B2III	0.10	9	1.65	*
8238	β Cep	37	B2III	0.00	9	67.0	*
8781	α Peg	41	B9.5III	0.00	7	69.1	var
8937	β Scl	11	B8p	0.00	23	3.32	
8988	ω2 Aqr	45	B9.5V	0.00	8	3.31	
9098	2 Cet	44	B9IV	0.00	6	2.07	*

Comments on Table 3

664	
1189/90	Combined magnitude
1463	z.o. bl. with spectrum of 1520. A β Cep variable
1520	Spectrum truncated by z.o. of 1463; possible mean graze
1790	Spectrum truncated by blending with 1876/9/80
1852	Blended with tail and second order of 1903, and other field stars - upper limit only.
1903	Spectrum truncated by blending with 1852
2128/08	Values of V, B-V used are for 2128 only
2282	Low altitude - some residual atmospheric extinction, esp. below 2000A, likely.
2288	Weak zero order signal.
2538	Note low elevation - possible shortwave extinction

3894 This is HD 85235 AB - not Osawa's No. 100 (which is BS 4072 and
not 30 U Ma, a mistake copied from Bertaud's list).

4295 Has a B excess.

7608 Spectrum below 2000A probably affected by blend with BS 7634 (6.09 A2)

8007 β Cep variable. BVX estimated against 8238.

8238 β Cep variable.

8781 variable

9098 Low quality spectrum; possible near graze

Tables 4-1 to 4-43. - Reduced Spectra

BS	Yale University Observatory Bright Star Catalogue Number
V	Visual magnitude
(B-V)XS	Colour excess $(B-V) - (B-V)_0$
LAMBDA (NM)	Effective wavelength in nanometers
FLUX	Normalised flux in units of 10^{-9} ergs/cm ² /sec/Å.
RDCRFLX	Ditto, corrected for reddening as described in the text.
MAG	Normalised magnitude i.e. $(m_\lambda - m_V)$
RDCRMAG	Ditto, corrected for reddening
WT	Signal/noise ratio for nearest smoothed data point.
RECIP-MU	Reciprocal wavelength in microns.

BS 226, V= 4.52 (B-V)XS 0.01

*FLUXES AND MAGS. NORMALISED TO V=0 (3.8×10^{-9} CGS/A)

LAMBDA [NM]	FLUX [(CGS/A)* 10^{-9}]	RDCRFLX	MAG	RDCRMAG	WT	RECIP-MU
180	12.56	13.12	-1.30	-1.35	2	5.56
185	16.10	16.77	-1.57	-1.61	2	5.41
190	15.02	15.62	-1.49	-1.53	2	5.26
195	13.21	13.76	-1.35	-1.40	3	5.13
200	11.83	12.35	-1.23	-1.28	3	5.00
205	10.65	11.13	-1.12	-1.17	4	4.88
210	10.02	10.49	-1.05	-1.10	4	4.76
215	10.34	10.83	-1.09	-1.14	3	4.65
220	11.07	11.61	-1.16	-1.21	4	4.55
225	11.69	12.28	-1.22	-1.27	4	4.44
230	11.95	12.55	-1.24	-1.30	4	4.35
235	11.84	12.42	-1.23	-1.29	5	4.26
240	11.59	12.13	-1.21	-1.26	5	4.17
245	11.07	11.56	-1.16	-1.21	4	4.08
250	10.22	10.66	-1.07	-1.12	4	4.00
255	9.41	9.80	-0.98	-1.03	4	3.92
260	8.62	8.97	-0.89	-0.93	4	3.85
265	8.12	8.43	-0.82	-0.86	3	3.77
270	8.23	8.54	-0.84	-0.88	3	3.70
275	8.79	9.10	-0.91	-0.95	3	3.64
280	9.50	9.82	-0.99	-1.03	2	3.57
285	9.88	10.21	-1.04	-1.07	2	3.51
290	9.56	9.86	-1.00	-1.03	2	3.45
295	7.29	7.51	-0.71	-0.74	2	3.39

BS 280, V= 4.30 (B-V)XS 0.00
 *FLUXES AND MAGS. NORMALISED TO V=0 (3.8×10^{-9} CGS/A)

LAMBDA [NM]	FLUX [(CGS/A)* 10^{-9}]	RDCRFLX	MAG	RDCRMAG	WT	RECIP-MU
175	30.18	30.18	-2.25	-2.25	2	5.71
180	18.86	18.86	-1.74	-1.74	3	5.56
185	15.65	15.65	-1.54	-1.54	3	5.41
190	15.26	15.26	-1.51	-1.51	3	5.26
195	15.54	15.54	-1.53	-1.53	4	5.13
200	16.60	16.60	-1.60	-1.60	5	5.00
205	16.36	16.36	-1.58	-1.58	6	4.88
210	15.69	15.69	-1.54	-1.54	6	4.76
215	15.45	15.45	-1.52	-1.52	6	4.65
220	14.76	14.76	-1.47	-1.47	6	4.55
225	13.99	13.99	-1.41	-1.41	5	4.44
230	13.02	13.02	-1.34	-1.34	5	4.35
235	12.17	12.17	-1.26	-1.26	5	4.26
240	11.73	11.73	-1.22	-1.22	5	4.17
245	11.52	11.52	-1.20	-1.20	5	4.08
250	11.31	11.31	-1.18	-1.18	5	4.00
255	11.22	11.22	-1.18	-1.18	5	3.92
260	11.05	11.05	-1.16	-1.16	5	3.85
265	10.55	10.55	-1.11	-1.11	4	3.77
270	10.18	10.18	-1.07	-1.07	4	3.70
275	9.48	9.48	-0.99	-0.99	4	3.64
280	8.99	8.99	-0.94	-0.94	3	3.57
285	8.87	8.87	-0.92	-0.92	3	3.51
290	9.78	9.78	-1.03	-1.03	2	3.45
295	10.97	10.97	-1.15	-1.15	2	3.39
300	12.54	12.54	-1.30	-1.30	2	3.33

BS 612, V= 4.68 (B-V)XS 0.00
 *FLUXES AND MAGS. NORMALISED TO V=0 (3.8×10^{-9} CGS/A)

LAMBDA [NM]	FLUX [(CGS/A)* 10^{-9}]	RDCRFLX	MAG	RDCRMAG	WT	RECIP-MU
175	13.36	13.36	-1.36	-1.36	1	5.71
180	14.19	14.19	-1.43	-1.43	2	5.56
185	15.75	15.75	-1.54	-1.54	2	5.41
190	14.70	14.70	-1.47	-1.47	3	5.26
195	13.32	13.32	-1.36	-1.36	3	5.13
200	12.41	12.41	-1.29	-1.29	3	5.00
205	11.36	11.36	-1.19	-1.19	3	4.88
210	10.65	10.65	-1.12	-1.12	4	4.76
215	10.75	10.75	-1.13	-1.13	3	4.65
220	11.10	11.10	-1.16	-1.16	3	4.55
225	11.42	11.42	-1.19	-1.19	4	4.44
230	11.49	11.49	-1.20	-1.20	4	4.35
235	11.34	11.34	-1.19	-1.19	4	4.26
240	11.21	11.21	-1.17	-1.17	4	4.17
245	10.97	10.97	-1.15	-1.15	3	4.08
250	10.54	10.54	-1.11	-1.11	4	4.00
255	10.21	10.21	-1.07	-1.07	4	3.92
260	9.96	9.96	-1.05	-1.05	4	3.85
265	9.72	9.72	-1.02	-1.02	3	3.77
270	9.88	9.88	-1.04	-1.04	3	3.70
275	10.05	10.05	-1.06	-1.06	3	3.64
280	10.13	10.13	-1.06	-1.06	3	3.57
285	9.99	9.99	-1.05	-1.05	2	3.51
290	10.06	10.06	-1.06	-1.06	2	3.45
295	9.97	9.97	-1.05	-1.05	2	3.39
300	11.63	11.63	-1.21	-1.21	2	3.33

BS 664, V= 4.08 (B-V)XS 0.03
 *FLUXES AND MAGS. NORMALISED TO V=0 (3.8*10⁻⁹ CGS/A)

LAMBDA [NM]	FLUX [(CGS/A)*10 ⁻⁹]	RDCRFLX	MAG	RDCRMAG	WT	RECIP-MU
175	19.09	21.94	-1.75	-1.90	1	5.71
180	12.64	14.40	-1.30	-1.45	2	5.56
185	8.89	10.04	-0.92	-1.06	2	5.41
190	6.96	7.83	-0.66	-0.79	2	5.26
195	5.88	6.64	-0.47	-0.61	2	5.13
200	5.55	6.30	-0.41	-0.55	2	5.00
205	5.36	6.12	-0.37	-0.52	2	4.88
210	5.34	6.11	-0.37	-0.52	2	4.76
215	5.64	6.49	-0.43	-0.58	3	4.65
220	5.99	6.91	-0.49	-0.65	3	4.55
225	6.18	7.16	-0.53	-0.69	3	4.44
230	6.18	7.15	-0.53	-0.69	3	4.35
235	6.06	6.98	-0.51	-0.66	3	4.26
240	6.01	6.89	-0.50	-0.65	3	4.17
245	5.99	6.83	-0.49	-0.64	3	4.08
250	5.96	6.76	-0.49	-0.62	3	4.00
255	6.07	6.85	-0.51	-0.64	3	3.92
260	6.41	7.20	-0.57	-0.69	3	3.85
265	6.75	7.56	-0.62	-0.75	3	3.77
270	7.50	8.36	-0.74	-0.86	3	3.70
275	8.63	9.58	-0.89	-1.00	3	3.64
280	9.88	10.93	-1.04	-1.15	3	3.57
285	11.41	12.57	-1.19	-1.30	2	3.51
290	13.66	14.99	-1.39	-1.49	3	3.45
295	15.29	16.72	-1.51	-1.61	3	3.39
300	17.20	18.75	-1.64	-1.73	3	3.33

BS 718, V= 4.27 (B-V)XS 0.02
 *FLUXES AND MAGS. NORMALISED TO V=0 (3.8×10^{-9} CGS/A)

LAMBDA [NM]	FLUX [(CGS/A)* 10^{-9}]	RDCRFLX	MAG	RDCRMAG	WT	RECIP-MU
180	7.69	8.39	-0.77	-0.86	1	5.56
185	10.53	11.43	-1.11	-1.20	1	5.41
190	9.72	10.51	-1.02	-1.10	2	5.26
195	8.22	8.92	-0.84	-0.93	2	5.13
200	6.78	7.38	-0.63	-0.72	2	5.00
205	5.55	6.06	-0.41	-0.51	2	4.88
210	4.71	5.15	-0.23	-0.33	2	4.76
215	4.43	4.86	-0.17	-0.27	2	4.65
220	4.41	4.85	-0.16	-0.27	2	4.55
225	4.53	5.00	-0.19	-0.30	2	4.44
230	4.61	5.08	-0.21	-0.31	2	4.35
235	4.60	5.05	-0.21	-0.31	2	4.26
240	4.57	5.00	-0.20	-0.30	2	4.17
245	4.45	4.85	-0.17	-0.27	2	4.08
250	4.21	4.58	-0.11	-0.20	2	4.00
255	4.00	4.34	-0.06	-0.14	1	3.92
260	3.87	4.18	-0.02	-0.10	2	3.85
265	3.86	4.17	-0.02	-0.10	2	3.77
270	4.21	4.52	-0.11	-0.19	2	3.70
275	4.91	5.27	-0.28	-0.35	2	3.64
280	5.71	6.11	-0.44	-0.52	2	3.57
285	6.44	6.87	-0.57	-0.64	2	3.51
290	6.99	7.44	-0.66	-0.73	1	3.45
295	6.57	6.98	-0.59	-0.66	1	3.39

BS 1088, V= 4.26 (B-V)XS 0.01
 *FLUXES AND MAGS. NORMALISED TO V=0 (3.8×10^{-9} CGS/A)

LAMBDA [NM]	FLUX [(CGS/ 10^{-9})]	RDCRFLX	MAG	RDCRMAG	WT	RECIP-MU
175	24.20	25.35	-2.01	-2.06	1	5.71
180	16.97	17.72	-1.62	-1.67	2	5.56
185	12.24	12.74	-1.27	-1.31	2	5.41
190	10.27	10.68	-1.08	-1.12	3	5.26
195	9.27	9.66	-0.97	-1.01	3	5.13
200	8.93	9.32	-0.93	-0.97	4	5.00
205	8.24	8.61	-0.84	-0.89	3	4.88
210	7.47	7.82	-0.73	-0.78	3	4.76
215	6.99	7.32	-0.66	-0.71	3	4.65
220	6.35	6.66	-0.56	-0.61	3	4.55
225	5.86	6.15	-0.47	-0.52	3	4.44
230	5.45	5.73	-0.39	-0.45	3	4.35
235	5.26	5.51	-0.35	-0.40	3	4.26
240	5.39	5.64	-0.38	-0.43	3	4.17
245	5.74	5.99	-0.45	-0.49	3	4.08
250	6.12	6.38	-0.52	-0.56	3	4.00
255	6.56	6.83	-0.59	-0.64	4	3.92
260	6.96	7.24	-0.66	-0.70	4	3.85
265	6.96	7.23	-0.66	-0.70	4	3.77
270	6.95	7.21	-0.66	-0.69	3	3.70
275	6.64	6.88	-0.61	-0.64	2	3.64
280	6.45	6.67	-0.57	-0.61	3	3.57
285	6.64	6.85	-0.61	-0.64	3	3.51
290	7.71	7.95	-0.77	-0.80	2	3.45
295	8.06	8.31	-0.82	-0.85	1	3.39

BS 1131, V= 3.83 (B-V)XS 0.32
 *FLUXES AND MAGS. NORMALISED TO V=0 (3.8×10^{-9} CGS/A)

LAMBDA [NM]	FLUX [(CGS/A)* 10^{-9}]	RDCRFLX	MAG	RDCRMAG	WT	RECIP-MU
185	16.43	60.28	-1.59	-3.00	3	5.41
190	12.19	42.66	-1.27	-2.63	3	5.26
195	8.77	32.36	-0.91	-2.33	3	5.13
200	6.44	24.98	-0.57	-2.04	2	5.00
205	5.22	21.23	-0.34	-1.87	2	4.88
210	4.75	20.26	-0.24	-1.82	2	4.76
215	5.02	22.30	-0.30	-1.92	3	4.65
220	5.71	26.43	-0.44	-2.11	3	4.55
225	6.37	30.75	-0.56	-2.27	3	4.44
230	6.89	32.84	-0.65	-2.34	3	4.35
235	7.24	32.66	-0.70	-2.34	3	4.26
240	7.59	32.36	-0.75	-2.33	4	4.17
245	7.87	31.72	-0.79	-2.30	3	4.08
250	8.00	30.66	-0.81	-2.27	3	4.00
255	8.17	29.78	-0.83	-2.24	3	3.92
260	8.41	29.25	-0.86	-2.22	4	3.85
265	8.48	28.23	-0.87	-2.18	4	3.77
270	8.82	28.10	-0.91	-2.17	3	3.70
275	9.19	27.99	-0.96	-2.17	3	3.64
280	9.56	27.94	-1.00	-2.17	2	3.57
285	10.03	28.22	-1.05	-2.18	2	3.51
290	11.13	30.14	-1.17	-2.25	2	3.45
295	12.08	31.49	-1.26	-2.30	2	3.39
300	14.04	35.21	-1.42	-2.42	2	3.33

BS 1134, V= 4.99 (B-V)XS 0.00
 *FLUXES AND MAGS. NORMALISED TO V=0 (3.8×10^{-9} CGS/A)

LAMBDA [NM]	FLUX [(CGS/A)* 10^{-9}]	RDCRFLX	MAG	RDCRMAG	WT	RECIP-MU
175	9.41	9.41	-0.98	-0.98	1	5.71
180	15.14	15.14	-1.50	-1.50	1	5.56
185	22.79	22.79	-1.94	-1.94	2	5.41
190	22.77	22.77	-1.94	-1.94	3	5.26
195	21.10	21.10	-1.86	-1.86	3	5.13
200	19.55	19.55	-1.78	-1.78	4	5.00
205	17.52	17.52	-1.66	-1.66	4	4.88
210	15.94	15.94	-1.56	-1.56	3	4.76
215	15.62	15.62	-1.53	-1.53	3	4.65
220	15.70	15.70	-1.54	-1.54	3	4.55
225	15.99	15.99	-1.56	-1.56	3	4.44
230	16.11	16.11	-1.57	-1.57	4	4.35
235	16.06	16.06	-1.56	-1.56	4	4.26
240	16.08	16.08	-1.57	-1.57	4	4.17
245	15.88	15.88	-1.55	-1.55	4	4.08
250	15.19	15.19	-1.50	-1.50	4	4.00
255	14.35	14.35	-1.44	-1.44	3	3.92
260	13.07	13.07	-1.34	-1.34	3	3.85
265	11.63	11.63	-1.21	-1.21	3	3.77
270	10.49	10.49	-1.10	-1.10	2	3.70
275	9.18	9.18	-0.96	-0.96	2	3.64
280	8.48	8.48	-0.87	-0.87	2	3.57
285	8.38	8.38	-0.86	-0.86	2	3.51
290	9.46	9.46	-0.99	-0.99	1	3.45
295	10.83	10.83	-1.14	-1.14	1	3.39
300	12.41	12.41	-1.29	-1.29	1	3.33

BS 1190, V= 4.26 (B-V)XS 0.00
 *FLUXES AND MAGS. NORMALISED TO V=0 (3.8×10^{-9} CGS/A)

LAMBDA [NM]	FLUX [(CGS/A)* 10^{-9}]	RDCRFLX	MAG	RDCRMAG	WT	RECIP-MU
185	5.02	5.02	-0.30	-0.30	1	5.41
190	3.65	3.65	0.04	0.04	1	5.26
195	2.74	2.74	0.36	0.36	1	5.13
200	2.49	2.49	0.46	0.46	1	5.00
205	2.59	2.59	0.41	0.41	1	4.88
210	2.91	2.91	0.29	0.29	2	4.76
215	3.48	3.48	0.10	0.10	2	4.65
220	4.18	4.18	-0.10	-0.10	2	4.55
225	4.67	4.67	-0.22	-0.22	3	4.44
230	4.96	4.96	-0.29	-0.29	3	4.35
235	5.06	5.06	-0.31	-0.31	2	4.26
240	5.11	5.11	-0.32	-0.32	3	4.17
245	5.09	5.09	-0.32	-0.32	3	4.08
250	4.96	4.96	-0.29	-0.29	3	4.00
255	4.87	4.87	-0.27	-0.27	2	3.92
260	4.84	4.84	-0.26	-0.26	2	3.85
265	4.84	4.84	-0.26	-0.26	2	3.77
270	5.14	5.14	-0.33	-0.33	3	3.70
275	5.73	5.73	-0.45	-0.45	3	3.64
280	6.55	6.55	-0.59	-0.59	2	3.57
285	7.69	7.69	-0.76	-0.76	2	3.51
290	9.49	9.49	-0.99	-0.99	2	3.45
295	11.00	11.00	-1.15	-1.15	2	3.39
300	12.69	12.69	-1.31	-1.31	2	3.33

BS 1228, V= 4.04 (B-V)XS 0.33
 *FLUXES AND MAGS. NORMALISED TO V=0 (3.8×10^{-9} CGS/A)

LAMBDA [NM]	FLUX [(CGS/A)* 10^{-9}]	RDCRFLX	MAG	RDCRMAG	WT	RECIP-MU
175	0.22	1.02	3.09	1.43	1	5.71
180	19.76	82.73	-1.79	-3.34	2	5.56
185	24.31	92.90	-2.01	-3.47	3	5.41
190	19.25	70.07	-1.76	-3.16	3	5.26
195	13.87	53.33	-1.41	-2.87	3	5.13
200	9.52	38.54	-1.00	-2.52	3	5.00
205	6.94	29.51	-0.65	-2.23	2	4.88
210	5.65	25.22	-0.43	-2.05	2	4.76
215	5.56	25.88	-0.41	-2.08	2	4.65
220	6.21	30.17	-0.53	-2.25	3	4.55
225	7.06	35.80	-0.67	-2.43	3	4.44
230	7.84	39.28	-0.79	-2.54	3	4.35
235	8.46	40.00	-0.87	-2.56	3	4.26
240	9.04	40.35	-0.94	-2.56	3	4.17
245	9.48	39.93	-0.99	-2.55	4	4.08
250	9.67	38.66	-1.01	-2.52	4	4.00
255	9.83	37.32	-1.03	-2.48	4	3.92
260	9.97	36.05	-1.05	-2.44	4	3.85
265	9.86	34.09	-1.04	-2.38	3	3.77
270	10.02	33.08	-1.05	-2.35	3	3.70
275	10.04	31.67	-1.05	-2.30	2	3.64
280	9.99	30.20	-1.05	-2.25	3	3.57
285	9.76	28.36	-1.02	-2.18	3	3.51
290	9.55	26.67	-1.00	-2.12	2	3.45
295	8.19	22.00	-0.83	-1.91	1	3.39
300	6.07	15.68	-0.51	-1.54	0	3.33

BS 1239, V= 3.80 (B-V)XS 0.00
 *FLUXES AND MAGS. NORMALISED TO V=0 (3.8*10⁻⁹ CGS/A)

LAMBDA [NM]	FLUX [(CGS/A)*10 ⁻⁹]	RDCRFLX	MAG	RDCRMAG	WT	RECIP-MU
175	37.46	37.46	-2.48	-2.48	2	5.71
180	28.81	28.81	-2.20	-2.20	3	5.56
185	23.50	23.50	-1.98	-1.98	4	5.41
190	19.89	19.89	-1.80	-1.80	4	5.26
195	17.61	17.61	-1.66	-1.66	4	5.13
200	16.89	16.89	-1.62	-1.62	5	5.00
205	16.07	16.07	-1.57	-1.57	5	4.88
210	15.53	15.53	-1.53	-1.53	6	4.76
215	15.87	15.87	-1.55	-1.55	6	4.65
220	16.23	16.23	-1.58	-1.58	6	4.55
225	16.35	16.35	-1.58	-1.58	6	4.44
230	16.07	16.07	-1.57	-1.57	6	4.35
235	15.59	15.59	-1.53	-1.53	6	4.26
240	15.29	15.29	-1.51	-1.51	6	4.17
245	15.00	15.00	-1.49	-1.49	6	4.08
250	14.55	14.55	-1.46	-1.46	6	4.00
255	14.25	14.25	-1.43	-1.43	6	3.92
260	14.00	14.00	-1.42	-1.42	6	3.85
265	13.62	13.62	-1.39	-1.39	5	3.77
270	13.71	13.71	-1.39	-1.39	5	3.70
275	13.82	13.82	-1.40	-1.40	4	3.64
280	14.08	14.08	-1.42	-1.42	4	3.57
285	14.50	14.50	-1.45	-1.45	3	3.51
290	15.59	15.59	-1.53	-1.53	3	3.45
295	15.81	15.81	-1.55	-1.55	2	3.39
300	16.04	16.04	-1.56	-1.56	2	3.33

BS 1463, V= 4.12 (B-V)XS 0.03
 *FLUXES AND MAGS. NORMALISED TO V=0 (3.8×10^{-9} CGS/A)

LAMBDA [NM]	FLUX [(CGS/A)* 10^{-9}]	RDCRFLX	MAG	RDCRMAG	WT	RECIP-MU
175	65.42	75.18	-3.09	-3.24	4	5.71
180	57.96	66.02	-2.96	-3.10	5	5.56
185	47.77	53.97	-2.75	-2.88	6	5.41
190	38.87	43.71	-2.52	-2.65	6	5.26
195	32.96	37.25	-2.35	-2.48	6	5.13
200	30.38	34.50	-2.26	-2.39	7	5.00
205	28.31	32.29	-2.18	-2.32	7	4.88
210	26.93	30.85	-2.13	-2.27	8	4.76
215	27.11	31.17	-2.13	-2.28	8	4.65
220	27.12	31.32	-2.13	-2.29	8	4.55
225	26.71	30.96	-2.12	-2.28	8	4.44
230	25.58	29.62	-2.07	-2.23	8	4.35
235	24.14	27.80	-2.01	-2.16	8	4.26
240	23.02	26.37	-1.96	-2.10	8	4.17
245	21.97	25.04	-1.90	-2.05	8	4.08
250	20.74	23.52	-1.84	-1.98	7	4.00
255	19.75	22.30	-1.79	-1.92	7	3.92
260	18.71	21.03	-1.73	-1.86	6	3.85
265	17.58	19.68	-1.66	-1.79	6	3.77
270	17.06	19.02	-1.63	-1.75	5	3.70
275	16.50	18.32	-1.59	-1.71	5	3.64
280	16.49	18.24	-1.59	-1.70	4	3.57
285	17.15	18.90	-1.64	-1.74	4	3.51
290	19.48	21.39	-1.77	-1.88	4	3.45
295	21.90	23.96	-1.90	-2.00	3	3.39
300	25.71	28.02	-2.08	-2.17	3	3.33

BS 1520, V= 4.02 (B-V)XS 0.01
 *FLUXES AND MAGS. NORMALISED TO V=0 (3.8×10^{-9} CGS/A)

LAMBDA [NM]	FLUX [(CGS/A)* 10^{-9}]	RDCRFLX	MAG	RDCRMAG	WT	RECIP-MU
175	35.75	37.45	-2.43	-2.48	2	5.71
180	29.19	30.48	-2.21	-2.26	3	5.56
185	25.28	26.33	-2.06	-2.10	4	5.41
190	21.74	22.60	-1.89	-1.94	4	5.26
195	19.09	19.88	-1.75	-1.80	4	5.13
200	17.66	18.42	-1.67	-1.71	5	5.00
205	16.08	16.80	-1.57	-1.61	5	4.88
210	14.76	15.44	-1.47	-1.52	5	4.76
215	14.27	14.95	-1.44	-1.49	5	4.65
220	13.62	14.29	-1.39	-1.44	6	4.55
225	12.89	13.54	-1.33	-1.38	5	4.44
230	11.81	12.40	-1.23	-1.28	5	4.35

BS 1542, V= 4.30 (B-V)XS 0.30
 *FLUXES AND MAGS. NORMALISED TO V=0 (3.8×10^{-9} CGS/A)

LAMBDA [NM]	FLUX [(CGS/A)* 10^{-9}]	RDCRFLX	MAG	RDCRMAG	WT	RECIP-MU
175	28.67	115.1	-2.19	-3.70	2	5.71
180	21.36	78.50	-1.87	-3.29	2	5.56
185	16.09	54.43	-1.57	-2.89	3	5.41
190	12.50	40.46	-1.29	-2.57	3	5.26
195	10.03	34.12	-1.05	-2.38	3	5.13
200	8.532	30.42	-0.88	-2.26	3	5.00
205	7.425	27.67	-0.73	-2.16	3	4.88
210	6.686	26.04	-0.61	-2.09	3	4.76
215	6.553	26.53	-0.59	-2.11	3	4.65
220	6.711	28.24	-0.62	-2.18	3	4.55
225	7.111	31.10	-0.68	-2.28	3	4.44
230	7.662	33.14	-0.76	-2.35	3	4.35
235	8.385	34.42	-0.86	-2.39	4	4.26
240	9.383	36.54	-0.98	-2.46	4	4.17
245	10.44	38.59	-1.10	-2.52	5	4.08
250	11.27	39.73	-1.18	-2.55	5	4.00
255	11.93	40.13	-1.24	-2.56	4	3.92
260	12.29	39.54	-1.27	-2.54	5	3.85
265	11.91	36.76	-1.24	-2.46	5	3.77
270	11.46	33.96	-1.20	-2.38	4	3.70
275	10.42	29.62	-1.10	-2.23	4	3.64
280	9.512	26.01	-1.00	-2.09	3	3.57
285	8.908	23.50	-0.92	-1.98	2	3.51
290	9.367	23.84	-0.98	-1.99	2	3.45
295	10.30	25.30	-1.08	-2.06	2	3.39
300	12.16	28.79	-1.26	-2.20	2	3.33

BS 1790, V= 1.64 (B-V)XS 0.01
 *FLUXES AND MAGS. NORMALISED TO V=0 (3.8×10^{-9} CGS/A)

LAMBDA [NM]	FLUX [(CGS/A)* 10^{-9}]	RDCRFLX	MAG	RDCRMAG	WT	RECIP-MU
175	83.53	87.49	-3.35	-3.41	19	5.71
180	62.36	65.12	-3.04	-3.08	22	5.56
185	48.03	50.02	-2.75	-2.80	23	5.41
190	38.68	40.22	-2.52	-2.56	25	5.26
195	32.53	33.89	-2.33	-2.38	26	5.13
200	29.47	30.75	-2.22	-2.27	27	5.00
205	26.94	28.15	-2.13	-2.17	28	4.88
210	25.16	26.33	-2.05	-2.10	29	4.76
215	25.00	26.20	-2.05	-2.10	29	4.65
220	24.87	26.09	-2.04	-2.09	30	4.55
225	24.57	25.81	-2.03	-2.08	30	4.44
230	23.74	24.92	-1.99	-2.04	29	4.35
235	22.70	23.79	-1.94	-1.99	29	4.26
240	22.03	23.05	-1.91	-1.96	29	4.17
245	21.50	22.45	-1.88	-1.93	29	4.08
250	20.88	21.77	-1.85	-1.90	28	4.00
255	20.65	21.50	-1.84	-1.88	27	3.92
260	20.85	21.68	-1.85	-1.89	27	3.85
265	21.07	21.88	-1.86	-1.90	26	3.77
270	22.40	23.23	-1.93	-1.97	26	3.70
275	24.67	25.54	-2.03	-2.07	25	3.64
280	27.52	28.46	-2.15	-2.19	24	3.57
285	31.23	32.26	-2.29	-2.32	23	3.51
290	36.77	37.93	-2.46	-2.50	23	3.45
295	39.68	40.89	-2.55	-2.58	22	3.39
300	40.63	41.81	-2.57	-2.60	19	3.33

BS 1791, V= 1.65 (B-V)XS 0.00
 *FLUXES AND MAGS. NORMALISED TO V=0 (3.8×10^{-9} CGS/A)

LAMBDA [NM]	FLUX [(CGS/A)* 10^{-9}]	RDCRFLX	MAG	RDCRMAG	WT	RECIP-MU
175	20.55	20.55	-1.83	-1.83	8	5.71
180	16.82	16.82	-1.62	-1.62	10	5.56
185	15.24	15.24	-1.51	-1.51	12	5.41
190	14.21	14.21	-1.43	-1.43	14	5.26
195	13.84	13.84	-1.40	-1.40	15	5.13
200	14.42	14.42	-1.45	-1.45	16	5.00
205	14.17	14.17	-1.43	-1.43	18	4.88
210	13.67	13.67	-1.39	-1.39	19	4.76
215	13.58	13.58	-1.38	-1.38	20	4.65
220	13.17	13.17	-1.35	-1.35	20	4.55
225	12.73	12.73	-1.31	-1.31	19	4.44
230	12.26	12.26	-1.27	-1.27	20	4.35
235	12.05	12.05	-1.25	-1.25	20	4.26
240	12.37	12.37	-1.28	-1.28	20	4.17
245	12.99	12.99	-1.33	-1.33	21	4.08
250	13.56	13.56	-1.38	-1.38	22	4.00
255	14.09	14.09	-1.42	-1.42	22	3.92
260	14.30	14.30	-1.44	-1.44	21	3.85
265	13.67	13.67	-1.39	-1.39	19	3.77
270	12.88	12.88	-1.32	-1.32	18	3.70
275	11.15	11.15	-1.17	-1.17	15	3.64
280	9.53	9.53	-1.00	-1.00	12	3.57
285	8.20	8.20	-0.83	-0.83	10	3.51
290	7.97	7.97	-0.80	-0.80	9	3.45
295	8.42	8.42	-0.86	-0.86	8	3.39
300	9.62	9.62	-1.01	-1.01	6	3.33

BS 1852, V= 2.20 (B-V)XS 0.09
 *FLUXES AND MAGS. NORMALISED TO V=0 (3.8×10^{-9} CGS/A)

LAMBDA [NM]	FLUX [(CGS/A)* 10^{-9}]	RDCRFLX	MAG	RDCRMAG	WT	RECIP-MU
205	40.48	60.06	-2.57	-3.00	25	4.88
210	36.88	55.45	-2.47	-2.91	26	4.76
215	35.65	54.23	-2.43	-2.89	26	4.65
220	34.46	53.02	-2.39	-2.86	26	4.55
225	33.46	52.09	-2.36	-2.84	26	4.44
230	32.03	49.70	-2.31	-2.79	26	4.35
235	30.56	46.67	-2.26	-2.72	25	4.26
240	29.76	44.74	-2.23	-2.68	25	4.17
245	29.26	43.30	-2.22	-2.64	25	4.08
250	28.68	41.85	-2.19	-2.60	24	4.00
255	28.62	41.19	-2.19	-2.59	24	3.92
260	29.04	41.24	-2.21	-2.59	24	3.85
265	29.18	40.92	-2.21	-2.58	23	3.77
270	30.34	42.02	-2.26	-2.61	22	3.70

BS 1876/79/80 (271-17), V= 3.20 (B-V)XS 0.14
 *FLUXES AND MAGS. NORMALISED TO V=0 (3.8×10^{-9} CGS/A)

LAMBDA [NM]	FLUX [(CGS/A)* 10^{-9}]	RDCRFLX	MAG	RDCRMAG	WT	RECIP-MU
175	94.12	180.0	-3.48	-4.19	8	5.71
180	66.61	122.3	-3.11	-3.77	9	5.56
185	57.71	101.9	-2.95	-3.57	10	5.41
190	52.38	90.62	-2.85	-3.44	11	5.26
195	48.95	86.66	-2.77	-3.39	12	5.13
200	48.32	87.44	-2.76	-3.40	15	5.00
205	45.80	84.61	-2.70	-3.37	16	4.88
210	43.21	81.49	-2.64	-3.33	15	4.76
215	42.54	81.68	-2.62	-3.33	16	4.65
220	41.20	80.56	-2.59	-3.32	18	4.55
225	39.55	78.73	-2.54	-3.29	17	4.44
230	37.07	73.43	-2.47	-3.21	15	4.35
235	34.40	66.48	-2.39	-3.11	14	4.26
240	32.37	61.06	-2.33	-3.01	15	4.17
245	30.54	56.20	-2.26	-2.92	14	4.08
250	28.44	51.21	-2.19	-2.82	13	4.00
255	26.62	46.89	-2.11	-2.73	13	3.92
260	24.47	42.23	-2.02	-2.61	12	3.85
265	22.20	37.57	-1.92	-2.49	10	3.77
270	20.53	34.08	-1.83	-2.38	9	3.70
275	18.35	29.87	-1.71	-2.24	7	3.64
280	16.84	26.93	-1.62	-2.13	7	3.57
285	15.90	24.99	-1.55	-2.04	6	3.51
290	16.45	25.43	-1.59	-2.06	5	3.45
295	17.17	26.11	-1.64	-2.09	5	3.39
300	19.03	28.46	-1.75	-2.19	4	3.33

BS 1903, $V = 1.70$ (B-V)XS 0.19
 *FLUXES AND MAGS. NORMALISED TO $V=0$ (3.8×10^{-9} CGS/A)

LAMBDA [NM]	FLUX [(CGS/A)* 10^{-9}]	RDCRFLX	MAG	RDCRMAG	WT	RECIP-MU
175	22.10	53.31	-1.91	-2.87	7	5.71
180	16.46	37.54	-1.59	-2.49	9	5.56
185	13.47	29.14	-1.37	-2.21	12	5.41
190	11.22	23.61	-1.18	-1.98	12	5.26
195	9.48	20.58	-0.99	-1.83	12	5.13
200	8.15	18.23	-0.83	-1.70	12	5.00
205	6.72	15.46	-0.62	-1.52	12	4.88
210	5.27	12.46	-0.35	-1.29	11	4.76
215	3.88	9.41	-0.02	-0.98	8	4.65

BS 2106, V= 4.35 (B-V)XS 0.02
 *FLUXES AND MAGS. NORMALISED TO V=0 (3.8×10^{-9} CGS/A)

LAMBDA [NM]	FLUX [(CGS/A)* 10^{-9}]	RDCRFLX	MAG	RDCRMAG	WT	RECIP-MU
180	21.75	23.72	-1.89	-1.99	2	5.56
185	23.09	25.04	-1.96	-2.05	3	5.41
190	20.64	22.32	-1.84	-1.92	3	5.26
195	18.54	20.12	-1.72	-1.81	3	5.13
200	17.63	19.19	-1.67	-1.76	3	5.00
205	16.50	18.01	-1.59	-1.69	4	4.88
210	15.65	17.13	-1.54	-1.63	5	4.76
215	15.71	17.24	-1.54	-1.64	5	4.65
220	15.75	17.34	-1.54	-1.65	4	4.55
225	15.61	17.22	-1.53	-1.64	4	4.44
230	15.07	16.61	-1.50	-1.60	4	4.35
235	14.30	15.72	-1.44	-1.54	5	4.26
240	13.66	14.96	-1.39	-1.49	5	4.17
245	12.99	14.17	-1.33	-1.43	4	4.08
250	12.15	13.22	-1.26	-1.35	4	4.00
255	11.45	12.41	-1.20	-1.29	4	3.92
260	10.76	11.63	-1.13	-1.21	4	3.85
265	10.15	10.94	-1.07	-1.15	3	3.77
270	10.04	10.80	-1.06	-1.13	3	3.70
275	10.19	10.92	-1.07	-1.15	2	3.64
280	10.73	11.47	-1.13	-1.20	3	3.57
285	11.65	12.42	-1.22	-1.29	2	3.51
290	13.19	14.03	-1.35	-1.42	2	3.45
295	13.28	14.10	-1.36	-1.42	2	3.39

BS -2128, V= 4.95 (B-V)XS 0.05 (271-06)
 *FLUXES AND MAGS. NORMALISED TO V=0 (3.8×10^{-9} CGS/A)

LAMBDA [NM]	FLUX [(CGS/A)* 10^{-9}]	RDCRFLX	MAG	RDCRMAG	WT	RECIP-MU
175	28.82	36.34	-2.20	-2.45	1	5.71
180	17.48	21.71	-1.66	-1.89	2	5.56
185	19.76	24.21	-1.79	-2.01	2	5.41
190	20.47	24.90	-1.83	-2.04	2	5.26
195	19.83	24.32	-1.79	-2.02	3	5.13
200	19.03	23.52	-1.75	-1.98	3	5.00
205	17.26	21.49	-1.64	-1.88	3	4.88
210	15.63	19.61	-1.54	-1.78	3	4.76
215	14.95	18.88	-1.49	-1.74	3	4.65
220	14.19	18.03	-1.43	-1.69	3	4.55
225	13.48	17.24	-1.37	-1.64	3	4.44
230	12.54	16.01	-1.30	-1.56	3	4.35
235	11.62	14.70	-1.21	-1.47	3	4.26
240	11.06	13.87	-1.16	-1.41	2	4.17
245	10.81	13.45	-1.14	-1.37	2	4.08
250	10.79	13.31	-1.13	-1.36	3	4.00
255	11.17	13.67	-1.17	-1.39	3	3.92
260	11.98	14.55	-1.25	-1.46	3	3.85
265	12.52	15.11	-1.29	-1.50	3	3.77
270	13.34	15.99	-1.36	-1.56	2	3.70
275	13.90	16.55	-1.41	-1.60	2	3.64
280	14.11	16.69	-1.42	-1.61	2	3.57
285	14.19	16.68	-1.43	-1.61	2	3.51
290	15.06	17.60	-1.50	-1.66	2	3.45
295	15.92	18.49	-1.56	-1.72	2	3.39
300	18.37	21.21	-1.71	-1.87	1	3.33

BS 2205, V= 5.05 (B-V)XS 0.00
 *FLUXES AND MAGS. NORMALISED TO V=0 (3.8×10^{-9} CGS/A)

LAMBDA [NM]	FLUX [(CGS/A)* 10^{-9}]	RDCRFLX	MAG	RDCRMAG	WT	RECIP-MU
175	81.26	81.26	-3.33	-3.33	2	5.71
180	64.11	64.11	-3.07	-3.07	3	5.56
185	52.17	52.17	-2.84	-2.84	3	5.41
190	43.19	43.19	-2.64	-2.64	4	5.26
195	37.24	37.24	-2.48	-2.48	4	5.13
200	34.87	34.87	-2.41	-2.41	4	5.00
205	32.92	32.92	-2.34	-2.34	5	4.88
210	31.87	31.87	-2.31	-2.31	5	4.76
215	32.78	32.78	-2.34	-2.34	5	4.65
220	33.68	33.68	-2.37	-2.37	5	4.55
225	33.72	33.72	-2.37	-2.37	5	4.44
230	32.45	32.45	-2.33	-2.33	5	4.35
235	30.26	30.26	-2.25	-2.25	5	4.26
240	27.98	27.98	-2.17	-2.17	5	4.17
245	25.41	25.41	-2.06	-2.06	5	4.08
250	22.53	22.53	-1.93	-1.93	4	4.00
255	20.14	20.14	-1.81	-1.81	4	3.92
260	18.10	18.10	-1.69	-1.69	3	3.85
265	17.03	17.03	-1.63	-1.63	3	3.77
270	17.47	17.47	-1.66	-1.66	3	3.70
275	19.15	19.15	-1.76	-1.76	3	3.64
280	21.32	21.32	-1.87	-1.87	3	3.57
285	23.19	23.19	-1.96	-1.96	2	3.51
290	23.94	23.94	-2.00	-2.00	2	3.45
295	19.44	19.44	-1.77	-1.77	1	3.39

BS 2282, V= 3.02 (B-V)XS 0.02
 *FLUXES AND MAGS. NORMALISED TO V=0 (3.8×10^{-9} CGS/A)

LAMBDA [NM]	FLUX [(CGS/A)* 10^{-9}]	RDCRFLX	MAG	RDCRMAG	WT	RECIP-MU
175	19.32	21.19	-1.77	-1.87	1	5.71
180	13.09	14.28	-1.34	-1.44	1	5.56
185	19.11	20.73	-1.75	-1.84	5	5.41
190	23.20	25.09	-1.96	-2.05	7	5.26
195	25.40	27.56	-2.06	-2.15	9	5.13
200	27.29	29.70	-2.14	-2.23	9	5.00
205	26.67	29.12	-2.12	-2.21	10	4.88
210	25.81	28.26	-2.08	-2.18	12	4.76
215	26.36	28.94	-2.10	-2.20	12	4.65
220	27.29	30.03	-2.14	-2.24	11	4.55
225	28.02	30.92	-2.17	-2.28	12	4.44
230	28.06	30.94	-2.17	-2.28	13	4.35
235	27.43	30.14	-2.15	-2.25	12	4.26
240	26.55	29.07	-2.11	-2.21	12	4.17
245	25.02	27.30	-2.05	-2.14	13	4.08
250	22.64	24.63	-1.94	-2.03	11	4.00
255	20.17	21.86	-1.81	-1.90	9	3.92
260	17.36	18.77	-1.65	-1.73	8	3.85
265	15.28	16.47	-1.51	-1.59	8	3.77
270	14.48	15.56	-1.45	-1.53	7	3.70
275	14.68	15.74	-1.47	-1.54	7	3.64
280	15.85	16.95	-1.55	-1.62	6	3.57
285	17.25	18.41	-1.64	-1.71	5	3.51
290	18.38	19.56	-1.71	-1.78	5	3.45
295	16.18	17.18	-1.57	-1.64	4	3.39
300	12.00	12.71	-1.25	-1.31	3	3.33

BS 2288, $V = 5.51$ (B-V)XS 0.06
 *FLUXES AND MAGS. NORMALISED TO $V=0$ (3.8×10^{-9} CGS/A)

LAMBDA [NM]	FLUX [(CGS/A)* 10^{-9}]	RDCRFLX	MAG	RDCRMAG	WT	RECIP-MU
180	36.37	47.18	-2.45	-2.73	1	5.56
185	30.20	38.54	-2.25	-2.52	1	5.41
190	29.11	36.81	-2.21	-2.47	2	5.26
195	28.16	35.97	-2.17	-2.44	2	5.13
200	27.41	35.35	-2.15	-2.42	2	5.00
205	24.97	32.48	-2.04	-2.33	3	4.88
210	22.66	29.74	-1.94	-2.23	3	4.76
215	21.97	29.06	-1.90	-2.21	3	4.65
220	21.96	29.28	-1.90	-2.22	2	4.55
225	22.49	30.22	-1.93	-2.25	2	4.44
230	22.92	30.71	-1.95	-2.27	3	4.35
235	23.09	30.63	-1.96	-2.27	3	4.26
240	23.25	30.52	-1.97	-2.26	3	4.17
245	23.00	29.87	-1.95	-2.24	3	4.08
250	22.12	28.46	-1.91	-2.19	3	4.00
255	21.34	27.21	-1.87	-2.14	3	3.92
260	21.00	26.53	-1.86	-2.11	2	3.85
265	21.32	26.72	-1.87	-2.12	2	3.77
270	23.58	29.30	-1.98	-2.22	2	3.70
275	28.02	34.52	-2.17	-2.40	2	3.64
280	32.97	40.32	-2.35	-2.56	3	3.57
285	37.59	45.64	-2.49	-2.70	2	3.51
290	40.82	49.21	-2.58	-2.78	2	3.45
295	35.77	42.80	-2.43	-2.63	1	3.39
300	24.51	29.12	-2.02	-2.21	1	3.33

BS 2538, V= 3.94 (B-V)XS 0.00
 *FLUXES AND MAGS. NORMALISED TO V=0 (3.8×10^{-9} CGS/A)

LAMBDA [NM]	FLUX [(CGS/A)* 10^{-9}]	RDCRFLX	MAG	RDCRMAG	WT	RECIP-MU
175	82.97	82.97	-3.35	-3.35	4	5.71
180	64.94	64.94	-3.08	-3.08	6	5.56
185	59.44	59.44	-2.99	-2.99	7	5.41
190	54.86	54.86	-2.90	-2.90	7	5.26
195	51.52	51.52	-2.83	-2.83	9	5.13
200	50.48	50.48	-2.81	-2.81	11	5.00
205	47.10	47.10	-2.73	-2.73	11	4.88
210	43.46	43.46	-2.65	-2.65	10	4.76
215	41.72	41.72	-2.60	-2.60	9	4.65
220	39.25	39.25	-2.54	-2.54	10	4.55
225	37.03	37.03	-2.47	-2.47	11	4.44
230	34.48	34.48	-2.39	-2.39	11	4.35
235	32.20	32.20	-2.32	-2.32	9	4.26
240	30.92	30.92	-2.28	-2.28	8	4.17
245	30.09	30.09	-2.25	-2.25	8	4.08
250	29.15	29.15	-2.21	-2.21	9	4.00
255	28.52	28.52	-2.19	-2.19	9	3.92
260	27.79	27.79	-2.16	-2.16	8	3.85
265	26.63	26.63	-2.11	-2.11	8	3.77
270	26.24	26.24	-2.10	-2.10	7	3.70
275	25.77	25.77	-2.08	-2.08	6	3.64
280	26.01	26.01	-2.09	-2.09	5	3.57
285	27.15	27.15	-2.13	-2.13	5	3.51
290	30.56	30.56	-2.26	-2.26	5	3.45
295	33.36	33.36	-2.36	-2.36	5	3.39
300	37.08	37.08	-2.47	-2.47	4	3.33

BS 2845, (271-10), V= 2.92 (B-V)XS 0.01
 *FLUXES AND MAGS. NORMALISED TO V=0 (3.8×10^{-9} CGS/A)

LAMBDA [NM]	FLUX [(CGS/A)* 10^{-9}]	RDCRFLX	MAG	RDCRMAG	WT	RECIP-MU
175	8.51	8.92	-0.88	-0.93	2	5.71
180	8.05	8.40	-0.81	-0.86	2	5.56
185	7.99	8.33	-0.81	-0.85	4	5.41
190	7.26	7.55	-0.70	-0.75	4	5.26
195	6.62	6.89	-0.60	-0.65	5	5.13
200	6.40	6.67	-0.57	-0.61	5	5.00
205	6.10	6.37	-0.51	-0.56	6	4.88
210	5.92	6.20	-0.48	-0.53	6	4.76
215	6.11	6.40	-0.52	-0.57	6	4.65
220	6.33	6.64	-0.55	-0.61	6	4.55
225	6.41	6.74	-0.57	-0.62	6	4.44
230	6.27	6.59	-0.54	-0.60	7	4.35
235	5.98	6.27	-0.49	-0.54	7	4.26
240	5.70	5.97	-0.44	-0.49	6	4.17
245	5.40	5.64	-0.38	-0.43	6	4.08
250	5.07	5.29	-0.31	-0.36	6	4.00
255	4.88	5.08	-0.27	-0.31	5	3.92
260	4.85	5.05	-0.27	-0.31	5	3.85
265	4.94	5.13	-0.28	-0.33	6	3.77
270	5.33	5.52	-0.37	-0.41	5	3.70
275	5.87	6.07	-0.47	-0.51	5	3.64
280	6.27	6.49	-0.54	-0.58	5	3.57
285	6.38	6.58	-0.56	-0.60	4	3.51
290	6.13	6.32	-0.52	-0.55	3	3.45
295	4.84	4.98	-0.26	-0.29	3	3.39
300	3.43	3.53	0.11	0.08	2	3.33

BS 2845, (271-60), V= 2.92 (B-V)XS 0.01
 *FLUXES AND MAGS. NORMALISED TO V=0 (3.8×10^{-9} CGS/A)

LAMBDA [NM]	FLUX [(CGS/A)* 10^{-9}]	RDCRFLX	MAG	RDCRMAG	WT	RECIP-MU
175	9.26	9.70	-0.97	-1.02	2	5.71
180	9.83	10.26	-1.03	-1.08	3	5.56
185	8.94	9.31	-0.93	-0.97	4	5.41
190	7.68	7.98	-0.76	-0.81	5	5.26
195	6.92	7.21	-0.65	-0.70	5	5.13
200	6.83	7.13	-0.64	-0.68	5	5.00
205	6.59	6.88	-0.60	-0.64	6	4.88
210	6.31	6.60	-0.55	-0.60	6	4.76
215	6.22	6.51	-0.53	-0.58	6	4.65
220	5.91	6.20	-0.48	-0.53	6	4.55
225	5.53	5.81	-0.41	-0.46	6	4.44
230	5.07	5.33	-0.31	-0.37	5	4.35
235	4.72	4.94	-0.23	-0.29	6	4.26
240	4.62	4.83	-0.21	-0.26	6	4.17
245	4.71	4.92	-0.23	-0.28	6	4.08
250	4.90	5.11	-0.28	-0.32	6	4.00
255	5.18	5.39	-0.34	-0.38	6	3.92
260	5.47	5.69	-0.40	-0.44	6	3.85
265	5.47	5.68	-0.40	-0.44	6	3.77
270	5.45	5.65	-0.39	-0.43	6	3.70
275	5.13	5.31	-0.33	-0.36	4	3.64
280	4.81	4.97	-0.26	-0.29	4	3.57
285	4.66	4.82	-0.22	-0.26	3	3.51
290	5.12	5.28	-0.32	-0.36	3	3.45
295	5.74	5.92	-0.45	-0.48	3	3.39
300	6.24	6.42	-0.54	-0.57	2	3.33

BS 3314, $V = 3.90$ (B-V)XS 0.00
 *FLUXES AND MAGS. NORMALISED TO $V=0$ (3.8×10^{-9} CGS/A)

LAMBDA [NM]	FLUX [(CGS/A)* 10^{-9}]	RDCRFLX	MAG	RDCRMAG	WT	RECIP-MU
175	8.99	8.99	-0.94	-0.94	0	5.71
180	7.55	7.55	-0.75	-0.75	1	5.56
185	7.14	7.14	-0.69	-0.69	2	5.41
190	6.34	6.34	-0.56	-0.56	2	5.26
195	5.58	5.58	-0.42	-0.42	2	5.13
200	5.08	5.08	-0.32	-0.32	2	5.00
205	4.58	4.58	-0.20	-0.20	2	4.88
210	4.25	4.25	-0.12	-0.12	2	4.76
215	4.29	4.29	-0.13	-0.13	2	4.65
220	4.50	4.50	-0.18	-0.18	2	4.55
225	4.73	4.73	-0.24	-0.24	2	4.44
230	4.87	4.87	-0.27	-0.27	2	4.35
235	4.88	4.88	-0.27	-0.27	3	4.26
240	4.83	4.83	-0.26	-0.26	3	4.17
245	4.62	4.62	-0.21	-0.21	3	4.08
250	4.24	4.24	-0.12	-0.12	3	4.00
255	3.81	3.81	-0.00	-0.00	2	3.92
260	3.36	3.36	0.13	0.13	2	3.85
265	3.13	3.13	0.21	0.21	2	3.77
270	3.31	3.31	0.15	0.15	2	3.70
275	4.02	4.02	-0.06	-0.06	2	3.64
280	5.00	5.00	-0.30	-0.30	2	3.57
285	5.89	5.89	-0.48	-0.48	2	3.51
290	6.01	6.01	-0.50	-0.50	2	3.45
295	3.91	3.91	-0.03	-0.03	1	3.39

BS 3690, V= 3.81 (B-V)XS 0.00
 *FLUXES AND MAGS. NORMALISED TO V=0 (3.8×10^{-9} CGS/A)

LAMBDA [NM]	FLUX [(CGS/A)* 10^{-9}]	RDCRFLX	MAG	RDCRMAG	WT	RECIP-MU
190	4.96	4.96	-0.29	-0.29	2	5.26
195	4.23	4.23	-0.12	-0.12	2	5.13
200	3.89	3.89	-0.02	-0.02	2	5.00
205	3.55	3.55	0.07	0.07	3	4.88
210	3.29	3.29	0.16	0.16	3	4.76
215	3.23	3.23	0.18	0.18	3	4.65
220	3.17	3.17	0.20	0.20	3	4.55
225	3.13	3.13	0.21	0.21	3	4.44
230	3.06	3.06	0.23	0.23	3	4.35
235	3.00	3.00	0.26	0.26	3	4.26
240	3.00	3.00	0.26	0.26	3	4.17
245	3.01	3.01	0.25	0.25	3	4.08
250	2.96	2.96	0.27	0.27	3	4.00
255	2.89	2.89	0.30	0.30	3	3.92
260	2.73	2.73	0.36	0.36	2	3.85
265	2.46	2.46	0.47	0.47	2	3.77
270	2.20	2.20	0.59	0.59	2	3.70
275	1.84	1.84	0.79	0.79	2	3.64
280	1.65	1.65	0.90	0.90	1	3.57
285	1.77	1.77	0.83	0.83	1	3.51
290	2.47	2.47	0.47	0.47	1	3.45
295	3.38	3.38	0.13	0.13	1	3.39
300	3.13	3.13	0.21	0.21	1	3.33

BS 3894, V= 4.59 (B-V)XS 0.00
 *FLUXES AND MAGS. NORMALISED TO V=0 (3.8×10^{-9} CGS/A)

LAMBDA [NM]	FLUX [(CGS/A)* 10^{-9}]	RDCRFLX	MAG	RDCRMAG	WT	RECIP-MU
190	2.37	2.37	0.51	0.51	1	5.26
195	2.36	2.36	0.52	0.52	1	5.13
200	2.53	2.53	0.44	0.44	1	5.00
205	2.53	2.53	0.44	0.44	2	4.88
210	2.48	2.48	0.46	0.46	1	4.76
215	2.49	2.49	0.46	0.46	1	4.65
220	2.50	2.50	0.45	0.45	1	4.55
225	2.55	2.55	0.43	0.43	2	4.44
230	2.65	2.65	0.39	0.39	2	4.35
235	2.84	2.84	0.32	0.32	2	4.26
240	3.14	3.14	0.21	0.21	2	4.17
245	3.48	3.48	0.10	0.10	2	4.08
250	3.72	3.72	0.02	0.02	2	4.00
255	3.87	3.87	-0.02	-0.02	2	3.92
260	3.81	3.81	-0.00	-0.00	2	3.85
265	3.47	3.47	0.10	0.10	2	3.77
270	3.06	3.06	0.23	0.23	2	3.70
275	2.55	2.55	0.43	0.43	1	3.64
280	2.52	2.52	0.45	0.45	1	3.57
285	3.26	3.26	0.17	0.17	1	3.51
290	5.02	5.02	-0.30	-0.30	1	3.45

BS 4033, V= 3.45 (B-V)XS 0.00
 *FLUXES AND MAGS. NORMALISED TO V=0 (3.8×10^{-9} CGS/A)

LAMBDA [NM]	FLUX [(CGS/A)* 10^{-9}]	RDCRFLX	MAG	RDCRMAG	WT	RECIP-MU
175	2.70	2.70	0.37	0.37	1	5.71
180	1.22	1.22	1.23	1.23	0	5.56
185	0.67	0.67	1.89	1.89	0	5.41
190	0.76	0.76	1.75	1.75	1	5.26
195	1.04	1.04	1.40	1.40	1	5.13
200	1.50	1.50	1.01	1.01	2	5.00
205	1.75	1.75	0.84	0.84	2	4.88
210	1.88	1.88	0.76	0.76	2	4.76
215	1.98	1.98	0.71	0.71	3	4.65
220	1.96	1.96	0.72	0.72	3	4.55
225	1.88	1.88	0.77	0.77	2	4.44
230	1.76	1.76	0.84	0.84	2	4.35
235	1.69	1.69	0.88	0.88	2	4.26
240	1.72	1.72	0.86	0.86	2	4.17
245	1.83	1.83	0.79	0.79	3	4.08
250	1.97	1.97	0.71	0.71	3	4.00
255	2.14	2.14	0.62	0.62	3	3.92
260	2.30	2.30	0.54	0.54	3	3.85
265	2.33	2.33	0.53	0.53	3	3.77
270	2.37	2.37	0.51	0.51	3	3.70
275	2.35	2.35	0.52	0.52	2	3.64
280	2.37	2.37	0.51	0.51	2	3.57
285	2.53	2.53	0.44	0.44	2	3.51
290	3.00	3.00	0.26	0.26	2	3.45
295	3.48	3.48	0.10	0.10	2	3.39
300	3.94	3.94	-0.04	-0.04	1	3.33

BS 4295, V= 2.37 (B-V)XS 0.00
 *FLUXES AND MAGS. NORMALISED TO V=0 (3.8×10^{-9} CGS/A)

LAMBDA [NM]	FLUX [(CGS/A)* 10^{-9}]	RDCRFLX	MAG	RDCRMAG	WT	RECIP-MU
175	4.00	4.00	-0.06	-0.06	2	5.71
180	4.40	4.40	-0.16	-0.16	3	5.56
185	4.63	4.63	-0.21	-0.21	4	5.41
190	4.16	4.16	-0.10	-0.10	6	5.26
195	3.66	3.66	0.04	0.04	6	5.13
200	3.32	3.32	0.15	0.15	6	5.00
205	2.95	2.95	0.27	0.27	6	4.88
210	2.66	2.66	0.39	0.39	6	4.76
215	2.55	2.55	0.44	0.44	6	4.65
220	2.46	2.46	0.47	0.47	6	4.55
225	2.41	2.41	0.50	0.50	6	4.44
230	2.35	2.35	0.52	0.52	6	4.35
235	2.31	2.31	0.54	0.54	6	4.26
240	2.34	2.34	0.53	0.53	6	4.17
245	2.40	2.40	0.50	0.50	6	4.08
250	2.46	2.46	0.47	0.47	6	4.00
255	2.56	2.56	0.43	0.43	7	3.92
260	2.69	2.69	0.38	0.38	6	3.85
265	2.75	2.75	0.35	0.35	6	3.77
270	2.88	2.88	0.30	0.30	6	3.70
275	2.98	2.98	0.26	0.26	5	3.64
280	3.05	3.05	0.24	0.24	5	3.57
285	3.10	3.10	0.22	0.22	5	3.51
290	3.25	3.25	0.17	0.17	4	3.45
295	3.24	3.24	0.17	0.17	4	3.39
300	3.40	3.40	0.12	0.12	3	3.33

BS 4660, V= 3.32 (B-V)XS 0.00
 *FLUXES AND MAGS. NORMALISED TO V=0 (3.8×10^{-9} CGS/A)

LAMBDA [NM]	FLUX [(CGS/A)* 10^{-9}]	RDCRFLX	MAG	RDCRMAG	WT	RECIP-MU
185	2.88	2.88	0.30	0.30	1	5.41
190	3.19	3.19	0.19	0.19	2	5.26
195	3.03	3.03	0.25	0.25	3	5.13
200	2.80	2.80	0.33	0.33	3	5.00
205	2.48	2.48	0.46	0.46	3	4.88
210	2.22	2.22	0.58	0.58	3	4.76
215	2.13	2.13	0.63	0.63	3	4.65
220	2.11	2.11	0.64	0.64	3	4.55
225	2.13	2.13	0.63	0.63	3	4.44
230	2.16	2.16	0.61	0.61	4	4.35
235	2.19	2.19	0.60	0.60	3	4.26
240	2.27	2.27	0.56	0.56	3	4.17
245	2.34	2.34	0.52	0.52	3	4.08
250	2.38	2.38	0.51	0.51	4	4.00
255	2.41	2.41	0.49	0.49	3	3.92
260	2.45	2.45	0.48	0.48	3	3.85
265	2.43	2.43	0.49	0.49	3	3.77
270	2.47	2.47	0.47	0.47	3	3.70
275	2.52	2.52	0.44	0.44	3	3.64
280	2.59	2.59	0.41	0.41	3	3.57
285	2.69	2.69	0.37	0.37	2	3.51
290	2.91	2.91	0.29	0.29	2	3.45
295	2.96	2.96	0.27	0.27	2	3.39
300	3.00	3.00	0.26	0.26	2	3.33

BS 6092, V= 3.90 (B-V)XS 0.00
 *FLUXES AND MAGS. NORMALISED TO V=0 (3.8*10⁻⁹ CGS/A)

LAMBDA [NM]	FLUX [(CGS/A)*10 ⁻⁹]	RDCRFLX	MAG	RDCRMAG	WT	RECIP-MU
175	39.59	39.59	-2.54	-2.54	3	5.71
180	28.59	28.59	-2.19	-2.19	4	5.56
185	21.27	21.27	-1.87	-1.87	4	5.41
190	17.20	17.20	-1.64	-1.64	4	5.26
195	14.91	14.91	-1.48	-1.48	4	5.13
200	14.24	14.24	-1.43	-1.43	5	5.00
205	13.59	13.59	-1.38	-1.38	5	4.88
210	13.14	13.14	-1.35	-1.35	6	4.76
215	13.34	13.34	-1.36	-1.36	6	4.65
220	13.43	13.43	-1.37	-1.37	6	4.55
225	13.28	13.28	-1.36	-1.36	6	4.44
230	12.77	12.77	-1.32	-1.32	6	4.35
235	12.10	12.10	-1.26	-1.26	6	4.26
240	11.60	11.60	-1.21	-1.21	6	4.17
245	11.11	11.11	-1.16	-1.16	6	4.08
250	10.52	10.52	-1.11	-1.11	5	4.00
255	10.04	10.04	-1.06	-1.06	5	3.92
260	9.60	9.60	-1.01	-1.01	4	3.85
265	9.21	9.21	-0.96	-0.96	5	3.77
270	9.32	9.32	-0.97	-0.97	4	3.70
275	9.82	9.82	-1.03	-1.03	4	3.64
280	10.74	10.74	-1.13	-1.13	4	3.57
285	11.94	11.94	-1.24	-1.24	4	3.51
290	13.20	13.20	-1.35	-1.35	3	3.45
295	12.00	12.00	-1.25	-1.25	3	3.39
300	8.38	8.38	-0.86	-0.86	2	3.33

BS 6588, V= 3.80 (B-V)XS 0.02
 *FLUXES AND MAGS. NORMALISED TO V=0 (3.8*10⁻⁹ CGS/A)

LAMBDA [NM]	FLUX [(CGS/A)*10 ⁻⁹]	RDCRFLX	MAG	RDCRMAG	WT	RECIP-MU
180	31.54	34.40	-2.30	-2.39	5	5.56
185	26.43	28.67	-2.11	-2.19	5	5.41
190	22.39	24.22	-1.93	-2.01	6	5.26
195	19.52	21.18	-1.78	-1.87	6	5.13
200	18.16	19.77	-1.70	-1.79	7	5.00
205	16.85	18.40	-1.62	-1.71	7	4.88
210	15.94	17.46	-1.56	-1.66	7	4.76
215	16.03	17.60	-1.56	-1.66	7	4.65
220	16.13	17.75	-1.57	-1.67	7	4.55
225	16.01	17.67	-1.56	-1.67	8	4.44
230	15.45	17.04	-1.52	-1.63	8	4.35
235	14.64	16.09	-1.46	-1.57	8	4.26
240	13.97	15.29	-1.41	-1.51	7	4.17
245	13.30	14.52	-1.36	-1.46	7	4.08
250	12.56	13.66	-1.30	-1.39	7	4.00
255	12.06	13.07	-1.25	-1.34	6	3.92
260	11.72	12.67	-1.22	-1.31	6	3.85
265	11.38	12.27	-1.19	-1.27	6	3.77
270	11.39	12.24	-1.19	-1.27	6	3.70
275	10.95	11.74	-1.15	-1.22	4	3.64
280	9.89	10.58	-1.04	-1.11	4	3.57
285	7.83	8.36	-0.79	-0.86	3	3.51
290	5.47	5.82	-0.39	-0.46	2	3.45

BS 7608, V= 5.12 (B-V)XS 0.03
 *FLUXES AND MAGS. NORMALISED TO V=0 (3.8×10^{-9} CGS/A)

LAMBDA [NM]	FLUX [(CGS/A)* 10^{-9}]	RDCRFLX	MAG	RDCRMAG	WT	RECIP-MU
190	20.73	23.32	-1.84	-1.97	3	5.26
195	16.99	19.20	-1.63	-1.76	2	5.13
200	14.64	16.63	-1.46	-1.60	2	5.00
205	12.71	14.50	-1.31	-1.45	2	4.88
210	11.28	12.92	-1.18	-1.33	2	4.76
215	10.76	12.38	-1.13	-1.28	3	4.65
220	10.47	12.08	-1.10	-1.26	3	4.55
225	10.40	12.06	-1.09	-1.25	3	4.44
230	10.31	11.94	-1.08	-1.24	2	4.35
235	10.24	11.79	-1.08	-1.23	2	4.26
240	10.32	11.82	-1.08	-1.23	2	4.17
245	10.31	11.75	-1.08	-1.23	3	4.08
250	10.00	11.34	-1.05	-1.19	3	4.00
255	9.50	10.73	-0.99	-1.13	3	3.92
260	8.53	9.58	-0.88	-1.00	2	3.85
265	7.24	8.11	-0.70	-0.82	2	3.77
270	5.95	6.64	-0.49	-0.61	1	3.70
275	4.30	4.77	-0.13	-0.25	1	3.64
280	3.36	3.72	0.13	0.02	1	3.57
285	3.42	3.77	0.12	0.01	1	3.51
290	5.09	5.58	-0.32	-0.42	1	3.45

BS 7852, V= 4.03 (B-V)XS 0.01
 *FLUXES AND MAGS. NORMALISED TO V=0 (3.8×10^{-9} CGS/A)

LAMBDA [NM]	FLUX [(CGS/A)* 10^{-9}]	RDCRFLX	MAG	RDCRMAG	WT	RECIP-MU
175	19.27	20.18	-1.76	-1.81	2	5.71
180	13.94	14.55	-1.41	-1.46	2	5.56
185	12.14	12.64	-1.26	-1.30	3	5.41
190	10.84	11.27	-1.14	-1.18	3	5.26
195	9.86	10.27	-1.04	-1.08	3	5.13
200	9.39	9.80	-0.98	-1.03	4	5.00
205	8.66	9.05	-0.89	-0.94	4	4.88
210	8.01	8.38	-0.81	-0.86	3	4.76
215	7.81	8.19	-0.78	-0.83	3	4.65
220	7.62	7.99	-0.75	-0.81	4	4.55
225	7.47	7.84	-0.73	-0.79	4	4.44
230	7.25	7.61	-0.70	-0.75	4	4.35
235	7.05	7.39	-0.67	-0.72	4	4.26
240	7.01	7.34	-0.67	-0.71	4	4.17
245	7.03	7.35	-0.67	-0.72	4	4.08
250	7.00	7.30	-0.66	-0.71	4	4.00
255	7.03	7.32	-0.67	-0.71	4	3.92
260	7.12	7.40	-0.68	-0.72	4	3.85
265	7.11	7.38	-0.68	-0.72	3	3.77
270	7.39	7.67	-0.72	-0.76	3	3.70
275	7.91	8.19	-0.80	-0.83	3	3.64
280	8.65	8.94	-0.89	-0.93	3	3.57
285	9.61	9.93	-1.01	-1.04	3	3.51

BS 8007, V= 6.44 (B-V)XS 0.10
 *FLUXES AND MAGS. NORMALISED TO V=0 (3.8×10^{-9} CGS/A)

LAMBDA [NM]	FLUX [(CGS/A)* 10^{-9}]	RDCRFLX H	MAG	RDCRMAG	WT	RECIP-MU
175	63.00	H	-3.05	-3.55	1	5.71
180	42.71	65.91	-2.63	-3.10	1	5.56
185	31.30	46.98	-2.29	-2.73	1	5.41
190	26.51	39.22	-2.11	-2.53	1	5.26
195	24.64	37.05	-2.03	-2.47	2	5.13
200	25.34	38.70	-2.06	-2.52	2	5.00
205	25.02	38.79	-2.05	-2.52	2	4.88
210	24.31	38.25	-2.01	-2.51	2	4.76
215	24.20	38.57	-2.01	-2.52	2	4.65
220	23.15	37.38	-1.96	-2.48	2	4.55
225	21.66	35.42	-1.89	-2.42	2	4.44
230	19.72	32.14	-1.79	-2.32	2	4.35
235	18.02	28.84	-1.69	-2.20	2	4.26
240	17.21	27.08	-1.64	-2.13	2	4.17
245	17.20	26.59	-1.64	-2.11	2	4.08
250	17.73	26.98	-1.67	-2.13	2	4.00
255	19.00	28.47	-1.75	-2.19	2	3.92
260	21.08	31.12	-1.86	-2.28	2	3.85
265	22.51	32.77	-1.93	-2.34	2	3.77
270	24.36	34.99	-2.02	-2.41	2	3.70
275	25.67	36.36	-2.07	-2.45	2	3.64
280	25.91	36.24	-2.08	-2.45	1	3.57
285	25.09	34.67	-2.05	-2.40	2	3.51
290	24.10	32.90	-2.01	-2.34	1	3.45
295	21.27	28.69	-1.87	-2.19	0	3.39
300	19.96	26.61	-1.80	-2.11	1	3.33

BS 8238, V= 3.18 (B-V)XS 0.00
 *FLUXES AND MAGS. NORMALISED TO V=0 (3.8×10^{-9} CGS/A)

LAMBDA [NM]	FLUX [(CGS/A)* 10^{-9}]	RDCRFLX	MAG	RDCRMAG	WT	RECIP-MU
175	62.26	62.26	-3.04	-3.04	8	5.71
180	51.73	51.73	-2.83	-2.83	9	5.56
185	41.75	41.75	-2.60	-2.60	11	5.41
190	34.87	34.87	-2.41	-2.41	12	5.26
195	31.27	31.27	-2.29	-2.29	12	5.13
200	31.40	31.40	-2.29	-2.29	14	5.00
205	31.30	31.30	-2.29	-2.29	15	4.88
210	31.48	31.48	-2.30	-2.30	17	4.76
215	33.07	33.07	-2.35	-2.35	17	4.65
220	34.36	34.36	-2.39	-2.39	17	4.55
225	34.65	34.65	-2.40	-2.40	18	4.44
230	33.84	33.84	-2.37	-2.37	18	4.35
235	32.52	32.52	-2.33	-2.33	18	4.26
240	31.57	31.57	-2.30	-2.30	18	4.17
245	30.68	30.68	-2.27	-2.27	16	4.08
250	29.43	29.43	-2.22	-2.22	16	4.00
255	28.36	28.36	-2.18	-2.18	17	3.92
260	26.92	26.92	-2.13	-2.13	15	3.85
265	24.94	24.94	-2.04	-2.04	13	3.77
270	23.35	23.35	-1.97	-1.97	12	3.70
275	20.90	20.90	-1.85	-1.85	10	3.64
280	19.10	19.10	-1.75	-1.75	9	3.57
285	18.20	18.20	-1.70	-1.70	9	3.51
290	19.79	19.79	-1.79	-1.79	8	3.45
295	22.44	22.44	-1.93	-1.93	7	3.39
300	26.04	26.04	-2.09	-2.09	6	3.33

BS 8781, V= 2.49 (B-V)XS 0.00
 *FLUXES AND MAGS. NORMALISED TO V=0 (3.8×10^{-9} CGS/A)

LAMBDA [NM]	FLUX [(CGS/A)* 10^{-9}]	RDCRFLX	MAG	RDCRMAG	WT	RECIP-MU
175	3.56	3.56	0.07	0.07	2	5.71
180	4.09	4.09	-0.08	-0.08	3	5.56
185	4.44	4.44	-0.17	-0.17	4	5.41
190	3.97	3.97	-0.05	-0.05	5	5.26
195	3.49	3.49	0.09	0.09	5	5.13
200	3.27	3.27	0.16	0.16	6	5.00
205	3.10	3.10	0.22	0.22	6	4.88
210	3.04	3.04	0.24	0.24	6	4.76
215	3.16	3.16	0.20	0.20	6	4.65
220	3.28	3.28	0.16	0.16	7	4.55
225	3.29	3.29	0.16	0.16	7	4.44
230	3.18	3.18	0.19	0.19	6	4.35
235	3.02	3.02	0.25	0.25	7	4.26
240	2.91	2.91	0.29	0.29	7	4.17
245	2.86	2.86	0.31	0.31	6	4.08
250	2.85	2.85	0.31	0.31	6	4.00
255	2.93	2.93	0.28	0.28	6	3.92
260	3.12	3.12	0.22	0.22	7	3.85
265	3.23	3.23	0.18	0.18	6	3.77
270	3.42	3.42	0.12	0.12	6	3.70
275	3.51	3.51	0.09	0.09	5	3.64
280	3.49	3.49	0.09	0.09	5	3.57
285	3.38	3.38	0.13	0.13	5	3.51
290	3.39	3.39	0.12	0.12	4	3.45
295	3.34	3.34	0.14	0.14	3	3.39
300	3.68	3.68	0.04	0.04	3	3.33

BS 8937, (271-11), V= 4.36 (B-V)XS 0.00
 *FLUXES AND MAGS. NORMALISED TO V=0 (3.8×10^{-9} CGS/A)

LAMBDA [NM]	FLUX [(CGS/A)* 10^{-9}]	RDCRFLX	MAG	RDCRMAG	WT	RECIP-MU
175	21.17	21.17	-1.86	-1.86	1	5.71
180	15.23	15.23	-1.51	-1.51	2	5.56
185	12.22	12.22	-1.27	-1.27	2	5.41
190	10.48	10.48	-1.10	-1.10	2	5.26
195	9.37	9.37	-0.98	-0.98	2	5.13
200	8.93	8.93	-0.93	-0.93	3	5.00
205	8.32	8.32	-0.85	-0.85	3	4.88
210	7.80	7.80	-0.78	-0.78	3	4.76
215	7.71	7.71	-0.77	-0.77	3	4.65
220	7.60	7.60	-0.75	-0.75	3	4.55
225	7.48	7.48	-0.74	-0.74	3	4.44
230	7.25	7.25	-0.70	-0.70	3	4.35
235	7.01	7.01	-0.67	-0.67	3	4.26
240	6.91	6.91	-0.65	-0.65	3	4.17
245	6.85	6.85	-0.64	-0.64	3	4.08
250	6.70	6.70	-0.62	-0.62	3	4.00
255	6.57	6.57	-0.59	-0.59	3	3.92
260	6.35	6.35	-0.56	-0.56	3	3.85
265	5.96	5.96	-0.49	-0.49	2	3.77
270	5.62	5.62	-0.43	-0.43	2	3.70
275	5.01	5.01	-0.30	-0.30	2	3.64
280	4.45	4.45	-0.17	-0.17	1	3.57
285	4.03	4.03	-0.06	-0.06	1	3.51
290	4.28	4.28	-0.13	-0.13	1	3.45
295	5.32	5.32	-0.37	-0.37	1	3.39
300	7.81	7.81	-0.78	-0.78	1	3.33

BS 8988, V= 4.48 (B-V)XS 0.00
 *FLUXES AND MAGS. NORMALISED TO V=0 (3.8*10⁻⁹ CGS/A)

LAMBDA [NM]	FLUX [(CGS/A)*10 ⁻⁹]	RDCRFLX	MAG	RDCRMAG	WT	RECIP-MU
185	4.89	4.89	-0.27	-0.27	1	5.41
190	4.99	4.99	-0.29	-0.29	2	5.26
195	4.59	4.59	-0.21	-0.21	1	5.13
200	4.14	4.14	-0.09	-0.09	1	5.00
205	3.61	3.61	0.05	0.05	2	4.88
210	3.22	3.22	0.18	0.18	2	4.76
215	3.12	3.12	0.21	0.21	2	4.65
220	3.16	3.16	0.20	0.20	2	4.55
225	3.27	3.27	0.16	0.16	2	4.44
230	3.35	3.35	0.14	0.14	2	4.35
235	3.39	3.39	0.12	0.12	2	4.26
240	3.44	3.44	0.11	0.11	2	4.17
245	3.44	3.44	0.11	0.11	2	4.08
250	3.35	3.35	0.14	0.14	2	4.00
255	3.27	3.27	0.16	0.16	2	3.92
260	3.20	3.20	0.19	0.19	1	3.85
265	3.15	3.15	0.20	0.20	1	3.77
270	3.29	3.29	0.16	0.16	2	3.70
275	3.60	3.60	0.06	0.06	1	3.64
280	4.03	4.03	-0.06	-0.06	1	3.57
285	4.52	4.52	-0.19	-0.19	2	3.51
290	5.06	5.06	-0.31	-0.31	1	3.45
295	4.90	4.90	-0.28	-0.28	1	3.39

BS 9098, V= 4.54 (B-V)XS 0.00
 *FLUXES AND MAGS. NORMALISED TO V=0 (3.8×10^{-9} CGS/A)

LAMBDA [NM]	FLUX [(CGS/A)* 10^{-9}]	RDCRFLX	MAG	RDCRMAG	WT	RECIP-MU
175	5.65	5.65	-0.43	-0.43	1	5.71
180	7.24	7.24	-0.70	-0.70	1	5.56
185	7.34	7.34	-0.71	-0.71	2	5.41
190	6.16	6.16	-0.52	-0.52	2	5.26
195	5.08	5.08	-0.32	-0.32	2	5.13
200	4.40	4.40	-0.16	-0.16	2	5.00
205	3.94	3.94	-0.04	-0.04	2	4.88
210	3.71	3.71	0.03	0.03	2	4.76
215	3.81	3.81	-0.00	-0.00	2	4.65
220	4.00	4.00	-0.06	-0.06	2	4.55
225	4.11	4.11	-0.08	-0.08	2	4.44
230	4.07	4.07	-0.07	-0.07	2	4.35
235	3.91	3.91	-0.03	-0.03	2	4.26
240	3.74	3.74	0.02	0.02	2	4.17
245	3.55	3.55	0.07	0.07	2	4.08
250	3.34	3.34	0.14	0.14	2	4.00
255	3.22	3.22	0.18	0.18	2	3.92
260	3.18	3.18	0.19	0.19	2	3.85
265	3.16	3.16	0.20	0.20	2	3.77
270	3.22	3.22	0.18	0.18	2	3.70
275	3.03	3.03	0.24	0.24	1	3.64
280	2.53	2.53	0.44	0.44	1	3.57
285	1.81	1.81	0.80	0.80	1	3.51

THE BACKGROUND BRIGHTNESS OF THE MILKY WAY
NEAR 2500 \AA BETWEEN $l'' = 72^\circ$ AND 126°

By
G. C. SUDBURY
and
M. F. INGHAM

The Background Brightness of the Milky Way near 2500 Å between $l^{\text{II}} = 72^\circ$ and 126°

by

G. C. SUDBURY

Royal Observatory,
Edinburgh EH9 3HJ

M. F. INGHAM

Department of Astrophysics,
South Parks Road, OxfordData from a rocket experiment show details which
were not known from ground-based observations.

GROUND-BASED surveys of the brightness of the Milky Way (see refs. 1-4, for example) have recently been supplemented by extraterrestrial observations (refs. 5-9 and unpublished work by Wolstencroft and Rose). We present and discuss here some sounding rocket data derived from four scans across the galactic plane between $l^{\text{II}} = 72^\circ$ and 126° at an effective wavelength of 2425 Å. These observations, while agreeing qualitatively with the ground-based observations, show certain details and quantitative aspects which may relate to the distribution of dust and stars and, when compared with other space observations, to the scattering and absorption properties of the interstellar dust in the ultraviolet.

The data have been derived from the output of a Royal Observatory, Edinburgh, spectrophotometer on board an ESRO Skylark rocket (payload S27/1), which was unstabilized but which had a controlled roll rate, launched on December 3, 1968, at 21 h 39 m UT from the Salto di Quirra range, Sardinia. Full details of the optics and pulse-counting techniques have been published elsewhere^{10,11}. The optical system is designed to scan the spectra of stars at 200 Å resolution but, when viewing a uniform background, behaves as a photometer with a bandpass at half height from 2020 to 2790 Å, a field width of 2.9° and an effective area of 0.5 square degrees. The absolute spectral response curve has been obtained by comparison of our own observation of Beta Tauri with that of Stecher¹². This fits satisfactorily to our ribbon lamp calibration at 2800 Å. The zero order response provides less than 10 per cent of the energy from a late B-type stellar spectrum and has been ignored as a component of the background.

Data Reduction

The attitude reconstruction is to an accuracy better than one degree and shows that a series of scans were made at about 18° intervals nearly orthogonal to the galactic plane. The background brightness distribution along four of the tracks, which were sufficiently free of the effects of the bright horizon (airglow and scattered atmospheric light) and stray moonlight,

is shown in Fig. 1 as a function of b^{II} . The positions of the tracks on the sky are shown in Fig. 2a and the measurements assembled as a tentative contour map in Fig. 2b. Each point in Fig. 1 represents the average of a set of ten successive readings (during this interval of 27.5 ms the field of view moves about 0.4°) in regions where the high-speed paper record was judged visually to be free of disturbance due to stellar signals, the threshold for recognition being about $V = 6.5$ (early B-type), 6.0 (late B-type) and 5.5 (early A-type stars). We traced

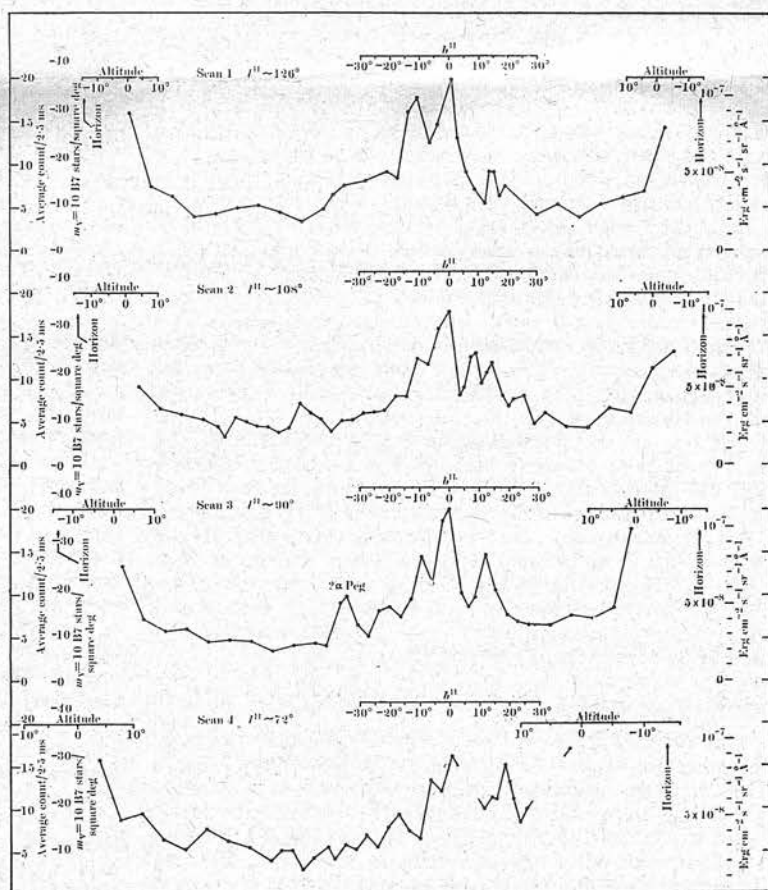


Fig. 1. Variation of 2500 Å background brightness along four tracks scanned on December 3, 1968.

doubtful sections on a star map and rejected intervals likely to have been affected by early type stars listed in the Yale Bright Star catalogue (cut-off about $V=6.5$).

A contribution due to the zodiacal light has been subtracted from arriving at the data shown. At visible wavelengths the scattering function is nearly isotropic where the angle of scattering is large¹³ and so the relative brightness depends mainly on the distribution of interplanetary dust. At shorter wavelengths, where the particles are larger relative to the wavelength of light, the assumption of isotropic scattering remains valid. We have therefore used the isophotes obtained at 5500 Å by Smith *et al.*¹⁴. An attenuation factor which was approximately 13 (taking one S_{10} unit = 1.25×10^{-9} erg cm⁻² s⁻¹ sr⁻¹ Å⁻¹ (ref. 15)*) was found to be the most satisfactory in producing symmetry between the residual brightness at large positive and negative galactic latitudes. Because the solar flux at 2800 Å (the effective wavelength of our instrument for the solar spectrum) is about one-seventh of that at 5500 Å, this scaling factor of 13 indicates that the albedo of the interplanetary dust particles in the middle ultraviolet is about half that in the visible. We also considered a scaling factor of 6.7, which would reduce the high southern latitude brightnesses to zero, but this would require a slightly higher albedo than in the visible for the interplanetary matter, leave an asymmetry (which could, however, be real (ref. 9 and unpublished work of Saito, Huru-hata and Dumont)) and seem unlikely on the astronomical and instrumental grounds which we discuss later.

Three ordinate scales are shown in Fig. 1: (a) The net average count reading over each integration interval of 2.5 ms. (b) The brightness in terms of numbers of $V=10$ stars of type corresponding to that of Beta Tauri per square degree, using our observation of the flux from Beta Tauri (B7III, $B-V=-0.13$), at 2500 Å and 210 Å resolution, as a reference. (c) The brightness in absolute units using the response curve derived as before.

Errors in deriving the response curve as well as those in the flux measurement of Beta Tauri will enter into scale (b) while obviously the absolute and relative calibration of Stecher are also implicit in scale (c). Scale (b) is likely to be reliable to about ± 25 per cent and scale (c) should be better than ± 50 per cent.

Background Brightness

Our residual light will comprise (a) the dark count of the photomultiplier tube (EMI D104) which we believe from preflight checks and inflight performance to average less than one per sample interval; (b) instrumental stray light, which from preflight checks is less than 0.1 per cent of the measured intensity within a spectrum, that is, its contribution is probably between one and three counts

*erg cm⁻² s⁻¹ sr⁻¹ Å⁻¹ \equiv W m⁻² sr⁻¹ nm⁻¹.

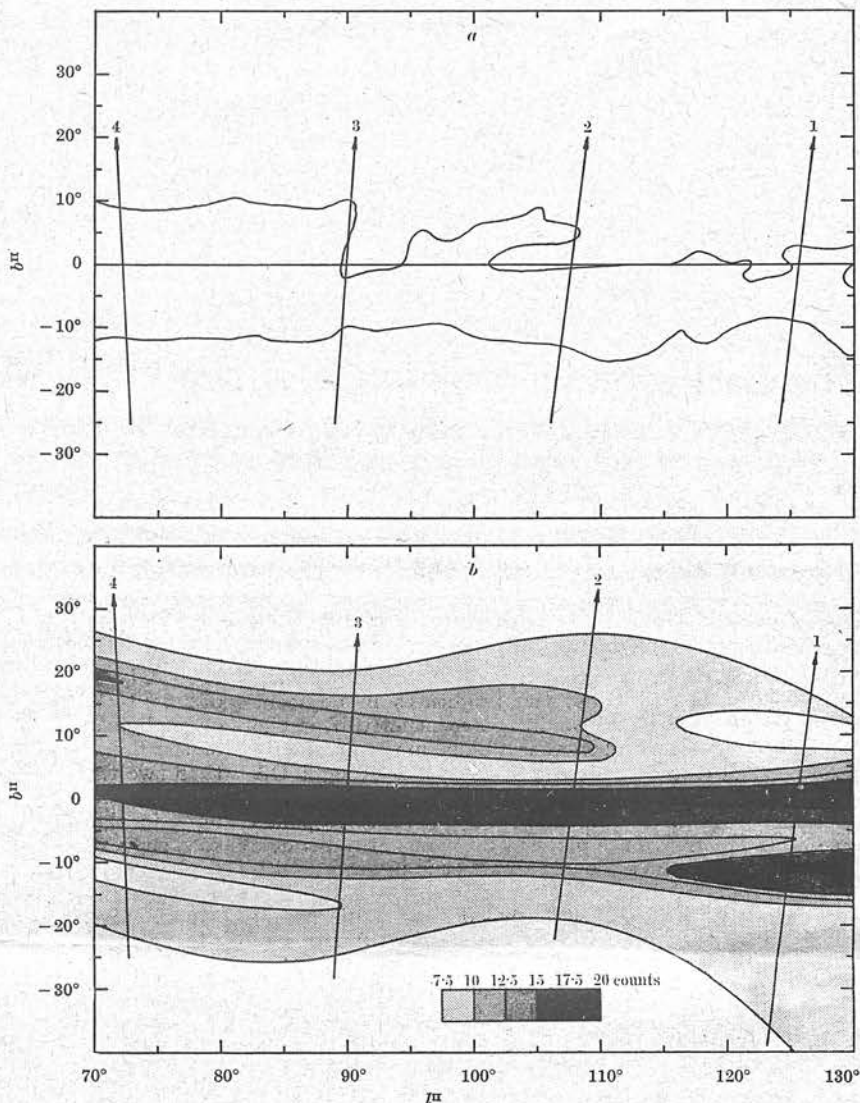


Fig. 2. a, Positions of the Milky Way crossing four tracks of Fig. 1 in l_{II} , b_{II} coordinates. b, Tentative contour map, derived from Fig. 1, near the galactic plane.

per sample interval; (c) galactic light, to which distant stars will contribute substantially when we view near the galactic plane; at high latitudes interstellar scattered light may predominate, supplemented perhaps by emissions from the galactic halo; (d) extragalactic light, including both continuum radiation and redshifted Lyman α from galaxies; and (e) residual atmospheric scattered light and airglow, which examination of the dependence on elevation shows to be negligible at altitudes greater than 20°.

Qualitatively our data show the general features of Milky Way brightness shown in star maps—the asymmetries with respect to the galactic plane, and the patches of obscuring matter. We have also looked at the integrated light maps of Roach and Megill³ and the background light maps of Elsasser and Haug², and the angular extension of the Milky Way to $b_{II} \sim +20^\circ$ seems to agree best with the colour index map of ref. 2. The secondary peaks in the brightness isophotes of our map some 10° away from the main galactic brightness maximum (Fig. 2b) suggest that at these latitudes we are looking at a distant “blue” region which is relatively much less obscured than at lower latitudes. Such an effect could be obtained from a distribution of dust and early type stars like that shown in Witt’s Fig. 3 (ref. 4) where the early type stars extend substantially beyond the dust boundary. We could then

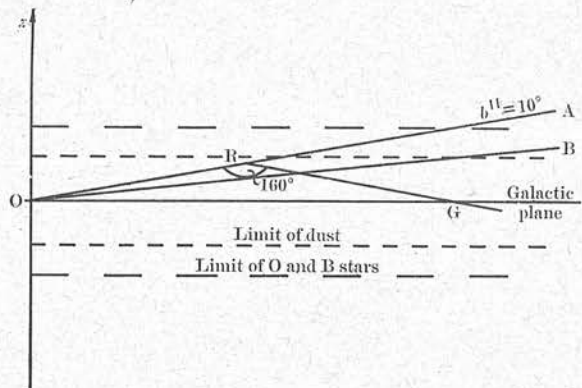


Fig. 3. Section of galactic model using plane-parallel dust and star distributions, showing lines of sight which correspond to the Fig. 2b isophotes.

have a situation where (a) within two or three degrees of the galactic plane (path OG in our Fig. 3) the background light would be due to the high concentration of early type stars close to the plane and relatively near to us; (b) around $b''=10^\circ$ (path OA) we would be looking through a considerable path length of stars in an unobscured region and with no great quantity of dust intervening; and (c) in the intermediate zone OB the relatively nearby stars are too few, and the stars in the unobscured region seen through too great a quantity of intervening obscuring matter, to equal the brightness in adjacent latitudes. Such an effect would be accentuated if, in the region we have observed, there is a bulge in the nominally plane parallel distribution, because the line of sight OA would then be more tangential to the layer of stars in the unobscured region. The elevation of about 10° corresponds to some 150 pc above the plane at a Cygnus arm distance of 1 kpc, so that the scale of this effect is in accord with the assumption of Witt.

One alternative possibility is that if there is substantial anisotropy in the forward angular scattering function of the interstellar grains at these wavelengths¹⁶ we could then be observing a maximum due to light scattered from the grains at an included angle of 160° (path GRO) from the high density of early type stars near the galactic plane. Although this is, in fact, the angle at which a maximum would occur near 2500 \AA from particles of radius $\sim 0.75 \mu\text{M}$, it obviously need not necessarily be a maximum in the angular function itself but only in its product with the illumination and the grain concentration, occurring at some 50–100 pc from the plane. The extinction along this path is less than along the direct path GO. Although the data of Lillie and Witt¹⁷ seem to indicate that we are observing early type stars rather than galactic background, it might be worth making observations from the ground around 3300 \AA to see if such an effect can be detected.

Turning to the quantitative aspects of our data, we find a range of rather more than 4 : 1 between the brightness in the galactic plane ($5 \times 10^{-8} \text{ erg cm}^{-2} \text{ s}^{-1} \text{ \AA}^{-1}$) and the value at high latitudes ($1.1 \times 10^{-8} \text{ erg cm}^{-2} \text{ s}^{-1} \text{ \AA}^{-1}$). Our values at $b''=0$ are an order of magnitude smaller than those obtained by Hayakawa *et al.*⁷ around 1400 \AA in the galactic anticentre region ($b'' \approx 200^\circ$ and $l''=240^\circ$) and an order larger than given by Kurt and Sunyaev^{5,6}. We point out that, on their own equivalence, the value of Hayakawa *et al.* is $2,000 m_v=10 \text{ A0 stars degree}^{-2}$ and seems very large compared with brightnesses similarly expressed in the visible region of the spectrum. Nevertheless, if we accept their value, and their hypothesis that the majority ($\sim 4 \times 10^{-7} \text{ erg cm}^{-2} \text{ s}^{-1} \text{ \AA}^{-1}$) of it is due to interstellar scattered light, our much lower value would support the views of Lillie and Witt¹⁷ and Nandy and Seddon¹⁸ that the maximum of extinction in the $2200\text{--}2500 \text{ \AA}$ region is due to a true absorption (low albedo) rather than a peak of scattering. One complication in the

comparison arises from the suggested anomalous spectral extinction properties in the anticentre region¹⁹ which might, in fact, cause the stellar contribution in this direction to be even greater than Hayakawa *et al.* have estimated. Code²⁰ and Bless²¹ have reported a rapid increase in flux below 2500 \AA from the galaxy M31.

It is also worth noting, however, the phenomena which Cooke *et al.*²² have suggested may account for the diffuse X-ray background which they have observed; it may be that the much reduced stellar flux in the ultraviolet enables the long wavelength "tail" of the X-ray background to be observed.

Our "extragalactic light" upper limit is also below that of ref. 7. Plotting as they did I versus $\text{cosec } b$ gives values of about $5\text{--}10 \times 10^{-9} \text{ erg cm}^{-2} \text{ s}^{-1} \text{ sr}^{-1} \text{ \AA}^{-1}$ at "cosec $b=0$ ", that is, in the absence of galactic light.

It is difficult to make a comparison with the data of Dimov *et al.*⁸ (in a band 700 \AA wide centred on 2800 \AA) because of their mode of presentation, large field and uncertainty of exact location. But if we take their V reference value arbitrarily as $250 S_{10}$ units, their "ultraviolet excess" is some $4\text{--}5 \times 10^{-8} \text{ erg cm}^{-2} \text{ sr}^{-1} \text{ \AA}^{-1}$, in good agreement with our value.

Assuming our four scans are typical and extrapolating over the whole sky, we arrive at an upper limit of $1.6 \times 10^{-17} \text{ erg cm}^{-3} \text{ \AA}^{-1}$ for the flux in the solar neighbourhood (excluding that due to "bright stars"), compared with Lillie's²³ value of $5 \times 10^{-17} \text{ erg cm}^{-3} \text{ \AA}^{-1}$ in the $2000\text{--}5600 \text{ \AA}$ band. (Habing²⁴ has calculated a "mean value" of $2.2 \times 10^{-17} \text{ ergs cm}^{-3} \text{ \AA}^{-1}$ at 2200 \AA , with an assumption of negligible albedo, when he finds less than a quarter of the flux is due to stars fainter than $m_v=6.5$.) More than two thirds of our flux is from $-25^\circ < b < +25^\circ$.

We conclude that the spatial distribution of background light in the 2500 \AA region and the Cygnus-Cassiopeia area suggests either that there is substantial light arising from relatively distant early type stars which are some 150 pc above the galactic plane, or that there is a peak in the effective angular scattering function at some 10° to the galactic plane in this region. Comparison of the absolute values of the flux measured at 2500 \AA with published data at 1400 \AA suggests that there is a minimum in the interstellar dust albedo corresponding to the peak of extinction, unless there is some unpredicted source of excess flux at the shorter wavelength or near $l''=180^\circ$.

In addition to those already mentioned¹⁰, we thank the European Space Operations Centre, G. M. Carstairs, Mrs D. E. Bashford and Mrs R. M. Tittensor, for help, and H. E. Butler, V. C. Reddish and R. Wolstencroft for advice and encouragement. The Royal Observatory, Edinburgh, is supported by the Science Research Council.

Received March 13, 1970.

- ¹ Pannekoek, A., and Koelbloed, D., *Publ. Astron. Inst. Amsterdam*, No. 9 (1949).
- ² Elsasser, H., and Haug, U., *Z. Astrophys.* 50, 121 (1960).
- ³ Roach, F. E., and Megill, L. R., *Astrophys. J.*, 133, 228 (1961).
- ⁴ Witt, A. N., *Astrophys. J.*, 152, 59 (1968).
- ⁵ Kurt, V. G., and Sunyaev, R. A., *Sov. Phys. Astron.*, 11, 928 (1968).
- ⁶ Kurt, V. G., and Sunyaev, R. A., *Proc. Luntenen Symp. IAU*, No. 36 (in the press).
- ⁷ Hayakawa, S., Yamashita, K., and Yoshioka, S., *Astrophys. and Space Sci.*, 5, 493 (1969).
- ⁸ Dimov, N. A., Severny, A. B., and Zvereva, A. H., *Proc. Luntenen Symp. IAU*, No. 36 (in the press).
- ⁹ Barth, C. A., *Proc. Luntenen Symp. IAU*, No. 36 (in the press).
- ¹⁰ Sudbury, G. C., *Appl. Opt.*, 8, 2013 (1969).
- ¹¹ Beattie, D. H., and Paterson, C. M., *Radio and Electron. Eng.* (in the press).
- ¹² Stecher, T. P., *Astron. J.*, 74, 98 (1969).
- ¹³ Ingham, M. F., *Mon. Not. Roy. Astron. Soc.*, 122, 157 (1961).
- ¹⁴ Smith, A. M., Roach, F. E., and Owen, R. W., *Planet. Space Sci.*, 13, 207 (1965).
- ¹⁵ Blackwell, D. E., Dewhurst, D. W., and Ingham, M. F., *Adv. Astron. Astrophys.*, 5, 1 (1967).
- ¹⁶ Slysh, V. I., *Nature*, 224, 159 (1969).
- ¹⁷ Lillie, C. F., and Witt, A. N., *Astrophys. Lett.*, 3, 207 (1969).
- ¹⁸ Nandy, K., and Seddon, H., *Nature*, 226, 63 (1970).
- ¹⁹ Ireland, J. G., and Nandy, K., *Astrophys. Space Sci.*, 5, 438 (1969).
- ²⁰ Code, A. D., *Publ. Astron. Soc. Pacific*, 81, 475 (1969).
- ²¹ Bless, R. C., *Proc. Luntenen Symp. IAU*, No. 36 (in the press).
- ²² Cooke, B. A., Griffiths, R. E., and Pounds, K. A., *Nature*, 224, 134 (1969).
- ²³ Lillie, C. F., *Bull. Amer. Astron. Soc.*, 1, 132 (1969).
- ²⁴ Habing, H. J., *Bull. Astro. Inst. Netherlands*, 19, 421 (1968).